KU Leuven
Biomedical Sciences Group
Faculty of Medicine
Department of Cardiovascular Sciences

SAFETY MARGINS FOR TISSUE MANIPULATION DURING MINIMALLY INVASIVE SURGERY

Rachel GEENENS

Promotor:	Prof. Dr. P. Herijgers
Co-promotor:	Prof. J. Vander Sloten & S. Vinckier
Chair:	Prof. K. Mubagwa
Jury members:	Prof. A. Luttun
	Prof. E. Verbeken
	Prof. J. Maessen
	Prof. F. Casselman

Dissertation presented in partial fulfillment of the requirements for the degree of Doctor in Biomedical Sciences

April 2016

TABLE OF CONTENTS

DANKWOORD

Een wijs man zei me ooit: “de weg naar een voltooide doctoraatthesis bestaat uit 1% inspiratie, 9% frustratie, en 90% transpiratie”. Gezien mijn verworven bekendheid als ‘de koukleum van ons lab en omstreken’ ligt de verhouding frustratie-transpiratie voor mij misschien een klein tikkeltje anders… Maar, Prof. Herijgers: ik wil u hierbij bedanken om me de voorbije jaren bij te staan met raad en daad doorheen ál deze facetten! Door u kreeg ik als bioloog de kans een biomedische thesis te maken en wegwijs te worden in de fascinerende wereld van de chirurgie. Bedankt om in mij te blijven geloven, ook als ik dit zelf niet meer deed…

Prof. Vander Sloten, Stefan en Nele, bedankt voor de begeleiding als copromotor en postdoc. Ook aan mijn juryleden, prof. Verbeken, prof. Luttun, prof. Casselman en prof. Maessen: bedankt voor uw input over dit doctoraatsproject. Het IWT Vlaanderen wil ik hierbij danken om mij een doctoraatsbeurs van 4 jaar toe te kennen.

Heel wat mensen hebben me doorheen de technische kant van mijn experimenten geholpen. Ann, An en Bjorn, Luc en Raf, Ines, Roxane: Bedankt!! Andy, zelfs toen je niet langer officieel deel van ons IDO-team was stond je paraat om holderdebolder een klemtoestel te ontwerpen, én mijn niet-bestaande programmeren-kennis aan te vullen. Ik ben je hier enorm dankbaar voor!!!

Ik ben ook zeker ‘mijn studentjes’ doorheen de jaren niet vergeten: Hannelore, Valérie, Gwen, Sarah, Arno, Rosalien, Silke en Ward! Een toffe werksfeer werd verder verzekerd door de collega’s van bij prof. Holvoet en prof. Sipido, de overflow meisjes en de uro-guys. Karel: je geweldige stripacts en 1-malig (boeee!) Samson optreden maakten het laboleven extra interessant en dragelijk ;) Lene, ook jou vergeet ik nooit, blijf zweven…

Els en Mieke, zonder jullie was ik nu nog steeds bezig met kleuringen, microscopie en analyses… En Mieke, ook bedankt om het befaamde verbod-op-meer-dan-1-koffie-per-dag-voor-Rachel te creëren, dat bleek inderdaad het beste voor íedereen :D Het was super om er naast collega’s ook vriendinnen bij te krijgen, die me steeds bleven oppeppen, zelfs na tegenslag # vijfduizend! Dit geldt ook voor mijn twee lieve bureau-genootjes, Nina en Tatiana. Tati, op een dag zullen onze rollen omgedraaid zijn, en zit ik nu vol trots toe te kijken hoe jij je awesome thesis verdedigt! Veel succes, geloof in jezelf, en ik blijf supporteren van op afstand… Ook mijn andere collega’s, uit de verte en dichtbij, wil ik graag bedanken; Wouter, Peter, Yvette, Annelies, Souad, Maud, Manu, Christophe, Sander en Aziza.

Het lijkt vaak niet zo, maar er is nog een sprankje leven buiten een doctoraatsthesis. Geweldige buren maken onze Langdorpse thuis nog toffer… Heidi, ik vind het super om een van de twee 'kiekens' te zijn (dixit Marc) - Namaste ;) Sophie, alsof mijn trouwdag nog niet schitterend (understatement) genoeg was, hou ik er ook nog een fotografisch wonder als vriendin aan over! Dat er nog vele (Bozar)-dates mogen volgen!! Mijn partner-in-PhD, Griet, wat deed het deugd es te kunnen ventileren tegen iemand in datzelfde soms zinkende schuitje! Evelyn, bedankt om eindeloos naar me te luisteren en er voor me te zijn, maar ook om es de zotte toer op te gaan! Ik denk niet dat ik nog veel mensen ga tegenkomen die me zo goed begrijpen als jij… Alle KEK mannen en vrouwen zijn natuurlijk ook een vermelding waard! Zeker onze enige echte limoncello-master Royke, die zijn talent terug mag bovenhalen komend weekend ;) En Ellen, mijn getuige-uit-de-miljoenen… De foto-updates uit Kalmthout zorgden *altijd* voor een lach op mijn gezicht, ook als mijn motivatie en optimisme héél ver te zoeken waren. One whatsappke a day keeps the stress - toch een beetje - away!! Meter mogen zijn van jullie prachtige dochter Julie is een eer, en betekent de wereld voor mij <3

Mama en papa, het voltooien van dit doctoraat had niet gekund zonder jullie eindeloze steun en vertrouwen al die jaren. Ook jullie geloven al bijna 30 jaar onvoorwaardelijk in mij en staan altijd klaar voor een babbelke, peptalk of klusweekend! Samen met de grootouders en alle familie zijn jullie zo belangrijk voor mij, en ik ben oneindig dankbaar voor de warme thuis waarin ik ben mogen opgroeien. Ook op mijn schoonfamilie-supporterclub kan ik altijd rekenen. Bedankt dat jullie er steeds voor me (geweest) zijn: vanaf die eerste verrassings-kennismaking in de Clijne Tafel, langheen vele blokpuddingskes en servet-dansjes, tot officieel de vrouw van jullie broer/(klein)zoon!

En dat brengt me bij de belangrijkste persoon voor mij… *Save the best for last* – zoals het hoort… Stijn, jij hebt me altijd gezegd: "op een dag zal ook jij hier staan en je doctoraat halen", en 't is nog waar ook... Je hebt me altijd gesteund en geholpen, mij met raad en daad bijgestaan, me door diepe dalen heen gesleurd en met mij de overwinningen gevierd. Zonder jou stond ik hier letterlijk niet, zoveel is zeker. Bedankt om er altijd te zijn voor mij… Love you Hubbie xx

Voor pepe

LIST OF ABBREVIATIONS

α-SMA	alpha smooth muscle actin
AP-1	activator protein-1
ACh	acetylcholine
ADP	adenosine diphosphate
ADPase	adenosine diphosphatase
ApoE	apolipoprotein E
bFGF	basic fibroblast growth factor
CAM	cell adhesion molecule
cGMP	cyclic guanosine monophosphate
CRP	c-reactive protein
CVD	cardiovascular disease
DAB	3,3'-diaminobenzidine
EC	endothelial cell
ECM	extracellular matrix
eNOS	endothelial nitric oxide synthase
EPCR	endothelial protein C receptor
EtOH	ethanol
FGF	fibroblast growth factor
ICAM-1	intercellular adhesion molecule 1
IDL	intermediate-density lipoprotein
IFN-γ	interferon-γ
IL	interleukin
LDL	low density lipoprotein
LDLR	low density lipoprotein receptor
LRP	low density lipoprotein receptor-related protein
M-CSF	macrophage colony stimulating factor
MCP-1	monocyte chemoattractant protein-1
MIS	minimally invasive surgery

MOF	minimum occlusion force
Mφ	macrophage
N	Newton
NADPH	nicotinamide adenine dinucleotide phosphate
Neo	Neomycin
NF-κB	nuclear factor kappa-light-chain-enhancer of activated B cells
NO	nitric oxide
oxLDL	oxidized low density lipoprotein
PC	preconstriction
PCR	polymerase chain reaction
PDGF	platelet-derived growth factor
PE	phenylephrin
RMIS	robotic minimally invasive surgery
SEM	scanning electron microscopy
SMC	Smooth muscle cell
SM-MHC	smooth mucle myosin heavy chain
SNP	sodium nitroprusside
SPC	stem/progenitor cell
TCFA	thin-capped fibroatheroma
t-PA	tissue-type plasminogen activator
TFPI	tissue factor pathway inhibitor
TGF-β	transforming growth factor beta
TNF-α	tumor necrosis factor alpha
VCAM-1	vascular cell adhesion molecule 1
VE-cadherin	vascular endothelial cadherin
VEGF	vascular endothelial growth factor
VLA-4	very late antigen 4
VLDL	very-low-density lipoprotein
VSMC	vascular smooth muscle cell
vWF	von Willebrand factor

CHAPTER I

INTRODUCTION

1.1. PROBLEM STATEMENT

1.1.1. EVOLUTION OF SURGERY

Surgical techniques and equipment have evolved tremendously during the last decades, striving to improve patient safety and satisfaction during and after surgery. Conventional, **open surgery** entails disadvantages including potentially prolonged recovery times, a significant traumatic stress response and pain for the patient, and a potential risk of intra- and postoperative complications such as infections. **Minimally invasive surgery** (MIS) was developed to further reduce these disadvantages by reducing incision size to about 3-12 mm diameter[1]. In 1987, the first laparoscopic cholecystectomy was carried out and the number of performed laparoscopic interventions has grown proportionally to the improvements in technology and technical skills of surgeons [2].

For **cardiac surgery**, mini-sternotomies, parasternal incisions and mini-thoracotomies were used in the first minimally invasive aortic valve operations[3,4] and it was shown that minimal access incisions provide adequate exposure for aortic and mitral valve repair/replacement[5] and coronary artery bypass operations[6]. More complex video-assisted procedures were first used for closed chest internal mammary artery harvests[7] and congenital heart operations[8], and the first video-directed mitral operation was performed by the end of the 1990's[9]. Advantages compared to conventional sternotomy are reduction of intraoperative blood loss, tissue trauma, risk of postoperative infection, patient discomfort, ventilator times and hospital stays[1,10,11].

Although MIS significantly limits tissue damage, which is beneficial for the patient[12], it causes some ergonomic **challenges** for the surgeon. The instrument tips only have four degrees of freedom resulting in decreased dexterity compared to the seven degrees of

freedom of the human hand. Hand-eye coordination is disturbed and physiologic tremors of the surgeon are transmitted over the instruments[12,13]. Furthermore, pivot of the instrument shafts in fixed access ports (trocars) creates the fulcrum effect[13]. Also, the forces that arise due to the friction between the instruments and the trocar may exceed 3 Newton and cause disturbed haptic sensations during MIS[14].

To overcome these disadvantages while enhancing the benefits of conventional MIS, robots were introduced in the operating theater[12]. Optimizations of these **surgical robots** led to the development of the Da Vinci™ system in 1997 and the first complete mitral valve repair using this surgical robot was performed in 2000[15]. This master-slave system comprises three components: a surgeon console, an instrument cart and a visioning platform. A 3-dimensional image is generated and displayed above the hands of the surgeon at the operating console (master), giving the impression of being at the surgical site[12]. The movements of the surgeons' hands are translated to the instruments located at the ends of the robot arms (slave)[16]. Another master-slave surgical robot is the Zeus™ system. Although it lacks a fully articulated wrist and allows only four degrees of freedom, the instrument diameter is only 3.9mm compared to the 7-mm Da Vinci™ arm. Visualization in the basic Zeus™ system is two-dimensional, although it can be used with an external three-dimensional visualization system[10]. This company was taken over by Intuitive Surgical (owning the Da Vinci Robot) who did not further commercialize this system. The Zeus System is therefore only of historical interest.

Today, robotic minimally invasive surgery (RMIS) has a wide range of applications in orthopedic, cardiothoracic and general surgery, urology and neurosurgery. Robots facilitate surgeons to carry out a variety of MIS procedures more effectively including radical prostatectomy[17], cholecystectomy[18] and cystectomy[19]. Currently the Da Vinci™

system, the only system approved by the US Food and Drug Administration, is used for cardiac surgery[20]. It has been used to perform mitral valve repairs (FIGURE 1.1), atrial fibrillation ablations, left ventricular lead placement, intracardiac tumor resections, congenital heart surgery procedures and coronary revascularizations[13].

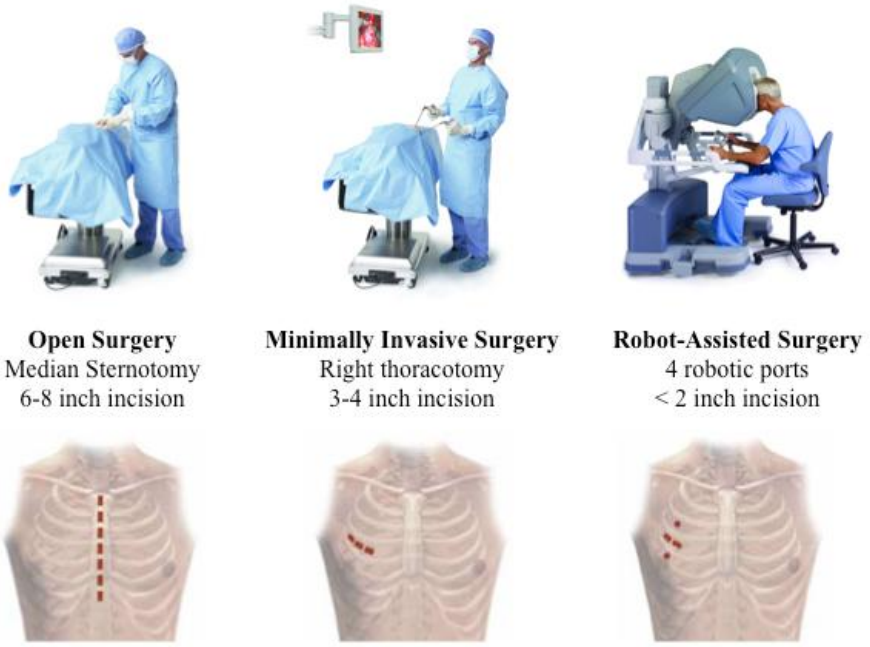

FIGURE 1.1: THE EVOLUTION OF SURGICAL APPROACH FOR MITRAL VALVE REPAIR. ADAPTED FROM [21,22]. WHILE OPEN SURGERY (LEFT) REQUIRES A FULL MEDIAN STERNOTOMY, INCISION SIZE IS LIMITED IN MINIMALLY INVASIVE PROCEDURES (MIDDLE) AND FURTHER IN CASE OF ROBOTIC SURGERY (RIGHT).

In comparison with MIS, RMIS has additional **advantages**. First, the inclusion of 7 degrees of freedom (including translation, rotation and gripping) to the instrument tips results in enhanced dexterity. Also, hardware and software filters compensate for the surgeons' tremor and create the possibility of motion scaling. Moreover, ergonomics as well as hand-eye coordination are improved and the fulcrum effect is eliminated. Finally, the 3-dimensional view with depth perception adds to a user-friendly working environment[12,13]. Advantages of conventional open surgery versus robot-assisted surgery are summarized in FIGURE 1.2.

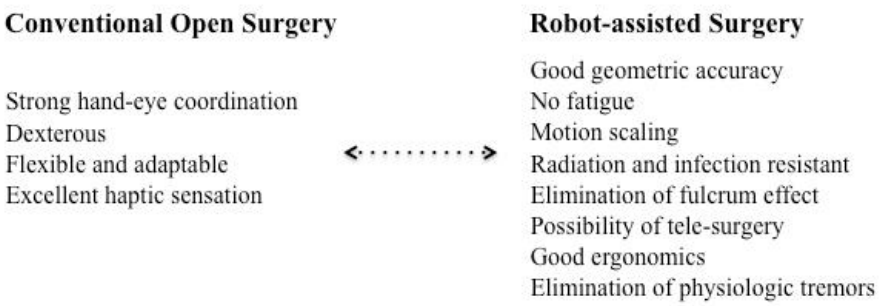

FIGURE 1.2: OVERVIEW OF THE ADVANTAGES OF OPEN SURGERY (LEFT) VERSUS ROBOT-ASSISTED SURGERY (RIGHT).

However, RMIS also has some **disadvantages**. Robotic systems and the disposables are a huge investment for hospitals (about 1.5 million dollar). Besides, these robots are large systems requiring extensive operating rooms[13]. Also, the physical disconnection between the instrument tips and the surgeons' hands completely abolishes tactile and force information (haptic feedback) for the surgeon while manipulating body tissues. This can lead to excessive load of soft tissue and thus the induction of unnecessary collateral damage[23].

1.1.2. HAPTIC FEEDBACK

The sense of touch is of great importance in everyday life and is believed to be essential for good clinical practice[24]. **Haptic feedback** generally encloses kinesthetic and cutaneous information including force, distributed pressure, temperature, vibrations and texture[25]. In surgery, it refers to the sense of touch that a surgeon experiences while manipulating body tissues. It requires intra-operative haptic sensing at the instrument tip and information display to the surgeon. The main goal of haptic sensing is to evaluate anatomical structures, detect local properties of tissue such as compliance and surface texture, and to allow the surgeon to commit appropriate force control for safe tissue manipulation[1].

To obtain **force feedback**, a system is required which measures or estimates forces applied to tissue by the instrument and gives feedback about this force to the surgeon[25]. Very effective, commercial force sensors are available but there are restrictions on size, geometry, cost, and biocompatibility for them to be implemented in the surgical robot[25–27]. Furthermore, standard sterilization for surgical instruments by autoclave can potentially destroy the sensors, while chemical protocols require much more time to ensure complete sterilization[1]. Size and complexity of force sensors depends on the degrees of freedom required for force measurement. For the Da Vinci™ system it would be ideal, though not always required or possible to have haptic feedback in all 7 degrees of freedom[1] since not all are actuated on the master[25].

The goal of implementing intraoperative force feedback in RMIS equipment is to provide **transparency** for the surgeon, to create the feeling as if his/her hands are manipulating the body tissues instead of the robot in between[25]. Several studies have shown that inclusion of haptic feedback while performing RMIS reduces injury during dissection and reduces collateral tissue damage[25–27]. Also for virtual reality training, improved performances concerning task completion time, accuracy, and number of errors have been demonstrated compared with task performances with only visual feedback[28].

In cardiac surgery, **lack of haptic information** reduces the performance of surgical tasks and accelerates visual fatigue[29]. For example, forces applied to sutures are critical in creating knots that are firm enough to hold, but do not break fine sutures or damage tissue[11]. Uncontrolled force application increases the risk for irreversible collateral injury, excessive hemorrhage or death[30]. Okamura and colleagues have shown that amplified force feedback is needed to accurately apply suture forces and that repeatability of suture ties is improved with the inclusion of force feedback[11]. Also, it

was found that the absence of haptic feedback while using a telerobotic system for blunt dissection increased tissue-damaging errors by a factor of 3[27,31].

The effect of haptic feedback implementation is still under investigation, as some groups believe that the effect may be overestimated since **experienced** surgeons are able to perform RMIS successfully without complementary force information[14,32]. However, Bethea et al. reported that even experienced surgeons often tear apart sutures and damage delicate tissues while training with surgical robots[30]. Wagner and Howe found that force feedback reduces potential tissue damage (measured by the level of applied force) for both surgeons as non-surgeons, although the latter show a significant increase in trial time[33].

Ideally, haptic feedback would be given in a direct way[34], but a fundamental limitation of giving direct force feedback is the trade-off between transparency and stability of the system. Therefore it might be better to opt for **sensory substitution** and to give force information via discrete audio signals or graphical display[11,35]. Okamura and colleagues have demonstrated that both auditory and visual feedback improve performance precision, but that visual feedback was more effective[11]. It was reported that graphical force feedback primarily benefits novices[36]. Also, the combination of vision and force feedback has been shown to be better than the availability of one of both[25]. An alternative way to provide physical constraints is via software-generated **virtual fixture assistance**[37]. This creates the possibility of shared autonomy: the surgeon remains in control of the procedure, while the robot adds safety, repeatability and accuracy[11].

The question remains if robotic systems can replace conventional laparoscopic instruments in less technical procedures. Improving and expanding the current laparoscopic procedures has the potential to overcome the limits of human ability. In the

future, an evaluation of cost-effectiveness or benefit of RMIS in comparison with conventional laparoscopic techniques has to be made[2,4].

1.2. BLOOD VESSELS IN HEALTH AND DISEASE

1.2.1. ANATOMY OF THE ARTERIAL WALL

The cardiovascular system is composed of the heart, blood, and blood vessels, which includes arteries, veins, and capillaries[38,39]. **Arteries** can be classified into elastic arteries, located near the heart and containing a high elastin to muscle ratio; and muscular arteries which contain fewer connective tissue fibers, have a large smooth muscle content and are found more peripherical[40]. Microscopically, the arterial wall consists of three layers: the (tunica) intima, the (tunica) media and the (tunica) adventitia (FIGURE 1.3)[41].

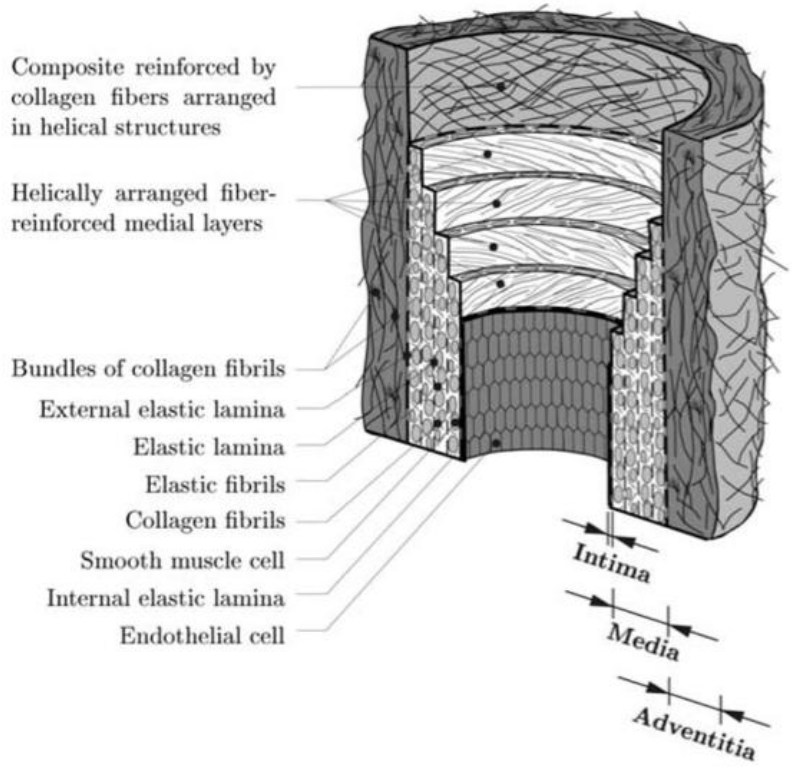

FIGURE 1.3: ARTERIAL ARCHITECTURE[41].

The **intima** consists of a single layer of endothelial cells (ECs, see 1.2.2) resting on a basal membrane (basal lamina). Being the innermost layer, it forms a barrier between the blood and the tunica media and has an important role in the regulation of the vascular tone, homeostasis and inflammation. The thickness of the subendothelial layer varies with topography, age (see 1.2.4) and disease (see 1.2.5), associated with alterations in the mechanical properties of the arterial wall[41].

The **media** consists of a three-dimensional network of circumferentially oriented smooth muscle cells (SMCs), elastin and collagen fibrils. In healthy arteries, the spindle-shaped vascular smooth muscle cells (VSMCs) allow blood vessel contraction and thus regulate blood vessel diameter, blood pressure and blood flow distribution[42]. They also secrete extracellular matrix (ECM) components which contribute to mechanical properties[43,44]. Elastic fibers consist of tropoelastin polymers cross-linked to fibrillin-rich microfibrils[45]. In muscular arteries, the lamina elastica interna and externa separate the media from the intima and the adventitia, respectively. The orientation and interconnection between elastic and collagen fibrils, elastic membranes and SMCs compose a fibrous helix, giving the media high strength and the ability to resist loads. The matrix fibers and cells are forming a functional lamellar unit, which is important for the adaptation to changes in arterial vascular wall stress[40,41].

The **adventitia** is the outermost layer and consists of fibroblasts and fibrocytes, elastic fibers, collagen fibers, the vasa vasorum and nerve structures. It is surrounded by loose connective tissue that stabilizes the blood vessel in the surrounding tissues[39]. Collagen fibrils are present as helical structures and contribute to stability and strength of the arterial wall. The adventitia has a role in initiation and propagation of inflammation, atherogenesis and arterial wall repair[41,46]. Pericytes are rare in adventitia of healthy

arteries, but their numbers increase strongly following injury. It has been described that they are implicated during wound healing and restenosis[47]. The adventitia, as well as the tunica intima and tunica media, also contains resident stem/progenitor cells (SPCs) as an endogenous repair mechanism[48].

1.2.2. ENDOTHELIAL CELLS

The **endothelial layer** is a highly dynamic organ system that participates in a variety of physiological processes, including the development and remodeling of the vasculature, the control of vascular tone and blood fluidity, and the trafficking of blood cells and nutrients. Furthermore, the endothelium is involved in a number of pathological conditions, such as atherosclerosis and cancer (via tumor angiogenesis)[39]. ECs are highly metabolically active and display remarkable heterogeneity in structure and function[49].

1.2.2.1. MORPHOLOGY

The vascular endothelium consists of a monolayer of about 10 trillion polygonal cells that line the 100 m^2 luminal surface of blood vessels[40]. ECs are typically flat, between 1-2 μm thick and 10-20 μm in diameter[40]. Arterial ECs are long and narrow or ellipsoidal, a reflection of their alignment in the direction of blood flow[39] and their cytoplasm contains a small amount of organelles, located in the perinuclear area. The most common organelles are the smooth endoplasmic reticulum, rough endoplasmic reticulum, ribosomes, lysosomes, Golgi apparatus and Weibel-Palade corpuscles. These corpuscles have the ability to store functional components such as Von Willebrand factor (vWF), interleukin (IL)-8, endothelin and P-selectin[40].

The endothelium is covered luminally with a vasculoprotective network of membrane-bound proteoglycans and glycoproteins. This **endothelial glycocalyx** is an important determinant of vascular permeability and influences blood cell – vessel wall

interactions. It repulses red blood cells from the endothelium and at the same time contains the EC adhesion molecules (CAMs, including integrins, selectins and immunoglobulin superfamily) that mediate leukocyte adhesion. CAMs have a major role in cell recruitment from the bloodstream and in cell signaling and other glycoproteins are important for coagulation, fibrinolysis and hemostasis. Factors that can damage the glycocalyx are hyperglycemia, ischemia/reperfusion injury and oxidized low density lipoproteins (oxLDL)[50].

Another characteristic of the endothelial layer is its **intercellular junctions**, of which the expression and organization varies throughout the vascular tree, corresponding to the site- specific functional requirements of the specific vessel[39]. Gap junctions are organized into connexons, channel-like structures composed of connexins. They mediate cell-cell communication, while intercellular adhesion is regulated by tight (zona occludens) and adherens (zona adherens) junctions, which interact with different signal transduction molecules and molecules that regulate cell growth and survival[51]. Adherens junctions are composed of cadherins such as vascular endothelial cadherin (VE-Cadherin), p120, γ-catenin and α-catenin[51,52]. Occludins are part of tight junctions, which form a barrier to transport between ECs (so-called paracellular transport) and help to maintain cell polarity between the luminal and abluminal side of the EC[49].

1.2.2.2. FUNCTION

The endothelium is **semi-permeable**, with a spatial heterogeneity in basal permeability that could be explained by the presence/absence of fenestrae, differences in junctional properties and/or differential activity of the transcytotic machinery[49]. Under basal conditions, molecules are continuously fluxed between the blood and the subendothelial

space. This can occur passively (paracellular) or via receptor(in)dependent transcellular transportation[49].

ECs can **respond** to chemical ligands and mechanical factors such as fluid shear stress and stretch. In straight parts of arteries, shear stretch and stress have well-defined directions, which helps in maintaining vascular homeostasis. However, at arterial curves or branches the mechanical stimuli do not have defined directions, resulting in a disruption of homeostasis[53–55]. Shear stress can activate mechanosensors on ECs, which triggers a cascade of signaling pathways resulting in modulated gene and protein expression that can regulate functional behavior of ECs[56,57].

Another function of ECs is **regulation of the vascular tone**. A rise in intracellular Ca^{2+} concentrations leads to the formation of a Ca^{2+}-calmodulin complex. This activates endothelial nitric oxide synthase (eNOS), which catalyzes the release of nitric oxide (NO) from L-Arginine. NO can diffuse through the EC membrane to activate guanylyl cyclase in the VSMCs. Subsequent formation of cyclic guanosine monophosphate (cGMP) induces muscle relaxation, leading to vasodilation. eNOS is activated by shear stress or signaling molecules such as bradykinin, adenosine, vascular endothelial growth factor (VEGF; in response to hypoxia), and serotonine (released during platelet aggregation)[58]. The endothelium can also induce VSMC hyperpolarization via an NO-independent pathway, which increases potassium conductance and subsequent propagation of depolarization[59]. Local production of endothelin, vasoconstrictor prostanoids and the conversion of angiotensin I to angiotensin II at the endothelial surface induce vasoconstriction[60,61].

In normal conditions, ECs express **anticoagulant** factors, inhibiting platelet activation (tissue factor pathway inhibitor (TFPI), heparin, thrombomodulin, endothelial protein C

receptor (EPCR), tissue-type plasminogen activator (t-PA), ecto-adenosine diphosphatase (ADPase), prostacyclin, and NO). NO inhibits platelet degranulation and aggregation via inhibition of thromboxane A2, which is a substrate for cGMP-dependent protein kinase[62–64].

1.2.3. ARTERIAL REMODELING

In normal arteries, remodeling is a homeostatic response to changes in blood flow and circumferential stretch to restore normal shear stress and wall tension, respectively[65,66]. Processes central in arterial remodeling are VSMC proliferation and differentiation, degradation and fracture of elastin fibers, and calcification plus deposition of ECM material[45]. When blood flow is higher, luminal size will increase so that the wall shear stress lowers, and vice versa. This mechanism has been shown to be endothelium-dependent[67,68]. Increased flow results in **outward remodeling**. NO is important in this process given its role in inducing metalloproteinases for matrix reorganization, inhibit proliferation and promotion of SMC apoptosis. **Inward remodeling** in response to low-flow states is mediated by production of growth factors such as transforming growth factor-β (TGF-β), which increase SMC proliferation and collagen deposition[65] (FIGURE 1.4).

Arterial remodeling refers to the whole range of structural and functional changes of the vascular wall that occur in response to disease, injury or aging[45]. The term thus covers *de novo* stenosis induced by physiological factors or pathology (see 1.2.4 and 1.2.5), transplant vasculopathy (beyond the scope of this thesis), restenosis (see 1.2.3.2), and wound healing following external mechanical injury (see 1.2.3.3). The variation in remodeling response throughout the vascular system and between patients can be explained by several factors. First, remodeling depends of the vascular bed that is

involved and the characteristics of the lesion, including plaque structure and VSMC quantity. Also, patient characteristics like age, smoking and hyperlipidemia play a role[69,70]. At last, local hemodynamics and calcium presence can predispose certain areas to the development of lesions[65].

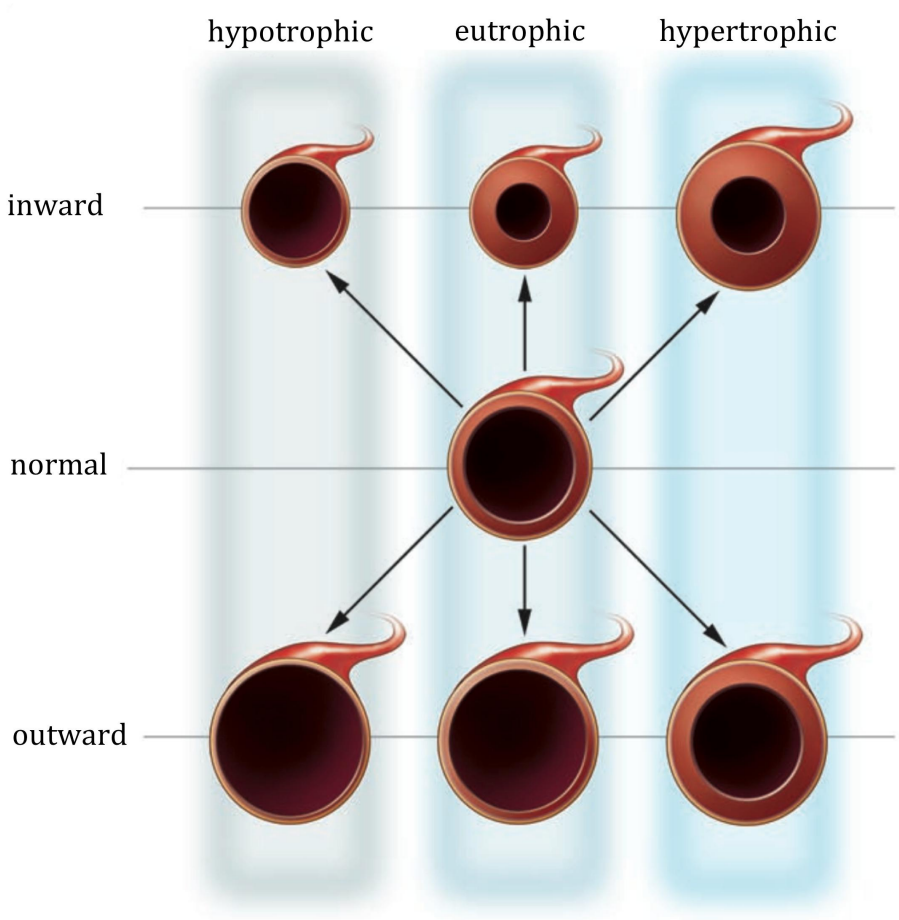

FIGURE 1.4: SCHEMATIC OVERVIEW OF OUTWARD AND INWARD ARTERIAL REMODELING (ADAPTED FROM [71]).

1.2.3.1. RESPONSE TO INJURY

The **endothelium** responds to injury by promoting the synthesis of procoagulating factors. A high affinity binding between thrombin and thrombomodulin, which is an EC-surface glycoprotein, results in platelet activation[72]. During activation, platelet granules release histamine, serotonin and adenosine diphosphate (ADP) resulting in the release

of NO and prostacyclin. The vWF is synthesized and secreted by ECs. It binds to glycoproteins GPIIb/IIIa and GPIb on the platelet membrane and forms a matrix for platelet aggregation[73,74]. This results in the formation of a limited clot, while maintaining blood in a fluid state (hemostasis).

Also, **damage** to the vascular wall causes disruption of the vascular tone, as well as the induction of EC activation and higher permeability of the endothelium[49]. Blood leukocytes adhere to the ECs via the interaction between endothelial selectins and leukocyte carbohydrate-based ligands. This initial connection is reinforced by firm adhesion between leukocyte integrins and endothelial intercellular adhesion molecule (ICAM)-1 and vascular cell adhesion molecule (VCAM)-1[75–77]. Leukocytes may pass through the endothelium between ECs (paracellular), or they may pass through the EC itself (transcellular)[78], followed by an inflammatory response in the vessel wall. These processes will be discussed in more detail in section 1.2.5.

Two mechanisms have been described for **repair** of a damaged endothelial layer. First, adjacent mature ECs can replicate and replace the lost or damaged cells, or resident SPCs can differentiate into ECs[48]. Furthermore, circulating endothelial progenitor cells can also play a role in maintenance and repair of the endothelium[79].

Differentiated, contractile **VSMCs** are elongated and spindle-shaped, and are characterized by abundant contractile filaments. They are non-migratory because of the relative absence of stimulatory factors and because the surrounding matrix is highly adhesive[80]. In response to injury or pathology, the VSMCs reobtain the embryonic potential of proliferation and migration[81]. They undergo a switch from their sessile, contractile phenotype to a mobile, synthetic, dedifferentiated phenotype and migrate to the intima where they produce ECM (**phenotypic switch**, FIGURE 1.5). Synthetic cells are

cobblestone-like, possess abundant rough endoplasmic reticulum[44] and are capable of cell division, while showing higher growth rates compared to contractile VSMCs. They express large quantities of growth factor receptors and secrete growth factors such as platelet-derived growth factor (PDGF) and TGF-β1[82].

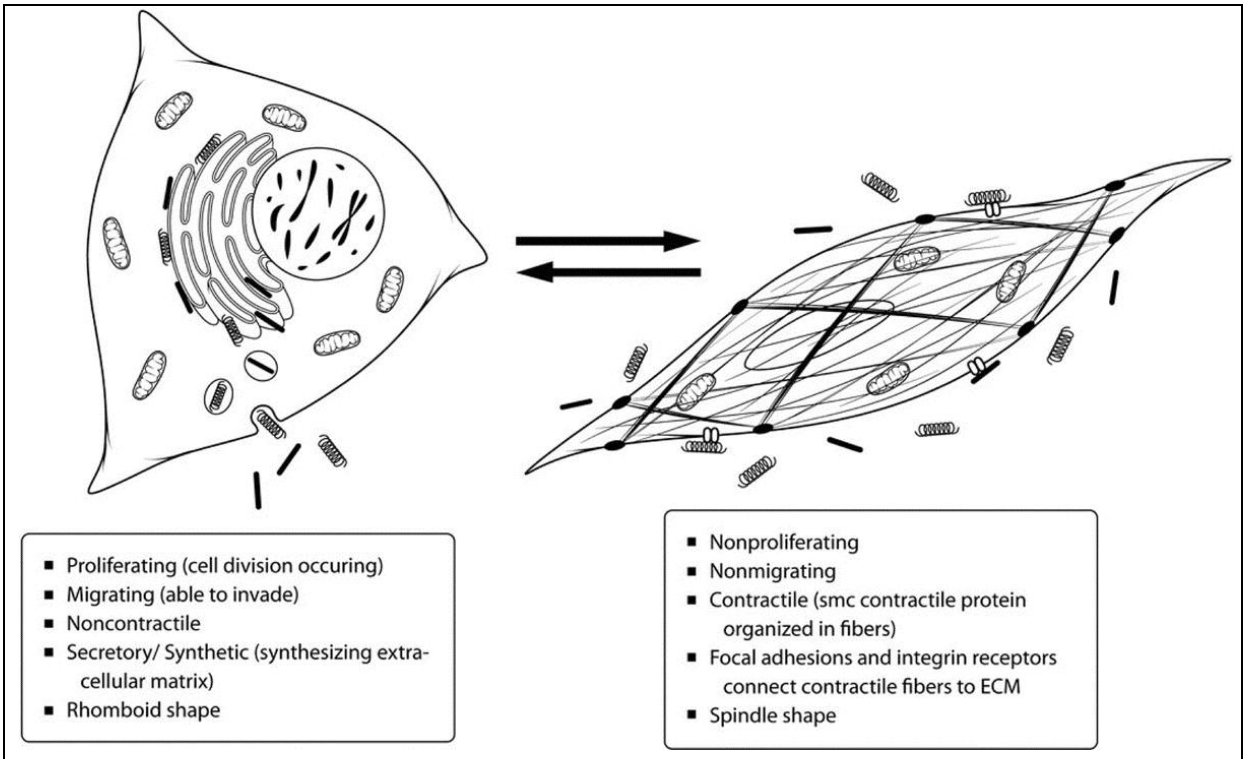

FIGURE 1.5: SCHEMATIC OVERVIEW OF VSMC PHENOTYPIC SWITCHING. THE CELL ON THE RIGHT REPRESENTS A DIFFERENTIATED, SESSILE SMC, CHARACTERIZED BY AN ABUNDANCE OF CONTRACTILE FIBERS. THE CELL ON THE LEFT IS A DEDIFFERENTIATED CELL, WHICH HAS AN IMPORTANT ROLE IN VASCULAR INJURY REPAIR BY PROLIFERATING, MIGRATING, AND MODULATING THE ECM[83].

Two biochemical factors that regulate phenotypic modulation are TGF-β, which stimulates the contractile phenotype by increasing alpha smooth muscle actin (α-SMA) and smooth muscle myosin heavy chain (SM-MHC)[84,85], and PDGF, which downregulates α-SMA and induces the synthetic phenotype[86,87]. Molecular markers for contractile cells are α-SMA, SM-MHC and smoothelin, while the synthetic phenotype can be detected via osteopontin[44,88].

SMC **migration** is initiated by the stimulation of cell surface receptors, causing activation of signal transduction pathways. This triggers remodeling of the cytoskeleton and activation of motor proteins, resulting in lamellipodia formation extending through actin polymerization. Focal formation and degradation of adhesive contact between the VSMC and the surrounding matrix support directed migration[80,89]. Proliferation of VSMCs and migration towards the injured site causes intimal thickening. This lesion can further progress into a mature atheroma[44], see section 1.2.5.

1.2.3.2. INTRAVASCULAR MECHANICAL INJURY: BALLOON ANGIOPLASTY, ATHERECTOMY AND STENTS (RESTENOSIS)

As will be described in section 1.2.5, atherosclerosis can narrow or fully occlude the blood vessel lumen. Minimally invasive procedures to reverse this occlusion are angioplasty and atherectomy, performed by balloons or lasers[90]. The hyperplastic reaction of the arterial wall in response to these procedures limits its long-term success. The incidence of acute occlusion after the intervention has been lowered by the use of intravascular stents, but the overall rate of restenosis is still approximately 20%. Drug-eluting stents reduce the restenosis rate in most studies to < 10%[89].

The remodeling process (**restenosis**) is defined as >75% cross-sectional area luminal narrowing by neointimal tissue[91]. It is characterized by early platelet aggregation and late thickening of the intima, induced by migration and proliferation of VSMCs and the accumulation of proteoglycan-collagenous ECM materials[69,90]. Restenosis occurs predominantly between 1 and 6 months after the procedure[92], but its time course is different between animal species and humans[91]. Intimal thickening has been reported to be at its maximum 28 days after balloon injury in animal models and at 6-12 months in human arteries[93]. The extent of injury is dependent of local flow characteristics, of lesion composition, structure, size and shape, as well as of medial VSMC abundance, phenotype

and distribution. For angioplasty, balloon size, inflation pressure and time also have an influence[69]. Predictors for in-stent restenosis include length of the stented segment, vessel diameter, final luminal area, and residual plaque burden outside the stent[94].

The **response** of the vascular wall to endothelial denudation induced by balloon angioplasty and stenting resembles a wound healing process and consists of thrombosis and inflammation (hours to days), cell proliferation and migration (days to weeks), and ECM remodeling (months)[89,91].

Immediately after injury, platelet adhesion and aggregation results in the formation of a thin **thrombus layer**. Platelets adhering directly to the injured site release their α-granules, containing chemokines which trigger an inflammatory response, and growth factors like TGF-β and PDGF, a chemoattractant for VSMCs, macrophages (Mφs) and neutrophils[69].

Second, the fibrin clot is replaced with **granulation tissue** by VSMCs and Mφs. The Mφs also phagocytize cell debris, secrete growth factors like fibroblast growth factor (FGF) and enhance the inflammatory response. Growth factors are responsible for VSMC and EC proliferation, which is required for arterial remodeling[91].

In a rat carotid injury model, **VSMC proliferation** in the media reached a maximum 72 hours after injury while intimal SMC proliferation peaked 7 days after injury[95]. Similar results were reported from rabbit iliac artery and baboon vascular grafts[96,97]. These findings suggest that a short burst of proliferation, shortly after injury, is sufficient for neointimal development. Proliferated VSMCs secrete ECM, explaining why after approximately 2 weeks the number of cells in the neo-intima remains constant and yet intimal thickness keeps increasing[70].

However, **VSMC replication** continues for up to 4 weeks[96]. It has been estimated that about 50% of medial VSMCs activated by balloon injury migrate and undergo approximately 3 to 5 rounds of division[98]. Some of the neo-intimal VSMC may also originate from adventitial fibroblasts, which could migrate to the site of injury and differentiate into myofibroblasts[99–101]. Also, smooth muscle progenitor cells can be mobilized from the bone marrow[102]. Noteworthy, it was demonstrated by Reidy and colleagues that SMC proliferation is not limited to the site of injury, but also occurs in up- and downstream locations[103].

Re-endothelization is aided by the mobilization of bone marrow-derived endothelial progenitor cells, which accelerate vascular repair[93,104] and may be influenced by local shear stress[105]. Tanaka et al. reported that activation of the regenerating endothelium, assessed by the expression of VCAM-1, advances in a wave from the border of injury[90]. It was shown that the area last covered by regenerated endothelium was associated with the greatest degree of intimal thickening[106], suggesting a role for ECs in tempering intimal growth. However, when large areas of endothelium are denuded, endothelium regeneration remains incomplete while intimal thickening does not continue infinitely. This means ECs are not the sole modulators in intimal growth arrest[69].

Interestingly, simple denudation and exposure to platelets may not be enough to **initiate intimal proliferation**. This is concluded from the observation that endothelial denudation without damage to the media does not result in intima proliferation, while deeper injury that includes medial SMC does[107,108]. Other factors that are important have been described. Basic fibroblast growth factor (bFGF) has been identified as a mediator of the initial wave of SMC replication. It is further stimulated by the production of growth factors and cytokines by the injured endothelium, platelets and infiltrated

inflammatory cells[109]. Also, leukocytes are recruited to the site of injury[104] and comprise between 1 and 11% of the total cell population in the neointima[70]. Tanaka et al. demonstrated a sustained activation of vascular cells and leukocytes up to 30 days after injury[90]. Moreover, SMC stretching has been shown to cause VSMC proliferation[110].

1.2.3.3. EXTRAVASCULAR MECHANICAL INJURY: CLAMPING AND SNARING (WOUND HEALING)

In a wide range of surgeries, blood vessels need to be temporarily occluded to stop blood flow through the exposed area[111]. To ensure efficiency, the **minimum occlusion force** (MOF) of the clamped blood vessel should be exceeded. According to Trobec and Gersak the actual clamping force should even be approximately three times greater than the MOF for safety[111]. At the other hand, clamping forces should be limited since excessive forces can induce irreversible damage to vessels[112].

The perfect vascular clamp would thus cause minimal trauma to a blood vessel while maintaining total occlusion of blood flow and providing sufficient traction to prevent clamp slippage. However, although many vascular clamps are described as being atraumatic, various degrees of vessel injury occur[113,114]. Several studies have compared the effects of different clamps on arterial tissue[113,115–119].

Possible macroscopic **complications** after clamping of the ascending aorta are the formation of an intimal tear with aneurysm formation[120] and acute aortic dissection[121]. Other complications of clamping injury include intimal tears and flaps, arterial thrombosis, embolization, and the late development of arterial stenosis[118]. Using histological techniques, the microscopic changes can be studied. Hangler et al. have shown using scanning electron microscopy (SEM) that external occlusion of human coronary arteries induces damage to the delicate endothelial layer[122]. This was confirmed in porcine aorta by Babin-Ebell et al.[123]. The functional integrity after

clamping can be quantified via isometric tension measurement. One of the first groups to use this methodology for this purpose was Barone et al. in 1989[113].

Lumen occlusion by internal shunts results in significantly more endothelial damage[122], while damage induced by silicone rubber looped tourniquets or suture snares is lower[118,124] compared to clamping injury. The damaged endothelium in small lesions can be **regenerated** by EC migration, while large areas need cell migration as well as proliferation[125,126]. This regenerated endothelium has a density of 150 to 200% compared to normal endothelium[127]. Although full re-endothelization can occur, impairment of endothelium-dependent relaxation and contraction has been observed while NO production was not impaired in the regenerated endothelium[128].

Apart from morphologic and physiologic changes, Dobrin et al. also examined (chronic) changes in the **mechanical properties** of non-atherosclerotic dog arteries after clamping[129]. A light clamping load (i.e. tightened until occlusion) induces a greater fraction of intimal hyperplasia and broken elastic laminae in the femoral arteries compared to the carotid arteries, while heavy clamping (i.e. as tight as possible) induces similar damage in both artery types. The application of vascular clamps with light or heavy force to the femoral arteries produced only minor changes in lumen dimension and distensibility. However, clamping the carotid artery with DeBakey clamps exhibited narrowing of the lumen[129].

The influence of **clamp duration** on the induced damage was histologically assessed by Moore et al. in infrarenal aorta an iliac vessels of adult mongrel dogs. They reported that the injury status of the arterial wall, assessed by SEM, was independent of clamping time (15 or 30 minutes)[118]. This is in contrast with later findings of Margovsky and coworkers in sheep. They found that up until 30 minutes, endothelial disruption is time-

dependent and 15 minutes of clamping induces significantly less endothelial damage than 30 minutes. However, no additional endothelial loss was observed for 30, 45 and 60 minutes of clamping[130]. The same group has shown that the **closing forces** generated by arterial clamps correlate positively with the extent and depth of artery wall injury after 15 minutes of clamping[131]. This finding was consistent with an earlier study of Slayback et al.[116].

An overview of acute histological and functional consequences of arterial clamping, linked to the extent of clamp force is presented in FIGURE 1.6. To our knowledge, the only researchers that have studied stress magnitudes and durations that can be safely applied to soft tissues are De et al. and Famaey et al.[132,133]. The study of De et al. was limited to a single animal experiment (pig), where different compression stresses were applied to the liver edge, jejunum, small bowel and ureter. Their preliminary data show a dose-dependent tissue response to stress magnitude, characterized by apoptosis and neutrophil infiltration in one or more of the tested tissues[132].

The research of Famaey et al.[133] was a preliminary proof of concept project within our research group and was further extended via this PhD thesis. Rat abdominal aorta was clamped *in vivo* for 2 minutes at 0.5 Newton (N), 5N or with a mosquito clamp, followed by functional and histological damage assessment. Acetylcholine (ACh)-induced relaxation was significantly impaired in the 5N and mosquito group, showing endothelial damage in the higher clamping loads. Absolute endothelium-independent relaxation induced by sodium nitroprusside (SNP) was impaired for all clamping loads. Transfluorescent visualization of haematoxylin-eosin stained paraffin cross-sections demonstrated endothelial denudation in the 0.5N group as well as flattening of the

elastic membranes in the 5N group. Mosquito clamping induced additional fragmentation [133].

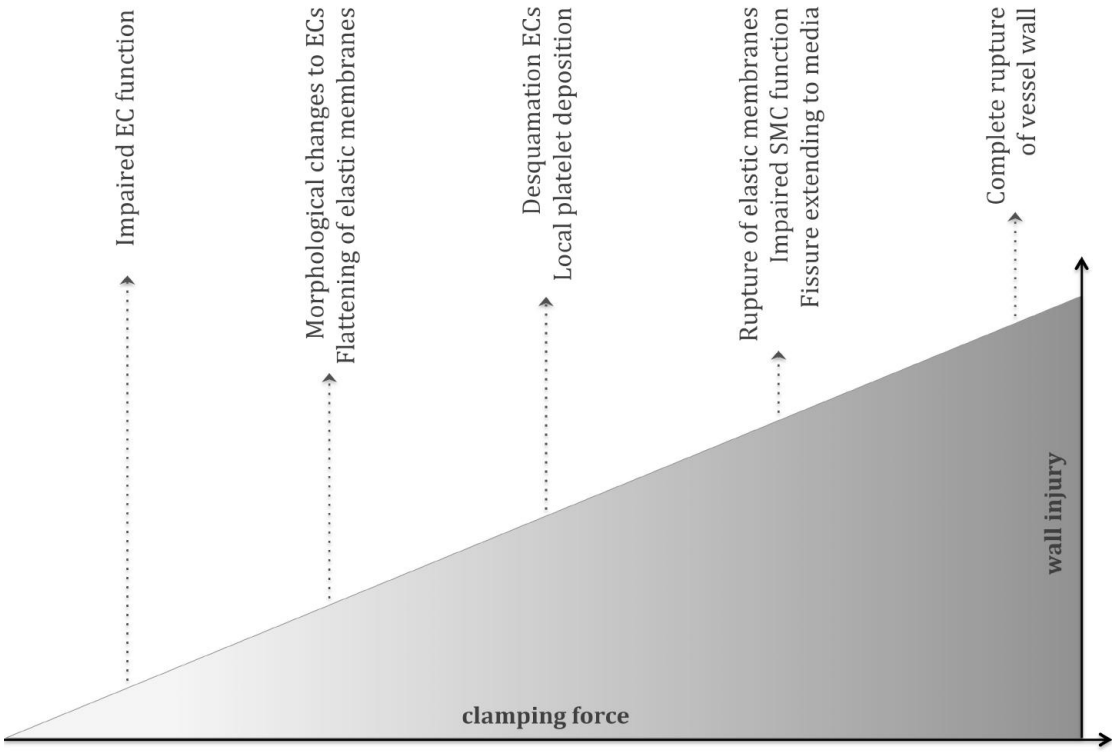

FIGURE 1.6: SUMMARY OF THE ACUTE EFFECTS OF ARTERIAL CLAMPING THAT OCCUR TO THE VESSEL WALL WITH A RISING CLAMP FORCE.

The possible **influence of vascular pathology** on clamping-induced damage was already assessed in 1976 by Slayback and colleagues. They reported that in the atherosclerotic group of vessels, it was difficult to plot a linear relationship between the amount of pressure applied and the extent of intimal damage[116]. Ten years later, Manship et al. [118] used SEM to characterize clamping-induced damage on atherosclerotic human arteries. They reported endothelial injury using vascular clamps, including intimal tears and flaps, while umbilical tape and silastic rubber did not cause detectable damage to the intima[118].

Long-term effects of external arterial occlusion have been assessed by Hsi et al. in Yucatan micro-swine at several time points (acute, 3 months, 6 months, 12 months)[134]. Suture loops induce extensive acute damage with only a slight degree of perivascular fibrosis or increase in adventitial thickening in time, while silastic loops only show damage on the long term. The use of bulldog clamps induces immediate slight injury which stays at the same level up to 12 months[134].

In this PhD dissertation the histological and functional changes due to controlled *in vivo* arterial loading were quantified both in an acute and long-term setting.

1.2.4. AGING

Population aging is a worldwide phenomenon. According to the United Nations, the proportion of elderly population in Europe (defined as people older than 65 years) will be 78.5% more in 2025 than in 1975[40]. **Vascular aging** is a normal physiological process associated with complex functional as well as structural alterations in the vasculature that renders the vascular system prone to disease[135]. It is associated with endothelial dysfunction and arterial remodeling, and leads to increased vascular stiffness (clinically measured as the carotid-femoral pulse wave velocity) and subsequently hypertension[136]. Elastic arteries are more prone to age-related changes than muscular arteries[137].

1.2.4.1. ENDOTHELIAL DYSFUNCTION

Aged vascular ECs become enlarged and flatten, and have an increasingly polyploid nucleus[138]. The arrangement and integrity of the cytoskeleton is altered, several inhibitors of the cell cycle are expressed and the regenerative capacity declines[139].

Senescent ECs increase production of vasoconstrictors like angiotensin II and endothelin and the production of vasodilators like NO and prostacyclin is reduced[139]. The decreased bioavailability of **NO** is due to an age-related decline in eNOS expression[140,141], a decreased intracellular L-arginine availability[142] and a functional inactivation of NO caused by age-associated oxidative stress[140,143]. Endothelium-derived NO is important for maintenance of tissue blood supply and confers significant vaso- and cardioprotective effects[135]. Impairment of endothelial function thus decreases vasodilator capacity and in turn leads to impairments in the control of vasomotor tone[140,144,145].

Important mechanisms involved in this age-related endothelial dysfunction are an increased production of **reactive oxygen species** due to an increased activity of nicotinamide adenine dinucleotide phosphate (NAD(P)H) oxidases[140,146,147]. Age-associated oxidative stress activates NF-κB (nuclear factor kappa-light-chain-enhancer of activated B cells), a redox-sensitive transcription factor that plays an important role in inflammatory phenotypic changes that occur during various pathophysiological conditions in blood vessels. Upon stimulation, NF-κB translocates to the nucleus and initiates inflammatory gene expression, which may further increase oxidative stress and thereby NF-κB activation itself[148]. Also, aging is associated with increasing levels of tumor necrosis factor alpha (TNF-α)[148], which promotes arterial inflammation and initiates programmed EC death[149].

1.2.4.2. ARTERIAL REMODELING DURING AGING

Age-related arterial remodeling is characterized by several macro- and microscopic changes[150].

First, the **thickness of the arterial wall** increases linearly nearly three-fold between the ages of 20 and 90 years[151]. The thickened tunica intima[152] contains matrix proteins, collagen, glycosaminoglycans and VSMCs[139]. Aged ECs have a pro-inflammatory phenotype. This is characterized by an increased expression of aortic intimal adhesion molecules and inflammatory cytokines like monocyte chemoattractant protein-1 (MCP-1)[153], and leads to increased adherence of monocytes to their surface[154]. Moreover, endothelial **permeability** has been shown to increase with age. These changes favor the passage of plasma macromolecules across the endothelium with subsequent trapping in the intima[155], adding to the process of intimal thickening.

Furthermore, for elastic arteries this age-associated increase in thickness is accompanied by an increase in arterial wall **stiffness** which leads to an increase in central pressure augmentation[156]. This is due to accelerated fragmentation and depletion of elastin by matrix metalloproteinases, as well as the deposition of collagen types I and III by VSMCs[157], which is aided by calcium deposition. With advancing age, adjacent collagen fibrils undergo non-enzymatic glycation and oxidation to form advanced glycation end products, which further increase the stiffness of the collagen network[139]. Also, VSMCs in adults mainly synthesize non-elastic collagen which results in stiffening of the vascular wall, further aided by calcium deposition[45]. Matrix metalloproteinases promote ECM degradation to facilitate migration of VSMC that have undergone phenotypic switch[44] (see 1.2.3.1.).

In this PhD thesis we determined whether middle-aged mouse arteries react differently to clamping compared to young vessels.

1.2.5. ATHEROSCLEROSIS

The age-related changes to the vascular wall described above are accelerated in the presence of cardiovascular diseases (CVD) like hypertension[158,159], metabolic syndrome[160] and atherosclerosis[161,162]. **Atherosclerosis** is a multifactorial CVD in which lipids, inflammation and shear stress are major contributing factors[163]. The pathology begins in childhood and usually manifests clinically from middle age[164]. Risk factors include hypertension, hyperlipidemia, diabetes mellitus and smoking[165].

Atherosclerotic lesions develop only at certain well-defined locations throughout the artery. This can be explained by the interaction between the blood and the endothelial layer. Thubrikar and Robicsek showed that **stress concentration** in the arterial wall due to intraluminal pressure leads to higher stretch, which relates to the sites of atherosclerotic lesion development[166]. Another related factor is **shear stress**. It arises from the friction between two virtual layers in a fluid and between a fluid and tissue and can be estimated with noninvasive imaging techniques such as magnetic resonance imaging and Doppler sonography[165]. Shear stress is subject- and vessel-specific and depends on age, blood pressure and body mass index. Vascular ECs subjected to elevated levels of wall shear stress have an elongated phenotype and align in the direction of blood flow, while low or oscillatory blood patterns are not associated with a specific morphology[165]. The shear stress between the blood and the endothelium triggers mechanotransduction pathways in the ECs via a primary cilium, present in regions of low and disturbed blood flow[167]. This results in changed expression of transcription factors like NF-κB and AP-1 (activator protein-1), inducing a pro- or anti-inflammatory EC phenotype[163]. For example, an acute increase in wall shear stress *in vitro* results in the acute release of vasodilators like NO, a key mediator in the atheroprotective effect of high shear stress[168].

At the other hand, it has been demonstrated that the regions of the vasculature exposed to oscillating or low shear stress may be susceptible to inflammation due to constitutive activation of NF-κB[163,169]. Low compared to oscillatory shear stress is a much stronger atherogenic stimulus and both types of shear stress induce plaques with a different composition, abundance of inflammatory cells, and vulnerability[163]. Moreover, exposure of the arterial wall to low shear stress may increase intercellular permeability[165,170]. If the concentration of **low density lipoproteins** (LDL) in the blood is high, it diffuses to the sub-endothelial space where it binds proteoglycans. This binding retains LDL and increases its susceptibility to be oxidized by NADH/NADPH oxidases, lipoxygenases and myeloperoxidase. OxLDL and released phospholipids further activate the ECs and this response is amplified by the binding of platelets to the EC surface. ECs respond by the production of TNF-α and IL-6, and the upregulation of selectins and immunoglobulin superfamily receptors on their surface. Interaction between these selectins (VCAM-1) and integrins (very late antigen 4 (VLA-4)) on blood monocytes causes the latter to roll over and bind to the endothelial surface.

MCP-1 and other chemokines cause diapedesis of **monocytes** into the intima, where macrophage colony stimulating factor (M-CSF) modulates their differentiation into Mφs. They are capable of producing cytokines which stimulate cellular proliferation, like IL-1, IL-6 and IL-8[171]. Two types of Mφ receptors are important for the further development of an atherosclerotic plaque.

- Engulfing of oxLDL by **scavenger receptors** on the Mφ surface causes intracellular accumulation of lipids into cytosolic droplets and transforms the Mφ into foam cells that produce metalloproteinases and can start replication.

- Binding of oxLDL to **toll-like receptors** activates the Mφs, leading to the secretion of PDGF, a chemoattractant for VSMCs in the media.

The **VSMC** undergo a switch from their sessile, contractile phenotype to a mobile, synthetic phenotype and migrate to the intima where they produce ECM components like type I and IV collagen, fibronectin and proteoglycans (phenotypic switch)[172–174]. Two biochemical factors that regulate phenotypic modulation are TGF-β, which stimulates the contractile phenotype by increasing α-SMA and SM-MHC[84,85], and PDGF, which downregulates α-SMA and induces the synthetic phenotype[86,87].

Endothelial and SMCs in accelerated vasculopathic lesions frequently express class I and II MHC antigens, induced by interferon-γ (IFN-γ). Antigenpresentation activates **T-cells** and induces innate immunity. In atherosclerotic lesions mainly CD4+ T-cells are found, and in early lesions natural killer T-cells are prevalent. The presence of cytokines promotes a Th1 response, further activating Mφs and the inflammatory response. In a progressed state, atherosclerotic plaques are present, which narrow the lumen of the blood vessel[70,175].

An advanced atherosclerotic plaque consists of a necrotic core and a fibrous cap, the composition of which determines the **stability** of the lesion. A stable atherosclerotic plaque is characterized by increased collagen content, decreased fraction of foam cells, absence of necrotic cores and a thick cap consisting of SMCs and fibrous tissue[176]. Autopsy studies disclosed that apoptosis of VSMCs and Mφs, loss of ECM integrity and inflammatory cell accumulation in the cap lead to plaque instability[177]. Rupture of this thin-capped fibroatheroma (TCFA) due to erosion or ulceration causes thrombosis, which can lead to unstable angina, stroke or myocardial infarction[178]. However, this concept of plaque (in)stability has recently been challenged by Libby and Pasterkamp.

They state that thin-capped plaques do not inevitably rupture. Moreover, plaques of other morphologies than TCFA may also result in thrombotic events[177]. It was also shown that the consequences of plaque disruption not only depend on plaque morphology, but also on the fluid phase of the blood[179].

Factors in the immune system that protect against atherosclerosis are IL-10[180], TGF-β [181] and B-cells[182,183]. The balance between inflammatory and anti-inflammatory activity controls the progression of atherosclerosis[182]. Systemic indicators of atherosclerotic inflammation are C-reactive protein (CRP) and IL-6[182,184].

In this PhD thesis the potential acute and long-term effects of atherosclerosis on clamping-induced arterial damage were assessed.

1.3. REFERENCES

1. Puangmali, P., Althoefer, K., Seneviratne, L. D., Murphy, D. & Dasgupta, P. State-of-the-art in force and tactile sensing for minimally invasive surgery. *IEEE Sens. J.* **8,** 371–380 (2008).
2. Jones, S. B. & Jones, D. B. Surgical aspects and future developments of laparoscopy. *Anesthesiology Clinics of North America* **19,** 107–124 (2001).
3. Cohn, L. H., Adams, D. H., Couper, G. S. & Bichell, D. P. Minimally invasive aortic valve replacement. *Semin. Thorac. Cardiovasc. Surg.* **9,** 331–6 (1997).
4. Cosgrove, D. M. & Sabik, J. F. Minimally invasive approach for aortic valve operations. *Ann. Thorac. Surg.* **62,** 596–7 (1996).
5. Navia, J. L. & Cosgrove, D. M. Minimally invasive mitral valve operations. *Ann. Thorac. Surg.* **62,** 1542–1544 (1996).
6. Ribakove, G. H. *et al.* Minimally invasive Port-Access coronary artery bypass grafting with early angiographic follow-up: Initial clinical experience. *J. Thorac. Cardiovasc. Surg.* **115,** 1101–1110 (1998).
7. Nataf, P. *et al.* Minimally invasive coronary surgery with thoracoscopic internal mammary artery dissection: surgical technique. *J. Card. Surg.* **11,** 288–92
8. Burke, R. P., Wernovsky, G., van der Velde, M., Hansen, D. & Castaneda, A. R. Video-assisted thoracoscopic surgery for congenital heart disease. *J. Thorac. Cardiovasc. Surg.* **109,** 499–507; discussion 508 (1995).
9. Chitwood, W. R. *et al.* Video-assisted minimally invasive mitral valve surgery: The 'micro-mitral' operation. *J. Thorac. Cardiovasc. Surg.* **113,** 413–414 (1997).

10. Kypson, A. P., Nifong, L. W. & Chitwood, W. R. Robotic Cardiac Surgery. *J. Long. Term. Eff. Med. Implants* **13,** 451–464 (2003).

11. Okamura, A. M. Methods for haptic feedback in teleoperated robot-assisted surgery. *Industrial Robot: An International Journal* **31,** 499–508 (2004).

12. Lanfranco, A. R., Castellanos, A. E., Desai, J. P. & Meyers, W. C. Robotic surgery: a current perspective. *Ann. Surg.* **239,** 14–21 (2004).

13. Satava, R. M., Bowersox, J. C. & Mack, M. Robotic surgery: state of the art and future trends. *Contemp Surg* **57,** 489–499 (2001).

14. Picod, G., Jambon, A. C., Vinatier, D. & Dubois, P. What can the operator actually feel when performing a laparoscopy? *Surg. Endosc. Other Interv. Tech.* **19,** 95–100 (2005).

15. Chitwood, W. R. *et al.* Robotic mitral valve repair: trapezoidal resection and prosthetic annuloplasty with the da vinci surgical system. *J. Thorac. Cardiovasc. Surg.* **120,** 1171–2 (2000).

16. Bodner, J., Wykypiel, H., Wetscher, G. & Schmid, T. First experiences with the da Vinci??? operating robot in thoracic surgery. in *European Journal of Cardio-thoracic Surgery* **25,** 844–851 (2004).

17. Wolfram, M. *et al.* Robotic-assisted laparoscopic radical prostatectomy: The Frankfurt technique. *World J. Urol.* **21,** 128–132 (2003).

18. Miller, D. W., Schlinkert, R. T. & Schlinkert, D. K. Robot-assisted laparoscopic cholecystectomy: initial Mayo Clinic Scottsdale experience. *Mayo Clin. Proc.* **79,** 1132–1136 (2004).

19. Miller, N. L. & Theodorescu, D. Status of robotic cystectomy in 2005. *World Journal of Urology* **24,** 180–187 (2006).

20. Bush, B., Nifong, L. W. & Chitwood, W. R. Robotics in cardiac surgery: past, present, and future. *Rambam Maimonides Med. J.* **4,** 1–8 (2013).

21. Sutter Health CMPC - http://www.cpmc.org/services/surgery/robotic/heart-mitralvalve-benefits.html. at <http://www.cpmc.org/services/surgery/robotic/heart-mitralvalve-benefits.html>

22. Robotic Assisted Laparoscopy - http://www.kenleong.com.au/roboticlaparoscopy.html.

23. Schirmbeck, E. U. *et al.* Evaluation of haptic in robotic heart surgery. *Int. Congr. Ser.* **1281,** 730–734 (2005).

24. Fager, P. J. & von Wowern, P. The use of haptics in medical applications. *Int. J. Med. Robot.* **1,** 36–42 (2004).

25. Okamura, A. M. Haptic feedback in robot-assisted minimally invasive surgery. *Curr. Opin. Urol.* **19,** 102–107 (2009).

26. Wagner, C. R., Stylopoulos, N., Jackson, P. G. & Howe, R. D. The Benefit of Force Feedback in Surgery: Examination of Blunt Dissection. *Presence: Teleoperators and Virtual Environments* **16,** 252–262 (2007).

27. Ortmaier, T. *et al.* Robot assisted force feedback surgery. *Springer Tracts Adv. Robot.* **31,** 361–379 (2007).

28. Jacobs, S., Holzhey, D., Strauss, G., Burgert, O. & Falk, V. The impact of haptic learning in telemanipulator-assisted surgery. *Surg. Laparosc. Endosc. Percutan. Tech.* **17,** 402–406 (2007).

29. Eva U. Braun, Hermann Mayer, Alois Knoll, R. L. and R. B. in *Medical Robotics* (ed. Bozovic, V.) 9–20 (I-Tech Education and Publishing, 2008). doi:10.5772/53

30. Bethea, B. T. *et al.* Application of haptic feedback to robotic surgery. *J. Laparoendosc. Adv. Surg. Tech. A* **14,** 191–195 (2004).

31. Wagner, C. R., Stylopoulos, N. & Howe, R. D. The role of force feedback in surgery: analysis of blunt dissection. *Proc. 10th Symp. Haptic Interfaces Virtual Environ. Teleoperator Syst. HAPTICS 2002* (2002). doi:10.1109/HAPTIC.2002.998943

32. Heijnsdijk, E. A. M., Pasdeloup, A., van der Pijl, A. J., Dankelman, J. & Gouma, D. J. The influence of force feedback and visual feedback in grasping tissue laparoscopically. *Surg. Endosc.* **18,** 980–985 (2004).

33. Wagner, C. R. & Howe, R. D. Force feedback benefit depends on experience in multiple degree of freedom robotic surgery task. *IEEE Trans. Robot.* **23,** 1235–1240 (2007).

34. Mahvash, M. *et al.* Force-feedback surgical teleoperator: Controller design and palpation experiments. in *Symposium on Haptics Interfaces for Virtual Environment and Teleoperator Systems 2008 - Proceedings, Haptics* 465–471 (2008). doi:10.1109/HAPTICS.2008.4479994

35. Kitagawa, M., Dokko, D., Okamura, A. M. & Yuh, D. D. Effect of sensory substitution on suture-manipulation forces for robotic surgical systems. *J. Thorac. Cardiovasc. Surg.* **129,** 151–158 (2005).

36. Reiley, C. E. *et al.* Effects of visual force feedback on robot-assisted surgical task performance. *J. Thorac. Cardiovasc. Surg.* **135,** 196–202 (2008).

37. Abbott, J., Panadda, M. & Allison, O. Haptic Virtual Fixtures for Robot-Assisted Manipulation. *Robot. Res.* 49–64 (2007). doi:10.1007/978-3-540-48113-3_5

38. Sherwood, L. *Human Physiology: From Cells to Systems*. *Human Physiology* **7th editio,** (2010).

39. Dela Paz, N. G. & D'Amore, P. A. Arterial versus venous endothelial cells. *Cell and Tissue Research* **335,** 5–16 (2009).

40. Mirea, O., Donoiu, I. & Pleşea, I. E. Arterial aging: a brief review. *Rom. J. Morphol. Embryol.* **53,** 473–7 (2012).

41. Holzapfel, G. A., Gasser, T. C. & Ogden, R. W. A new constitutive framework for arterial wall mechanics and a comparative study of material models. *J. Elast.* **61,** 1–48 (2000).

42. Owens, G. K., Kumar, M. S. & Wamhoff, B. R. Molecular regulation of vascular smooth muscle cell differentiation in development and disease. *Physiol. Rev.* **84,** 767–801 (2004).

43. Alexander, M. R. & Owens, G. K. Epigenetic Control of Smooth Muscle Cell Differentiation and Phenotypic Switching in Vascular Development and Disease. *Annual Review of Physiology* **74,** 13–40 (2012).

44. Rensen, S. S. M., Doevendans, P. A. F. M. & van Eys, G. J. J. M. Regulation and characteristics of vascular smooth muscle cell phenotypic diversity. *Neth. Heart J.* **15,** 100–8 (2007).

45. Van Varik, B. J. *et al.* Mechanisms of arterial remodeling: Lessons from genetic diseases. *Frontiers in Genetics* **3,** (2012).

46. Maiellaro, K. & Taylor, W. R. The role of the adventitia in vascular inflammation. *Cardiovasc. Res.* **75,** 640–648 (2007).

47. Tigges, U., Komatsu, M. & Stallcup, W. B. Adventitial pericyte progenitor/mesenchymal stem cells participate in the restenotic response to arterial injury. *J. Vasc. Res.* **50,** 134–44 (2013).

48. Luttun, A. & Carmeliet, P. in *Stem Cells: From Basic Research to Therapy, Volume Two* 104–144 (Enfield, USA: Science Publishers, 2014).

49. Aird, W. C. Phenotypic heterogeneity of the endothelium: I. Structure, function, and mechanisms. *Circ. Res.* **100,** 158–73 (2007).

50. Reitsma, S., Slaaf, D. W., Vink, H., Van Zandvoort, M. A. M. J. & Oude Egbrink, M. G. A. The endothelial glycocalyx: Composition, functions, and visualization. *Pflugers Archiv European Journal of Physiology* **454,** 345–359 (2007).

51. Bazzoni, G. & Dejana, E. Endothelial cell-to-cell junctions: molecular organization and role in vascular homeostasis. *Physiol. Rev.* **84,** 869–901 (2004).

52. *Cell Junctions: Adhesion, Development, and Disease*. (Wiley-VCH Verlag GmbH & Co. KGaA, 2008). doi:10.1002/9783527622092

53. Chien, S. Molecular and mechanical bases of focal lipid accumulation in arterial wall. in *Progress in Biophysics and Molecular Biology* **83,** 131–151 (2003).

54. Colangelo, S., Langille, B. L. & Gotlieb, A. I. Three patterns of distribution characterize the organization of endothelial microfilaments at aortic flow dividers. *Cell Tissue Res.* **278,** 235–242 (1994).

55. Nerem, R. M. Hemodynamics and the vascular endothelium. *J. Biomech. Eng.* **115,** 510–514 (1993).

56. Li, Y.-S. J., Haga, J. H. & Chien, S. Molecular basis of the effects of shear stress on vascular endothelial cells. *J. Biomech.* **38,** 1949–71 (2005).

57. Chien, S. Mechanotransduction and endothelial cell homeostasis: the wisdom of the cell. *Am. J. Physiol. Heart Circ. Physiol.* **292,** H1209–24 (2007).

58. Govers, R. & Rabelink, T. J. Cellular regulation of endothelial nitric oxide synthase. *Am. J. Physiol. Renal Physiol.* **280,** F193–F206 (2001).

59. Busse, R. *et al.* EDHF: Bringing the concepts together. *Trends in Pharmacological Sciences* **23,** 374–380 (2002).

60. Saye, J. A., Singer, H. A. & Peach, M. J. Role of endothelium in conversion of angiotensin I to angiotensin II in rabbit aorta. *Hypertension* **6,** 216–21

61. Kinlay, S. *et al.* Role of endothelin-1 in the active constriction of human atherosclerotic coronary arteries. *Circulation* **104,** 1114–8 (2001).

62. Nguyen, B. L., Saitoh, M. & Ware, J. A. Interaction of nitric oxide and cGMP with signal transduction in activated platelets. *Am. J. Physiol.* **261,** H1043–H1052 (1991).

63. Durante, W., Kroll, M. H., Vanhoutte, P. M. & Schafer, A. I. Endothelium-derived relaxing factor inhibits thrombin-induced platelet aggregation by inhibiting platelet phospholipase C. *Blood* **79,** 110–116 (1992).

64. Wang, G. R., Zhu, Y., Halushka, P. V, Lincoln, T. M. & Mendelsohn, M. E. Mechanism of platelet inhibition by nitric oxide: in vivo phosphorylation of thromboxane receptor by cyclic GMP-dependent protein kinase. *Proc. Natl. Acad. Sci. U. S. A.* **95,** 4888–4893 (1998).

65. Ward, M. R., Pasterkamp, G., Yeung, A. C. & Borst, C. Arterial remodeling. Mechanisms and clinical implications. *Circulation* **102,** 1186–1191 (2000).

66. Langille, B. L. Arterial remodeling: relation to hemodynamics. *Can. J. Physiol. Pharmacol.* **74,** 834–841 (1996).

67. Kamiya, A. & Togawa, T. Adaptive regulation of wall shear stress to flow change in the canine carotid artery. *Am. J. Physiol.* **239,** H14–H21 (1980).

68. Langille, B. L. & O'Donnell, F. Reductions in arterial diameter produced by chronic decreases in blood flow are endothelium-dependent. *Science* **231,** 405–407 (1986).

69. Liu, M. W., Roubin, G. S. & King, S. B. Restenosis after coronary angioplasty. Potential biologic determinants and role of intimal hyperplasia. *Circulation* **79,** 1374–1387 (1989).

70. Ferns, G. A. A., Stewart-Lee, A. L. & Anggard, E. E. Arterial response to mechanical injury: Balloon catheter de-endothelialization. *Atherosclerosis* **92,** 89–104 (1992).

71. Carretero, O. A. Vascular remodeling and the kallikrein-kinin system. *J. Clin. Invest.* **115,** 588–91 (2005).

72. Marcus, A. J. *et al.* Inhibition of platelet function by an aspirin-insensitive endothelial cell ADPase: Thromboregulation by endothelial cells. *J. Clin. Invest.* **88,** 1690–1696 (1991).

73. Pytela, R., Pierschbacher, M. D., Ginsberg, M. H., Plow, E. F. & Ruoslahti, E. Platelet membrane glycoprotein IIb/IIIa: member of a family of Arg-Gly-Asp--specific adhesion receptors. *Science (80-.).* **231,** 1559–1562 (1986).

74. Titani, K., Takio, K., Handa, M. & Ruggeri, Z. M. Amino acid sequence of the von Willebrand factor-binding domain of platelet membrane glycoprotein Ib. *Proc. Natl. Acad. Sci. U. S. A.* **84,** 5610–5614 (1987).

75. Butcher, E. C. Leukocyte-endothelial cell recognition: three (or more) steps to specificity and diversity. *Cell* **67,** 1033–6 (1991).

76. Springer, T. A. Traffic signals for lymphocyte recirculation and leukocyte emigration: the multistep paradigm. *Cell* **76,** 301–14 (1994).

77. Aurrand-Lions, M., Johnson-Leger, C. & Imhof, B. A. The last molecular fortress in leukocyte trans-endothelial migration. *Nat. Immunol.* **3,** 116–8 (2002).

78. Carman, C. V. & Springer, T. A. A transmigratory cup in leukocyte diapedesis both through individual vascular endothelial cells and between them. *J. Cell Biol.* **167,** 377–388 (2004).

79. Asahara, T. *et al.* Isolation of putative progenitor endothelial cells for angiogenesis. *Science* **275,** 964–967 (1997).

80. Gerthoffer, W. T. Mechanisms of vascular smooth muscle cell migration. *Circulation Research* **100,** 607–621 (2007).

81. Stintzing, S. *et al.* Differentiation patterning of vascular smooth muscle cells (VSMC) in atherosclerosis. *Virchows Arch.* **455,** 171–185 (2009).

82. Hao, H., Gabbiani, G. & Bochaton-Piallat, M. L. Arterial smooth muscle cell heterogeneity: Implications for atherosclerosis and restenosis development. *Arteriosclerosis, Thrombosis, and Vascular Biology* **23,** 1510–1520 (2003).

83. Milewicz, D. M. *et al.* Genetic variants promoting smooth muscle cell proliferation can result in diffuse and diverse vascular diseases: evidence for a hyperplastic vasculomyopathy. *Genet. Med.* **12,** 196–203 (2010).

84. Shah, N. M., Groves, A. K. & Anderson, D. J. Alternative neural crest cell fates are instructively promoted by TGFbeta superfamily members. *Cell* **85,** 331–343 (1996).

85. Hautmann, M. B., Madsen, C. S. & Owens, G. K. A transforming growth factor beta (TGFbeta) control element drives TGFbeta-induced stimulation of smooth muscle alpha-actin gene expression in concert with two CArG elements. *J. Biol. Chem.* **272,** 10948–10956 (1997).

86. Li, X. *et al.* Suppression of smooth-muscle alpha-actin expression by platelet-derived growth factor in vascular smooth-muscle cells involves Ras and cytosolic phospholipase A2. *Biochem. J.* **327 (Pt 3,** 709–716 (1997).

87. Kotani, M. *et al.* Chimeric DNA-RNA hammerhead ribozyme targeting PDGF A-chain mRNA specifically inhibits neointima formation in rat carotid artery after balloon injury. *Cardiovasc. Res.* **57,** 265–276 (2003).

88. Miano, J. M., Cserjesi, P., Ligon, K. L., Periasamy, M. & Olson, E. N. Smooth muscle myosin heavy chain exclusively marks the smooth muscle lineage during mouse embryogenesis. *Circ. Res.* **75,** 803–812 (1994).

89. Marx, S. O., Totary-Jain, H. & Marks, A. R. Vascular smooth muscle cell proliferation in restenosis. *Circ Cardiovasc Interv* **4,** 104–11 (2011).

90. Tanaka, H. *et al.* Sustained activation of vascular cells and leukocytes in the rabbit aorta after balloon injury. *Circulation* **88,** 1788–1803 (1993).

91. Chaabane, C., Otsuka, F., Virmani, R. & Bochaton-Piallat, M.-L. Biological responses in stented arteries. *Cardiovasc. Res.* **99,** 353–363 (2013).

92. Kimura, T. *et al.* Remodeling of human coronary arteries undergoing coronary angioplasty or atherectomy. *Circulation* **96,** 475–483 (1997).

93. Virmani, R., Kolodgie, F. D., Farb, A. & Lafont, A. Drug eluting stents: are human and animal studies comparable? *Heart* **89,** 133–138 (2003).

94. Endo, A. *et al.* Arterial remodeling influences the development of intimal hyperplasia after stent implantation. *J. Am. Coll. Cardiol.* **37,** 70–75 (2001).

95. Clowes, A. W., Reidy, M. A. & Clowes, M. M. Kinetics of cellular proliferation after arterial injury. I. Smooth muscle growth in the absence of endothelium. *Lab. Invest.* **49,** 327–333 (1983).

96. Hanke, H., Strohschneider, T., Oberhoff, M., Betz, E. & Karsch, K. R. Time course of smooth muscle cell proliferation in the intima and media of arteries following experimental angioplasty. *Circ. Res.* **67,** 651–659 (1990).

97. Geary, R. L., Kohler, T. R., Vergel, S., Kirkman, T. R. & Clowes, A. W. Time course of flow-induced smooth muscle cell proliferation and intimal thickening in endothelialized baboon vascular grafts. *Circ. Res.* **74,** 14–23 (1994).

98. Clowes, A. W. & Schwartz, S. M. Significance of quiescent smooth muscle migration in the injured rat carotid artery. *Circ. Res.* **56,** 139–145 (1985).

99. Shi, Y. *et al.* Adventitial myofibroblasts contribute to neointimal formation in injured porcine coronary arteries. *Circulation* **94,** 1655–1664 (1996).

100. Wilcox, J. N. *et al.* Contribution of adventitial myofibroblasts to vascular remodeling and lesion formation after experimental angioplasty in pig coronary arteries. *Ann. N. Y. Acad. Sci.* **811,** 437–47 (1997).

101. Scott, N. A. *et al.* Identification of a potential role for the adventitia in vascular lesion formation after balloon overstretch injury of porcine coronary arteries. *Circulation* **93,** 2178–2187 (1996).

102. Sata, M. *et al.* Hematopoietic stem cells differentiate into vascular cells that participate in the pathogenesis of atherosclerosis. *Nat. Med.* **8,** 403–409 (2002).

103. Reidy, M. A. Proliferation of smooth muscle cells at sites distant from vascular injury. *Arteriosclerosis* **10,** 298–305

104. Padfield, G. J., Newby, D. E. & Mills, N. L. Understanding the Role of Endothelial Progenitor Cells in Percutaneous Coronary Intervention. *Journal of the American College of Cardiology* **55,** 1553–1565 (2010).

105. Langille, B. L., Reidy, M. A. & Kline, R. L. Injury and repair of endothelium at sites of flow disturbances near abdominal aortic coarctations in rabbits. *Arteriosclerosis* **6,** 146–54

106. Björkerud, S. & Bondjers, G. Arterial repair and atherosclerosis after mechanical injury. *Atherosclerosis* **18,** 235–255 (1973).

107. Tada, T. & Reidy, M. A. Endothelial regeneration. IX. Arterial injury followed by rapid endothelial repair induces smooth-muscle-cell proliferation but not intimal thickening. *Am. J. Pathol.* **129,** 429–433 (1987).

108. Walker, L. N., Ramsay, M. M. & Bowyer, D. E. Endothelial healing following defined injury to rabbit aorta. *Atherosclerosis* **47,** 123–130 (1983).

109. Jackson, C. L. & Reidy, M. A. Basic fibroblast growth factor: its role in the control of smooth muscle cell migration. *Am. J. Pathol.* **143,** 1024–31 (1993).

110. Sarembock, I. J. *et al.* Influence of inflation pressure and balloon size on the development of intimal hyperplasia after balloon angioplasty. A study in the atherosclerotic rabbit. *Circulation* **80,** 1029–1040 (1989).

111. Trobec, R. & Gersak, B. Direct measurement of clamping forces in cardiovascular surgery. *Med. Biol. Eng. Comput.* **35,** 17–20 (1997).

112. Gersak, B. Comparison between absorbable and nonabsorbable sutures in arterial anastomoses in growing dogs. *J. Cardiovasc. Surg. (Torino).* **32,** 757–760 (1991).

113. Barone, G. W., Conerly, J. M., Farley, P. C., Flanagan, T. L. & Kron, I. L. Assessing clamp-related vascular injuries by measurement of associated vascular dysfunction. *Surgery* **105,** 465–471 (1989).

114. Darçin, O. T. *et al.* Pressure-controlled Vascular Clamp: A Novel Device for Atraumatic Vessel Occlusion. *Ann. Vasc. Surg.* **18,** 254–256 (2004).

115. Henson, G. F. & Rob, C. G. A comparative study of the effects of different arterial clamps on the vessel wall. *Br. J. Surg.* **43,** 561–564 (1956).

116. Slayback, J. B., Bowen, W. W. & Hinshaw, D. B. Intimal injury from arterial clamps. *Am. J. Surg.* **132,** 183–188 (1976).

117. Harvey, J. G. & Gough, M. H. A comparison of the traumatic effects of vascular clamps. *Br. J. Surg.* **68,** 267–72 (1981).

118. Manship, L. L., Moore, W. M., Bynoe, R. & Bunt, T. J. Differential endothelial injury caused by vascular clamps and vessel loops. II. Atherosclerotic vessels. *Am. Surg.* **51,** 401–6 (1985).

119. Coelho, J. C. *et al.* Arteriographic and ultrasonic evaluation of vascular clamp injuries using an in vitro human experimental model. *Surg. Gynecol. Obstet.* **155,** 506–12 (1982).

120. Boruchow, I. B., Iyengar, R. & Jude, J. R. Injury to ascending aorta by partial-occlusion clamp during aorta-coronary bypass. *J. Thorac. Cardiovasc. Surg.* **73,** 303–5 (1977).

121. Litchford, B., Okies, J. E., Sugimura, S. & Starr, A. Acute aortic dissection from cross-clamp injury. *J. Thorac. Cardiovasc. Surg.* **72,** 709–13 (1976).

122. Hangler, H., Mueller, L., Ruttmann, E., Antretter, H. & Pfaller, K. Shunt or snare: coronary encothelial damage due to hemosttic devices for beating heart coronary surgery. *Ann. Thorac. Surg.* **86,** 1873–7 (2008).

123. Babin-Ebell, J., Gimpel-Henning, K., Sievers, H.-H. & Scharfschwerdt, M. Influence of clamp duration and pressure on endothelial damage in aortic cross-clamping. *Interact. Cardiovasc. Thorac. Surg.* **10,** 168–71 (2010).

124. Perrault, L. P. *et al.* Snaring of the target vessel in less invasive bypass operations does not cause endothelial dysfunction. *Ann. Thorac. Surg.* **63,** 751–755 (1997).

125. Reidy, M. A. & Schwartz, S. M. Endothelial regeneration. III. Time course of intimal changes after small defined injury to rat aortic endothelium. *Lab. Invest.* **44,** 301–308 (1981).

126. Schwartz, S. M., Haudenschild, C. C. & Eddy, E. M. Endothelial regneration. I. Quantitative analysis of initial stages of endothelial regeneration in rat aortic intima. *Lab. Invest.* **38,** 568–580 (1978).

127. Griffin, G. K. *et al.* IL-17 and TNF-alpha sustain neutrophil recruitment during inflammation through synergistic effects on endothelial activation. *J Immunol* **188,** 6287–6299 (2012).

128. Shimokawa, H., Flavahan, N. A. & Vanhoutte, P. M. Natural course of the impairment of endothelium-dependent relaxations after balloon endothelium removal in porcine coronary arteries. Possible dysfunction of a pertussis toxin-sensitive G protein. *Circ. Res.* **65,** 740–753 (1989).

129. Dobrin, P. B., McGurrin, J. F. & McNulty, J. A. Chronic histologic changes after vascular clamping are not associated with altered vascular mechanics. *Ann. Vasc. Surg.* **6,** 153–9 (1992).

130. Margovsky, A. I., Lord, R. S. & Chambers, A. J. The effect of arterial clamp duration on endothelial injury: an experimental study. *Aust. N. Z. J. Surg.* **67,** 448–451 (1997).

131. Margovsky, A. I., Chambers, A. J. & Lord, R. S. The effect of increasing clamping forces on endothelial and arterial wall damage: an experimental study in the sheep. *Cardiovasc. Surg.* **7,** 457–63 (1999).

132. De, S. *et al.* Assessment of Tissue Damage due to Mechanical Stresses. *Int. J. Rob. Res.* **26,** 1159–1171 (2007).

133. Famaey, N. *et al.* In vivo soft tissue damage assessment for applications in surgery. *Med. Eng. Phys.* **32,** 437–43 (2010).

134. Hsi, C. *et al.* Experimental coronary artery occlusion: relevance to off-pump cardiac surgery. *Asian Cardiovasc. Thorac. Ann.* **10,** 293–7 (2002).

135. Ungvari, Z., Kaley, G., de Cabo, R., Sonntag, W. E. & Csiszar, A. Mechanisms of vascular aging: New perspectives. *J. Gerontol. A. Biol. Sci. Med. Sci.* **65 A,** 1028–1041 (2010).

136. Herrera, M. D., Mingorance, C., Rodríguez-Rodríguez, R. & Alvarez de Sotomayor, M. Endothelial dysfunction and aging: An update. *Ageing Research Reviews* **9,** 142–152 (2010).

137. Benetos, A., Laurent, S., Hoeks, A. P., Boutouyrie, P. H. & Safar, M. E. Arterial alterations with aging and high blood pressure. A noninvasive study of carotid and femoral arteries. *Arterioscler. Thromb.* **13,** 90–97 (1993).

138. Asai, K. *et al.* Peripheral vascular endothelial dysfunction and apoptosis in old monkeys. *Arterioscler. Thromb. Vasc. Biol.* **20,** 1493–1499 (2000).

139. Najjar, S. S., Scuteri, A. & Lakatta, E. G. Arterial aging: Is it an immutable cardiovascular risk factor? *Hypertension* **46,** 454–462 (2005).

140. Csiszar, A. *et al.* Aging-induced phenotypic changes and oxidative stress impair coronary arteriolar function. *Circ. Res.* **90,** 1159–1166 (2002).

141. Tanabe, T. *et al.* Exercise training improves ageing-induced decrease in eNOS expression of the aorta. *Acta Physiol. Scand.* **178,** 3–10 (2003).

142. Berkowitz, D. E. *et al.* Arginase Reciprocally Regulates Nitric Oxide Synthase Activity and Contributes to Endothelial Dysfunction in Aging Blood Vessels. *Circulation* **108,** 2000–2006 (2003).

143. Sun, D. *et al.* Reduced release of nitric oxide to shear stress in mesenteric arteries of aged rats. *Am. J. Physiol. Heart Circ. Physiol.* **286,** H2249–56 (2004).

144. Lévy, B. I. Artery changes with aging: degeneration or adaptation? *Dialogues Cardiovasc. Med.* **6,** 104–111 (2001).

145. Ungvari, Z., Parrado-Fernandez, C., Csiszar, A. & De Cabo, R. Mechanisms underlying caloric restriction and lifespan regulation: Implications for vascular aging. *Circulation Research* **102,** 519–529 (2008).

146. van der Loo, B. *et al.* Enhanced peroxynitrite formation is associated with vascular aging. *J. Exp. Med.* **192,** 1731–1744 (2000).

147. Donato, A. J. *et al.* Direct evidence of endothelial oxidative stress with aging in humans: Relation to impaired endothelium-dependent dilation and upregulation of nuclear factor-κB. *Circ. Res.* **100,** 1659–1666 (2007).

148. Csiszar, A., Wang, M., Lakatta, E. G. & Ungvari, Z. Inflammation and endothelial dysfunction during aging: role of NF-kappaB. *J. Appl. Physiol.* **105,** 1333–1341 (2008).

149. Ungvari, Z., Csiszar, A. & Kaley, G. Vascular inflammation in aging. *Herz* **29,** 733–740 (2004).

150. Hallock, P. & Benson, I. C. STUDIES ON THE ELASTIC PROPERTIES OF HUMAN ISOLATED AORTA. *J. Clin. Invest.* **16,** 595–602 (1937).

151. Nagai, Y. *et al.* Increased carotid artery intimal-medial thickness in asymptomatic older subjects with exercise-induced myocardial ischemia. *Circulation* **98,** 1504–1509 (1998).

152. Virmani, R. *et al.* Effect of aging on aortic morphology in populations with high and low prevalence of hypertension and atherosclerosis. Comparison between occidental and Chinese communities. *Am. J. Pathol.* **139,** 1119–1129 (1991).

153. Spinetti, G. *et al.* Rat aortic MCP-1 and its receptor CCR2 increase with age and alter vascular smooth muscle cell function. *Arterioscler. Thromb. Vasc. Biol.* **24,** 1397–1402 (2004).

154. Orlandi, A., Marcellini, M. & Spagnoli, L. G. Aging influences development and progression of early aortic atherosclerotic lesions in cholesterol-fed rabbits. *Arterioscler. Thromb. Vasc. Biol.* **20,** 1123–1136 (2000).

155. Fry, D. L. Mass transport, atherogenesis, and risk. *Arteriosclerosis* **7,** 88–100 (1987).

156. Nichols, W. W. Clinical measurement of arterial stiffness obtained from noninvasive pressure waveforms. *American Journal of Hypertension* **18,** (2005).

157. O'Rourke, M. F. & Nichols, W. W. Aortic diameter, aortic stiffness, and wave reflection increase with age and isolated systolic hypertension. *Hypertension* **45,** 652–8 (2005).

158. Nichols, W. W., Nicolini, F. A. & Pepine, C. J. Determinants of isolated systolic hypertension in the elderly. *J. Hypertens. Suppl.* **10,** S73–S77 (1992).

159. Taddei, S. *et al. Hypertension causes premature aging of endothelial function in humans. Hypertension* **29,** (1997).

160. Scuteri, A. *et al.* Metabolic syndrome amplifies the age-associated increases in vascular thickness and stiffness. *J. Am. Coll. Cardiol.* **43,** 1388–1395 (2004).

161. Burke, G. L. *et al.* Arterial Wall Thickness Is Associated With Prevalent Cardiovascular Disease in Middle-Aged Adults : The Atherosclerosis Risk in Communities (ARIC) Study. *Stroke* **26,** 386–391 (1995).

162. van Popele, N. M. *et al.* Association between arterial stiffness and atherosclerosis: the Rotterdam Study. *Stroke.* **32,** 454–460 (2001).

163. Helderman, F. *et al.* Effect of shear stress on vascular inflammation and plaque development. *Curr. Opin. Lipidol.* **18,** 527–533 (2007).

164. Deanfield, J. E., Halcox, J. P. & Rabelink, T. J. Endothelial function and dysfunction: Testing and clinical relevance. *Circulation* **115,** 1285–1295 (2007).

165. Shaaban, A. M. & Duerinckx, A. J. Wall Shear Stress and Early Atherosclerosis. *Am. J. Roentgenol.* **174,** 1657–1665 (2000).

166. Thubrikar, M. J. & Robicsek, F. Pressure-induced arterial wall stress and atherosclerosis. *Annals of Thoracic Surgery* **59,** 1594–1603 (1995).

167. Van Der Heiden, K. *et al.* Monocilia on chicken embryonic endocardium in low shear stress areas. *Dev. Dyn.* **235,** 19–28 (2006).

168. Ballermann, B. J., Dardik, A., Eng, E. & Liu, A. Shear stress and the endothelium. *Kidney Int. Suppl.* **67,** S100–S108 (1998).

169. Partridge, J. *et al.* Laminar shear stress acts as a switch to regulate divergent functions of NF-kappaB in endothelial cells. *FASEB J.* **21,** 3553–3561 (2007).

170. Okano, M. & Yoshida, Y. Junction complexes of endothelial cells in atherosclerosis-prone and atherosclerosis-resistant regions on flow dividers of brachiocephalic bifurcations in the rabbit aorta. *Biorheology* **31,** 155–61

171. Libby, P., Schwartz, D., Brogi, E., Tanaka, H. & Clinton, S. K. A cascade model for restenosis. A special case of atherosclerosis progression. *Circulation* **86,** III47–I52 (1992).

172. Katsuda, S. *et al.* Collagens in human atherosclerosis. Immunohistochemical analysis using collagen type-specific antibodies. *Arterioscler. Thromb.* **12,** 494–502 (1992).

173. Clausell, N., Molossi, S. & Rabinovitch, M. Increased interleukin-1 beta and fibronectin expression are early features of the development of the postcardiac transplant coronary arteriopathy in piglets. *Am. J. Pathol.* **142,** 1772–1786 (1993).

174. Carey, D. J. Vascular smooth muscle extracellular matrix. *J. Vasc. Surg.* **15,** 917–919 (1992).

175. Hansson, G. K., Jonasson, L., Holm, J., Clowes, M. M. & Clowes, A. W. Gamma-interferon regulates vascular smooth muscle proliferation and Ia antigen expression in vivo and in vitro. *Circ. Res.* **63,** 712–719 (1988).

176. Dickson, B. C. & Gotlieb, A. I. Towards understanding acute destabilization of vulnerable atherosclerotic plaques. *Cardiovasc. Pathol.* **12,** 237–248 (2003).

177. Libby, P. & Pasterkamp, G. Requiem for the 'vulnerable plaque'. *Eur. Heart J.* **36,** 2984–7 (2015).

178. Kolodgie, F. D. *et al.* The thin-cap fibroatheroma: a type of vulnerable plaque: the major precursor lesion to acute coronary syndromes. *Curr. Opin. Cardiol.* **16,** 285–292 (2001).

179. Libby, P. & Theroux, P. Pathophysiology of coronary artery disease. *Circulation* **111,** 3481–8 (2005).

180. Mallat, Z. *et al.* Protective role of interleukin-10 in atherosclerosis. *Circ. Res.* **85,** e17–e24 (1999).

181. Robertson, A. K. L. *et al.* Disruption of TGF-β signaling in T cells accelerates atherosclerosis. *J. Clin. Invest.* **112,** 1342–1350 (2003).

182. Hansson, G. K. Inflammation, atherosclerosis, and coronary artery disease. *N. Engl. J. Med.* **352,** 1685–1695 (2005).

183. Caligiuri, G., Nicoletti, A., Poirierand, B. & Hansson, G. K. Protective immunity against atherosclerosis carried by B cells of hypercholesterolemic mice. *J. Clin. Invest.* **109,** 745–753 (2002).

184. Lindahl, B., Toss, H., Siegbahn, A., Venge, P. & Wallentin, L. *Markers of myocardial damage and inflammation in relation to long-term mortality in unstable coronary artery disease. FRISC Study Group. Fragmin during Instability in Coronary Artery Disease. NEJM* **343,** (2000).

CHAPTER II

PROJECT AIMS

Evolution of surgical techniques towards robotic minimally invasive procedures entails major advantages for the patients as well as for the surgeon. However, the lack of intra-operative tactile and force information (haptic feedback) and the limited field of view of the optic camera can lead to unnecessary collateral damage to soft tissues. Blood vessels, for example, could be unwillingly compressed by instruments or their shafts outside the field of view during robotic manipulations. **The implementation of haptic information in robotic systems, to limit the exerted forces on soft tissues could improve patient safety during minimally invasive surgery.**

In order to define safety thresholds above which damage becomes unacceptable, we want to investigate the relationship between application of a predefined clamping load on mouse aortas and the hereby induced tissue damage. Furthermore, it is unknown whether these safety thresholds are invariable irrespective of age and potential pathology, i.e. if we should take in to account **patient-specific physiological or pathological factors**. Knowledge of this relationship for healthy, aged and diseased arteries will clarify whether patient-specificity should be accounted for.

Aim 1 We want to determine the relationship between mechanical arterial clamping and the induced tissue damage.

Hypothesis 1.1 We hypothesize that an increasing clamping load will result in increasing damage to the arterial wall (chapter 3 and 5).

Aim 2 We want to investigate the effect of aging and pathology on the relationship between mechanical arterial clamping and the induced tissue damage.

Hypothesis 2.1 We hypothesize that a specific clamping load (0.5N or 2.0N) will induce more extensive damage to aged mouse aortas (chapter 3).

Hypothesis 2.2 We hypothesize that a specific clamping load (0.6N or 1.27N) will induce more extensive damage to diseased (atherosclerotic) mouse aortas (chapter 5).

Aim 3 We want to study the long-term response of the arterial wall to mechanical clamping.

Hypothesis 3.1 We hypothesize that arterial clamping will result in acute injury to which the vascular wall will respond by wound healing response, characterized by inflammation (chapter 5).

CHAPTER III

ARTERIAL VASOREACTIVITY IS EQUALLY AFFECTED BY *IN VIVO* CROSS-CLAMPING WITH INCREASING LOADS IN YOUNG AND MIDDLE-AGED MOUSE AORTAS.

Adapted from:

Geenens R, Famaey N, Gijbels A, Verhulst V, Vinckier S, Vander Sloten J, Herijgers P. Arterial vasoreactivity is equally affected by *in vivo* cross-clamping with increasing loads in young and middle-aged mouse aortas. Ann Thorac Cardiovasc Surg. 2015 Nov 6. [Epub ahead of print]

3.1. ABSTRACT

3.1.1. BACKGROUND

To compensate for the lack of haptic feedback by surgical robots, limitation of exerted forces could be implemented. The limits should be based on the observed relationship between tissue load and induced damage. This study examines whether age-related changes influence this relationship.

3.1.2. METHODS

Descending thoracic aortas of male C57BL/6J mice of 10, 25 and 40 weeks were clamped *in vivo* (no clamp, 0.5N or 2.0N) for 2 minutes. Functional integrity was tested *in vitro* by studying endothelium-dependent and –independent vasoreactivity.

3.1.3. RESULTS

Endothelium-dependent relaxation deteriorated with increased clamping force at all ages. Clamping did not influence endothelium-independent vasodilation. Age (10, 25 and 40 weeks) did not significantly impact on the effect of clamping on endothelium-dependent and independent vasoreactivity.

3.1.4. CONCLUSIONS

Within the tested conditions, mechanical clamping induces damage to the vascular endothelium, but not to the SMCs. Age has no effect on the obtained results in mice from 10 to 40 weeks old.

3.2. INTRODUCTION

Robotic surgery is increasingly applied in cardiovascular surgery to reduce surgical trauma and improve patient satisfaction[1]. The lack of haptic feedback increases the risk of tissue overload, since the surgeon is not aware of sometimes excessive force exerted on the tissue. Tissue out of the visual field is at the highest risk of accidental mechanical overload. Previously, we and others have shown that the amount of force applied on an artery is directly related to the degree of damage on functional, microscopic and even macroscopic level[2–7] and that the extent of damage is partly time-dependent[8].

Robotic surgery could overcome this problem in two potential ways. The most obvious possibility is to integrate haptic feedback in robotic instruments. However, this complicates the design of the robotic interface and will always occur with a considerable time delay, slowing down the operation. An alternative approach, that our research group is currently exploring, proposes the limitation of the maximally allowable exerted force by robotic instruments on the tissue. This can be easily implemented in the robotic system. This limit should be chosen to avoid unacceptable collateral tissue damage that is permanent or has important functional consequences. Proper implementation of these limits requires knowledge on the quantitative relation between mechanical loading and tissue damage. As a research model, we used the clamping of mouse thoracic aortae to determine these limits. Mouse models allow to test the effect of clinically relevant conditions such as age and gender. Also, frequent pathologies can be studied by using transgenic mouse models.

It has not been examined if the aging process influences this relationship. Aging is associated with complex functional and structural alterations in the vasculature that renders the vascular system prone to disease and alters the biomechanical

characteristics[9]. Aged vascular ECs become enlarged and flattened, have an increasingly polyploid nucleus[10] and altered production of vasoconstrictory and vasodilatory substances[11,12]. Also, endothelial permeability has been shown to increase with age. This favors the passage of plasma macromolecules across the endothelium with subsequent trapping in the intima[13], inducing thickening of the intima[11,13–16]. EC aging is thus associated with loss of functional integrity and entails a shift towards a pro-inflammatory and pro-apoptotic state, which enhances monocyte transmigration into the vessel wall[17,18].

This study aims at establishing the quantitative relationship between the mechanical load by arterial clamping and the induced damage to the endothelial and medial vascular layer. Secondly, we aim to test the hypothesis that *in vivo* arterial clamping would cause more severe damage in mouse aortas of middle-aged compared to younger animals.

3.3. MATERIAL AND METHODS

3.3.1. SURGICAL PROCEDURE

All animal experiments are prospective and were approved by the ethical committee of the KU Leuven (project P009/2011). C57BL/6J mice (The Jackson Laboratory) were housed in a 12-hour light/dark cycle and fed normal chow at libitum. Male animals were used to avoid inter-gender differences. Mice of 10 (n = 20), 25 (n = 21) and 40 (n = 20) weeks old were anesthetized (ip, medetomidine 0.5mg/kg, Orion Pharma and ketamine 50mg/kg, Eurovet), intubated and ventilated with room air (250µl stroke volume, 140 strokes/min). Rectal temperature was kept at 37°C. Left thoracotomy was performed, followed by retraction of the left lung. The descending thoracic aorta was carefully

isolated from surrounding tissue and either used as a control sample (unclamped, 0.0N) or clamped *in vivo* for 2 minutes at 0.5 or 2.0N using a manual custom-designed system that allows online monitoring and control of the applied force level (FIGURE 3.1). The clamping jaws (5mm wide) are not serrated to allow homogenous distribution of the clamping forces on the vessel. Afterwards, the clamp was removed and segments of the aorta were immediately excised and transferred to organ baths for assessment of vasoreactivity.

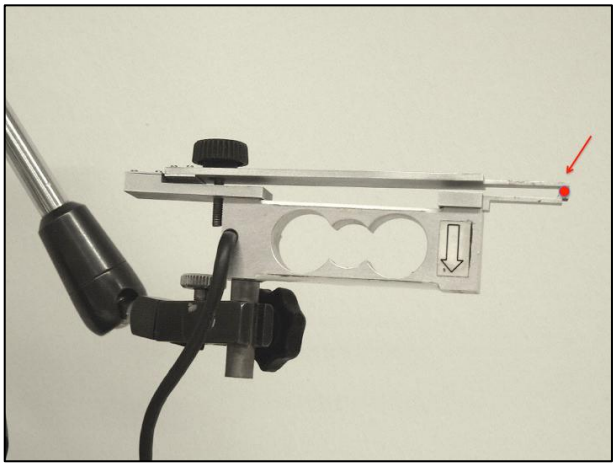

FIGURE 3.1: THE DEVICE USED FOR IN VIVO ARTERIAL CLAMPING. IT CAN BE MANUALLY OPERATED WITH THE BLACK WHEEL, AND CONNECTION OF A FORCE TRANSDUCER ALLOWS ONLINE MONITORING OF THE FORCE (N). THE CLAMPING SURFACES ARE NOT SERRATED, ENABLING A RELATIVELY HOMOGENEOUS DISTRIBUTION OF THE FORCE OVER THE CLAMPED SURFACE.

3.3.2. ISOMETRIC TENSION MEASUREMENT

For isometric tension tests, the aortic segments (3.14 ± 0.6mm in length) were mounted in a water-jacketed organ chamber containing Krebs solution (containing in mM: NaCl 118.3, KCl 4.7, KH_2PO_4 1.2, $MgSO_4$ 1.2, $NaHCO_3$ 25, Na_2Ca EDTA 0.026, Glucose 5.5, $CaCl_2$ 2.5) at 37°C, aerated by 95% O_2/ 5% CO_2. Tension was measured isometrically with Type372 force transducers (Hugo Sachs Elektronics) connected to a data acquisition

system (NI-USB-6009, National Instruments). Segments were gradually stretched over 1 hour until a stable preload of 30 mN was reached. This preload was predetermined to obtain maximal response of the segment to 40 mmol/l K^+. After preload adjustment, preconstriction (PC) was induced by PE (Sigma-Aldrich, 10^{-6}M). Subsequent cumulative addition of ACh (Sigma-Aldrich, 10^{-7}M, 10^{-6}M) allowed assessment of endothelium-dependent vasodilation. Tissues were washed 3 times with fresh Krebs solution before a new drug was tested. Endothelium-independent vasodilation was examined by adding a direct NO donor (SNP, 10^{-6}M, Fluka) following PC.

3.3.3. ANALYSIS AND STATISTICS

Preload was subtracted from the isometric tension value. All values were normalized for the length of the tested segment and grouped according to age and clamping load. Relative vasodilation is expressed as % reversal of constriction induced by PE. Results are displayed as median (interquartile range) unless otherwise stated. Statistical analyses were performed with GraphPad and $P < 0.05$ was considered statistically significant. ANOVA or Kruskal-Wallis test with Dunn's Multiple Comparison test was performed.

3.4. RESULTS

Endothelial functional integrity after *in vivo* aortic clamping (0.0N, 0.5N or 2.0N) was assessed in 61 male C57BL/6J mice of 10, 25 and 40 weeks. The exact number of experiments per condition is listed in FIGURES 3.2 AND 3.3. PC values before ACh and before SNP administration, and absolute and relative relaxation due to ACh and SNP are presented in TABLE 3.1.

TABLE 3.1: RESULTS (MEDIANS WITH THEIR INTERQUARTILE RANGE) OF THE FUNCTIONAL INTEGRITY ASSESSMENT AFTER DIFFERENT LOADING LEVELS AND FOR DIFFERENT AGES.

PC1: PC BEFORE ACH ADMINISTRATION, PC2: PC BEFORE SNP ADMINISTRATION, ACH ABS: ABSOLUTE VALUE OF RELAXATION DUE TO ACH, ACH %: RELATIVE DEGREE OF RELAXATION DUE TO ACH, SNP ABS: ABSOLUTE VALUE OF RELAXATION DUE TO SNP, SNP %: RELATIVE DEGREE OF RELAXATION DUE TO SNP. PC, ACH ABS AND SNP ABS ARE EXPRESSED AS G/MM.

		0.0N	0.5N	2.0N
10 weeks	PC1	0.16 (0.07,0.21)	0.09 (0.07,0.10)	0.11 (0.09,0.13)
	ACh abs	0.16 (0.06,0.18)	0.03 (0.01,0.03)	0.03 (0.01,0.03)
	ACh %	86.54 (72.16,100.00)	29.63 (18.18,36.36)	22.62 (11.70,34.66)
	PC2	0.23 (0.15,0.29)	0.12 (0.05,0.13)	0.12 (0.10,0.14)
	SNP abs	0.31 (0.21,0.34)	0.15 (0.12,0.17)	0.15 (0.14,0.17)
	SNP %	133.4 (114.4,143.1)	142.3 (110.6,251.6)	135.3 (106.6,160.5)
25 weeks	PC1	0.12 (0.09,0.13)	0.14 (0.11,0.23)	0.15 (0.12,0.18)
	ACh abs	0.06 (0.04,0.10)	0.04 (0.00,0.06)	0.02 (0.00,0.04)
	ACh %	74.19 (35.14,88.89)	30.56 (0.00,60.00)	22.22 (0.00, 25.00)
	PC2	0.18 (0.15,0.21)	0.17 (0.13,0.22)	0.17 (0.11,0.21)
	SNP abs	0.20 (0.18,0.25)	0.22 (0.16,0.26)	0.21 (0.13,0.25)
	SNP %	112.0 (104.2,121.2)	128.7 (114.0,142.4)	119.4 (109.4,132.2)
40 weeks	PC1	0.17 (0.13,0.32)	0.11 (0.09,0.16)	0.07 (0.05,0.18)
	ACh abs	0.07 (0.06,0.13)	0.01 (0.00,0.03)	0.02 (0.01,0.05)
	ACh %	54.29 (29.16,65.37)	8.52 (-2.47,28.07)	43.96 (11.41,47.79)
	PC2	0.21 (0.18,0.27)	0.11 (0.09,0.23)	0.14 (0.05,0.22)
	SNP abs	0.26 (0.24,0.31)	0.17 (0.11,0.25)	0.20 (0.09,0.24)
	SNP %	121.2 (109.3,140.0)	118.3 (108.8,125.0)	145.5 (107.8,187.0)

3.4.1. THE EFFECTS OF ARTERIAL CLAMPING

Overall, increasing clamping force resulted in a significantly lower endothelium-dependent vasodilation, for all ages. This is evident both when expressed as absolute relaxation (FIGURE 3.2A) or relative to PC (FIGURE 3.2B). The endothelium-independent vasodilation was not influenced by the imposed clamping forces (FIGURE 3.3).

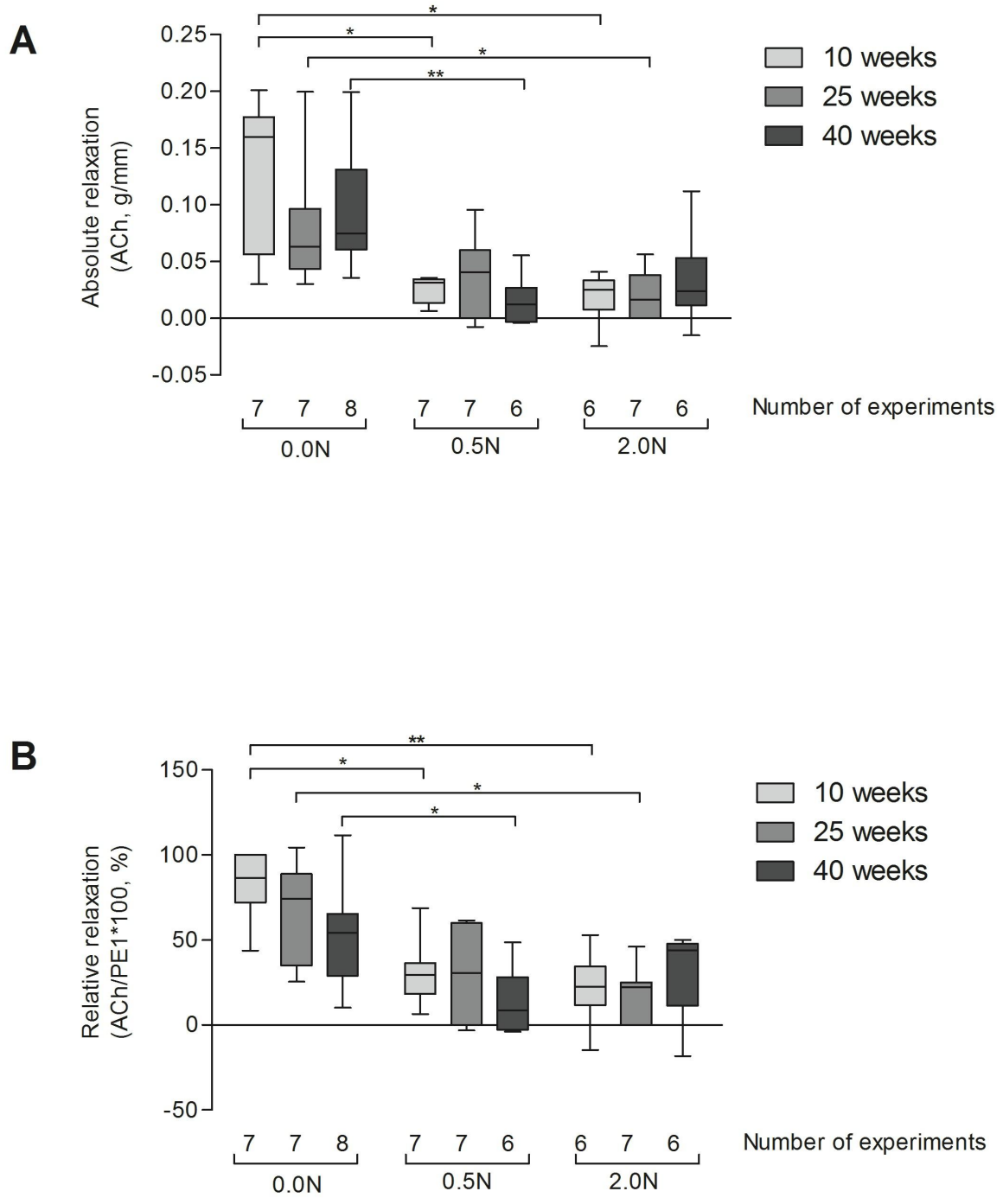

FIGURE 3.2: ENDOTHELIUM-DEPENDENT RELAXATION AFTER *IN VIVO* CLAMPING IN MICE OF 10, 25 AND 40 WEEKS.

A: RELAXATION DUE TO ACH, EXPRESSED AS G/MM

B: PERCENTAGE RELAXATION BY ACH AFTER PE PRECONSTRICTION

DATA ARE DISPLAYED AS MEDIAN (IQR) AND WHISKERS SHOW MINIMUM AND MAXIMUM.

* $P < 0.05$ AND ** $P < 0.01$

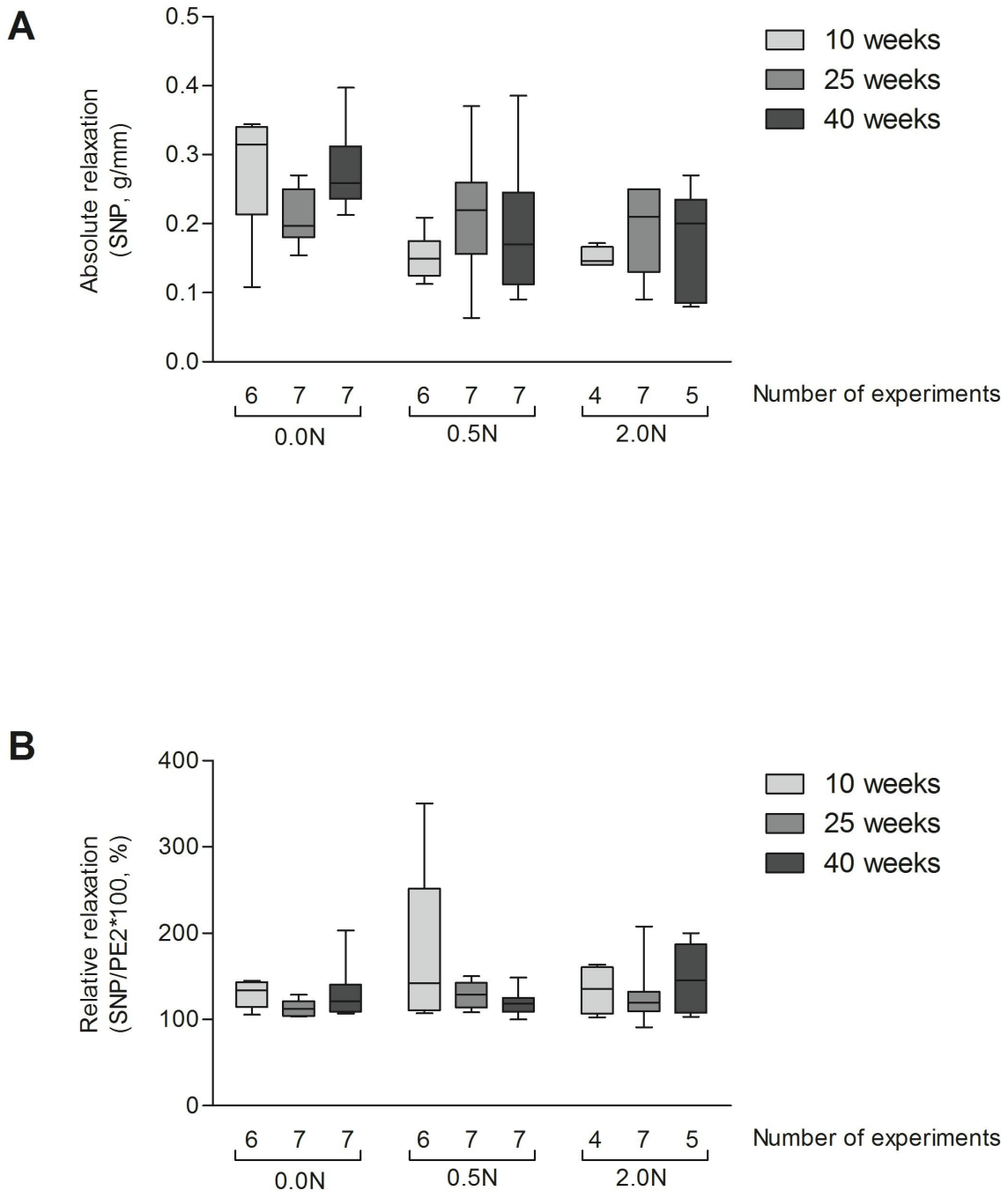

FIGURE 3.3: ENDOTHELIUM-INDEPENDENT RELAXATION AFTER *IN VIVO* CLAMPING IN MICE OF 10, 25 AND 40 WEEKS.

A: RELAXATION DUE TO SNP, EXPRESSED AS G/MM

B: PERCENTAGE OF RELAXATION BY SNP AFTER PE PRECONSTRICTION

DATA ARE DISPLAYED AS MEDIAN (IQR) AND WHISKERS SHOW MINIMUM AND MAXIMUM.

3.4.2. THE EFFECTS OF AGE

No significant difference for functional integrity in endothelium-dependent and –independent vasodilation is observed between mice of 10-weeks, 25-weeks and 40-weeks. Unclamped segments of 10-week, 25-week and 40-week old mice show no difference in PC before ACh addition ($p = 0.16$), absolute ($p = 0.57$) and relative relaxation ($p = 0.16$) to ACh, PC before SNP addition ($p = 0.30$) and absolute ($p = 0.062$) and relative relaxation ($p = 0.11$) to SNP. After clamping segments at 0.5N, less contraction of SMCs was observed, indicated by a lower PC value caused by PE before ACh addition ($p = 0.012$). No significant difference was observed for endothelium-dependent vasodilation (absolute ($p = 0.51$) and relative ($p = 0.29$)), PC before SNP addition ($p = 0.24$) and absolute ($p = 0.31$) and relative endothelium-independent relaxation ($p = 0.58$). Finally, segments clamped at 2.0N did not exhibit reduced PC caused by PE before ACh addition ($p = 0.25$), absolute ($p = 0.88$) and relative ($p = 0.48$) endothelium-dependent relaxation, PC before SNP addition ($p = 0.43$) and endothelium-independent relaxation (absolute ($p = 0.50$) and relative ($p = 0.80$)) (FIGURE 3.2 AND 3.3).

3.5. DISCUSSION

It has been described that mechanical manipulation of soft tissue causes damage[4–7] and that higher clamping forces induce higher tissue damage[2,3]. In this study, we tested the vascular integrity after *in vivo* clamping of thoracic mouse aortas for 2 minutes, a model for accidental unwanted force exertion, e.g. during robotic surgery. We hypothesized that *in vivo* clamping of a thoracic mouse aorta at a high load (2.0N) would cause more severe damage compared to segments clamped at a lower load (0.5N). These forces are relevant in the light that in preliminary experiments, 0.3N was just enough for artery occlusion.

Our results show that endothelium-dependent relaxation (tested by ACh) is reduced by *in vivo* aortic clamping up to 2.0N. The effect of *in vivo* force exertion on the endothelium is thus clearly demonstrated in our study. For the lower clamping level of 0.5N, as well as for the segments clamped at 2.0N, the effect of ACh is significantly diminished compared to the unclamped specimens. However, we did not find a statistically significant difference between clamping at the high (2.0N) and low (0.5N) level. This suggests that *in vivo* clamping at 0.5N already induces maximal damage to the endothelium.

Endothelium-independent vessel relaxation was studied by means SNP. Here, no statistical differences could be observed. We conclude that clamping up to 2.0N does not lead to a demonstrable effect on the SMCs, at least not in the conditions that we have tested. However, for the absolute relaxation by SNP, we can see a trend towards lower relaxation in the clamped segments. This effect is not seen for relative relaxation. This observation was also made by Famaey et al.[2] and can be explained by the fact that SNP as well as PE act directly on the SMCs and their effect is thus equally dependent on the amount of intact SMCs.

Aging influences all tissues of the body, including the cardiovascular system. It has been shown that functional integrity of the vascular endothelium deteriorates with age[19]. Aged SMCs show dysfunction[12,20]. Since mechanical manipulation of soft tissue may cause damage, we hypothesized that *in vivo* clamping of thoracic mouse aorta would cause more severe damage to middle-aged arteries compared to younger ones.

We observed a trend of diminished relaxation in response to ACh in 40 week old mice compared to the younger age groups, but this difference was not statistically significant. This could be explained by lack of power or the fact that the chosen age groups might be

too close together. An age group of mice older than 40 weeks could have shown other results.

In previous arterial clamping studies, clamp duration was chosen to be up to 15 minutes[3,21,22]. However, the tested specimens were carotid, coronary and femoral arteries. Babin-Ebell et al. studied aortic cross-clamping as we did and clamped for 30 minutes *ex vivo*[23]. Since our experiments are *in vivo*, we limited clamping time to avoid distal ischemia. During previous research in our lab, clamp duration was 2 minutes and here a representative load-damage curve was obtained for rat aorta[2]. A short clamping duration is also more relevant in the context of the larger framework of this study aiming to reduce accidentally induced damage during MIS by maneuvering surgical instruments to the desired location.

In general, previous clamping experiments studied the tissue response to different vascular clamps, or to different pinching forces induced by changing the amount of notch closure[2–7]. We used a tailored custom-made clamping device to load the arteries with a well-defined amount of force. This way a quantitative load-damage relation can be obtained. Note that this study has provided the relation between the macroscopic clamping force, expressed in Newtons, and the damage expressed as a percentage of functional integrity of the endothelium. To allow a more general interpretation and use of these values, i.e. intra- and extrapolation to other loading situations, a mathematical model describing the, not necessarily linear, load-damage relation on a local tissue level is required. Combining this mathematical model with the finite element method, the macroscopic loading as e.g. performed in the current experiments can be translated to a local tissue load value (*in casu* mechanical stress) and correlated to the experimentally obtained damage values. This will yield species- and tissue-specific damage parameters

for the mathematical model as a basis for the force limits that can be implemented on a robotic system to prevent accidental damage of tissues[24,25].

To summarize, we have shown that *in vivo* clamping of mice thoracic aorta at 0.5N or 2.0N induces endothelial damage. We could not find significantly different clamping damage in mice of 10 weeks, 25 weeks and 40 weeks of age. The next step in the research process will aim at expanding the current testing conditions, e.g. to study longterm effects of clamping and to obtain relevant load-damage data in transgenic mouse models, thereby investigating the effect of pathology on the damage mechanisms. Future work will also be directed towards the translation of these results obtained in small animals to larger animals and human samples, such that ultimately, the concept of safety thresholds can be brought into clinical practice.

3.6. REFERENCES

1. Rodriguez, E. & Chitwood, W. R. Robotics in cardiac surgery. *Scandinavian Journal of Surgery* **98,** 120–124 (2009).
2. Famaey, N. *et al.* In vivo soft tissue damage assessment for applications in surgery. *Med. Eng. Phys.* **32,** 437–43 (2010).
3. Margovsky, A. I., Chambers, A. J. & Lord, R. S. The effect of increasing clamping forces on endothelial and arterial wall damage: an experimental study in the sheep. *Cardiovasc. Surg.* **7,** 457–63 (1999).
4. Barone, G. W., Conerly, J. M., Farley, P. C., Flanagan, T. L. & Kron, I. L. Assessing clamp-related vascular injuries by measurement of associated vascular dysfunction. *Surgery* **105,** 465–471 (1989).
5. Hangler, H., Mueller, L., Ruttmann, E., Antretter, H. & Pfaller, K. Shunt or snare: coronary encothelial damage due to hemosttic devices for beating heart coronary surgery. *Ann. Thorac. Surg.* **86,** 1873–7 (2008).
6. Slayback, J. B., Bowen, W. W. & Hinshaw, D. B. Intimal injury from arterial clamps. *Am. J. Surg.* **132,** 183–188 (1976).
7. Vural, A. H. *et al.* Intracoronary Shunt Versus Bulldog Clamp in Off-Pump Bypass Surgery. Endothelial Trauma: Shunt Versus Clamp. *J. Surg. Res.* **150,** 261–265 (2008).
8. Margovsky, A. I., Lord, R. S. & Chambers, A. J. The effect of arterial clamp duration on endothelial injury: an experimental study. *Aust. N. Z. J. Surg.* **67,** 448–451 (1997).
9. Ungvari, Z., Kaley, G., de Cabo, R., Sonntag, W. E. & Csiszar, A. Mechanisms of vascular aging: New perspectives. *J. Gerontol. A. Biol. Sci. Med. Sci.* **65 A,** 1028–1041 (2010).

10. Asai, K. *et al.* Peripheral vascular endothelial dysfunction and apoptosis in old monkeys. *Arterioscler. Thromb. Vasc. Biol.* **20,** 1493–1499 (2000).

11. Lévy, B. I. Artery changes with aging: degeneration or adaptation? *Dialogues Cardiovasc. Med.* **6,** 104–111 (2001).

12. Ferrari, A. U., Radaelli, A. & Centola, M. Invited review: aging and the cardiovascular system. *J. Appl. Physiol.* **95,** 2591–2597 (2003).

13. Fry, D. L. Mass transport, atherogenesis, and risk. *Arteriosclerosis* **7,** 88–100 (1987).

14. Gerrity, R. G. & Cliff, W. J. The aortic tunica intima in young and aging rats. *Exp. Mol. Pathol.* **16,** 382–402 (1972).

15. Haudenschild, C. C., Prescott, M. F. & Chobanian, A. V. Aortic endothelial and subendothelial cells in experimental hypertension and aging. *Hypertension* **3,** I148–53 (1981).

16. Guyton, J. R., Lindsay, K. L. & Dao, D. T. Comparison of aortic intima and inner media in young adult versus aging rats. Stereology in a polarized system. *Am. J. Pathol.* **111,** 234–246 (1983).

17. Hariri, R. J. *et al.* Aging and arteriosclerosis. Cell cycle kinetics of young and old arterial smooth muscle cells. *Am. J. Pathol.* **131,** 132–136 (1988).

18. Wang, J. C. & Bennett, M. Aging and atherosclerosis: Mechanisms, functional consequences, and potential therapeutics for cellular senescence. *Circulation Research* **111,** 245–259 (2012).

19. Seals, D. R., Jablonski, K. L. & Donato, A. J. Aging and vascular endothelial function in humans. *Clin. Sci. (Lond).* **120,** 357–375 (2011).

20. Yildiz, O. Vascular smooth muscle and endothelial functions in aging. in *Annals of the New York Academy of Sciences* **1100,** 353–360 (2007).

21. Darçin, O. T. *et al.* Pressure-controlled Vascular Clamp: A Novel Device for Atraumatic Vessel Occlusion. *Ann. Vasc. Surg.* **18,** 254–256 (2004).

22. Hsi, C. *et al.* Experimental coronary artery occlusion: relevance to off-pump cardiac surgery. *Asian Cardiovasc. Thorac. Ann.* **10,** 293–7 (2002).

23. Babin-Ebell, J., Gimpel-Henning, K., Sievers, H.-H. & Scharfschwerdt, M. Influence of clamp duration and pressure on endothelial damage in aortic cross-clamping. *Interact. Cardiovasc. Thorac. Surg.* **10,** 168–71 (2010).

24. Famaey, N., Vander Sloten, J. & Kuhl, E. A three-constituent damage model for arterial clamping in computer-assisted surgery. *Biomech. Model. Mechanobiol.* **12,** 123–136 (2013).

25. Famaey, N., Sommer, G., Vander Sloten, J. & Holzapfel, G. A. Arterial clamping: Finite element simulation and in vivo validation. *J. Mech. Behav. Biomed. Mater.* **12,** 107–118 (2012).

CHAPTER IV

THE QUEST FOR A SUITABLE ATHEROSCLEROSIS MODEL

4.1. ABSTRACT

4.1.1. BACKGROUND

To investigate whether atherosclerotic arteries show a different response to mechanical clamping, a good animal model is needed. While insulin-resistant JCR:LA-*cp* rats show only poor atherosclerosis development, low density lipoprotein receptor (*LDLR*) knockout mice develop advanced atherosclerotic lesions when fed western diet[1]. In the first phase of this project we set up breeding of this strain and optimized the genotyping protocol. Also, we investigated which length of western diet feeding corresponds to the extent of pathology development in male *LDLR-/-* mice we need for this study.

4.1.2. METHODS

Polymerase chain reaction and gel electrophoresis were performed to genotype the mice. Mac-3 and sirius red staining allowed assessment of the extent of atherosclerosis development throughout the vasculature. We compared the pathology in mice fed western diet for 7, 14, 19 and 24 weeks, started at 5 weeks of age.

4.1.3. RESULTS

Genotyping confirmed full knockout of the *LDLR* gene in all mice. Analysis of the histologic stainings showed mature atherosclerotic lesion formation at the aortic valves and aortic arch of mice that were fed western diet for 14, 19 and 24 weeks. On these time points, fatty streaks and beginning atherosclerosis lesions were detected throughout the descending thoracic aorta.

4.1.4. CONCLUSIONS

Since 14 weeks of western feeding results in obvious atherosclerosis development in male *LDLR-/-* mice we decided to define the optimal length of western diet feeding for our experiments as 15 weeks, starting from 5 weeks of age.

4.2. INTRODUCTION

A wide variety of **animal models** are available to gain insight in molecular pathway regulation, genetic defects and other underlying causes of human CVDs. While pigs are expensive, require large housing space, and are difficult to genetically modify, their size facilitates noninvasive measurements of arteries, and they have a human-like lipoprotein profile. Nonhuman primates share the (dis)advantages of pigs. The species most susceptible to dietary cholesterol overload is the rabbit[2]. Especially Watanabe hereditary hypercholesterolemic rabbits fed a cholesterol-rich diet develop lesions very similar to the pathology observed in homozygous familial hypercholesterolemic patients. Transgenic rabbits have been generated[3], but genetic modification remains easier in mice.

Preliminary experiments in our research group had gained insight in the response of rat arteries to mechanical clamping[4]. Therefore, we decided to use the insulin-resistant **JCR:LA-*cp* rat** to investigate the influence of pathology on the relationship between arterial clamping and induced damage. This rat strain incorporates the autosomal recessive *cp*-gene, which leads to development of obesity and profound insulin resistance in homozygotes (cp:cp) that closely resembles the condition in humans[5]. Although it has been suggested that high plasma insulin levels are involved in the pathogenesis of atherosclerosis[6], this statement has not been universally accepted[7]. And indeed, preliminary observations in our center showed the absence of atherosclerotic lesions in the JCR:LA-*cp* rat arteries (8-9 weeks of age) despite the published reports that claim otherwise. Therefore, this animal model did not comply with our study aim and we decided to perform our experiments in mice.

The availability of transgenic mouse models makes mice very valuable for basic research studies, especially since they are also relatively easy to handle and breading costs are low[2]. Despite these advantages, it is important to keep the **differences between mouse and human** atherosclerosis in mind. In humans, it takes years for atherosclerosis to develop, and the lesions are most prominent in the aortic arch, the carotids and the coronary arteries. On the contrary, atherosclerotic plaques in genetically modified mice develop over a time frame of months and are mainly located in the aortic arch and sinus, as well as in the innominate artery. This may (partly) be due to the much higher heart rate in mice (> 400 bpm) than humans (70-100 bpm) and hence disturbed blood flow. Total normal plasma cholesterol in mice (50-100 mg/dl) is also lower compared to humans (150-300 mg/dl). Additionally, while low density lipoprotein (LDL) is the major lipoprotein in humans, in mice this is HDL[2]. The presence of high plasma levels of anti-atherogenic HDL and low levels of VLDL and LDL causes wildtype mice to be quite resistant to the development of CVD. Therefore, murine atherosclerotic models are based on generating a non-HDL characterized hypercholesterolemia, induced by genetic modification and/or western-type diet feeding. From the available genetic mouse backgrounds, C57BL/6J has been shown to be most susceptible to atherosclerotic lesion formation[8,9].

One of the frequently used mouse models is a mouse knockout for apolipoprotein E (***ApoE***), a component of very low density lipoprotein (VLDL) which has a role in its clearance from the plasma. Spontaneous plaque formation is observed in *ApoE* knockout mice. Feeding these mice a high-fat diet accelerates pathology development and more severe atherosclerotic lesions will be present. However, an important shortcoming of the *ApoE* knockout mouse model is that their lipoprotein profiles are dissimilar to those

in humans. While human cholesterol is mainly contained in LDL particles, cholesterol in *ApoE-/-* mice is mostly found in VLDL/IDL (intermediate-density lipoprotein) fractions. Moreover, since ApoE has numerous other known functions affecting Mφ biology, immune function and adipose tissue biology[2], defects in its gene could influence other mechanisms and thus complicate result interpretation.

Human type II hyperlipoproteinemia or familial hypercholesterolemia is the most common genetic hyperlipidemic disorder. It is characterized by elevated plasma LDL levels because defects in the gene coding for the **LDLR** results in defective clearance of LDL. LDL binding to the LDLR (with 1:1 stoichiometry) involves a specific area of the apoB molecule termed the LDL receptor binding domain. Once the LDL particle is internalized into hepatocytes, it is trafficked and catabolized within various endosomes/lysosomes and the cholesterol enters a for the most part nonexchangeable pool where it is re-esterified and used to lipidate nascent ApoB-VLDL precursor particles[10]. Elimination of the *LDLR* gene in mice fed western-type diet results in elevated cholesterol levels, mainly in the IDL/LDL fraction, so this mouse model resembles the human plasma lipoprotein profile better than the *ApoE* knockout mice. Also, LDLR does not have a large variety of functions besides lipoprotein uptake and clearance. Furthermore, arterial lesions in human familial hypercholesterolemia share some characteristics with mouse lesions like plaque formation at the aortic valves and root[2]. However, lipoproteins containing ApoB48 can still be cleared via the low-density lipoprotein receptor-related protein (LRP), resulting in only modest development of atherosclerosis[11]. Given these significant advantages, we wanted to evaluate if the *LDLR-/-* strain would develop atherosclerotic lesions and hence would be useful for our

studies. Additionally, we wanted to evaluate at which time point mice should be assessed as we need to optimize the presence of lesions and the time/ cost of housing.

4.3. MATERIAL AND METHODS

4.3.1. BREEDING

All animal experiments were approved by the animal ethics committee of the KU Leuven (project P009/2011). Breeding pairs of the B6.129S7-Ldlrtm1Her/J mouse strain (The Jackson Laboratory, Stock #2207, C57BL/6J background) were housed in a 12-hour light/dark cycle and fed at libitum. Male offspring was genotyped (see 4.3.2) and fed standard chow at libitum. At 5 weeks of age, diet was changed to western diet (Ssniff® EF R/M acc. TD88137 mod.), which induces atherosclerotic lesion formation in these knockout animals throughout the arterial tree[1]. 4 mice were sacrificed, each at a different time point (7, 14, 19 and 24 weeks of western diet feeding) to assess atherosclerosis development (see 4.3.3) and optimize the period of western diet feeding for our study design.

4.3.2. GENOTYPING

DNA purification Tails (5mm) were cut and incubated overnight in 300µl lysis buffer containing 3µl proteinase K (55°C). After thorough shaking the lysate was centrifuged (10min, 14000rpm) and the supernatant was poured in 600µl isopropanol. This mixture was shaken and centrifuged (10min, 14000rpm), followed by dissolving the pellet in 250µl distilled water and incubation at 55°C for 2 hours.

Polymerase chain reaction (PCR) The *LDLR* gene is knocked out via the insertion of a neomycin resistance cassette. Therefore, two PCRs were performed, with primers for the *LDLR* and neomycin (*Neo*) resistance gene respectively. For every sample the following components were added: 10µl GoTaq® G2 Hot Start Green Master Mix

(Promega), 1µl forward primer (10µM), 1µl reverse primer (10µM), 5.5µl RNase-free H_2O, and 0.5µl dimetylsulfoxide (DMSO). Primers were ordered from Invitrogen. Their sequences and the PCR conditions are specified in TABLE 4.1.

TABLE 4.1: PRIMER SEQUENCES AND PCR CONDITIONS FOR THE LOW DENSITY LIPOPROTEIN RECEPTOR (*LDLR*) AND NEOMYCIN (*NEO*) PRIMER SETS. FW: FORWARD PRIMER, RV: REVERSE PRIMER

LDLR	NEO
FW 5' CCA TAT GCA TCC CCA GTC TT 3'	FW 5' CCA TAT GCA TCC CCA GTC TT 3'
RV 5' GCG ATG GAT ACA CTC ACT GC 3'	RV 5' AAT CCA TCT TGT TCA ATG GCC GAT C 3'
94°C 5'	94°C 5'
35x { 95°C 30"	95°C 1'
65°C 30"	60°C 1' } 35x
72°C 30"	72°C 1'
72°C 10'	72°C 10'
4°C ∞	4°C ∞

Gelelectrophoresis The PCR product and Eurogentec SmartLadder SF (100 to 1000 bp) were loaded on a 2% agarose gel (4µl ethidium bromide per 100 ml 1x TAE buffer[1]), followed by electrophoresis (Biorad PowerPac 300, 1x Tris-acetaat-EDTA buffer, 115V, 30min). The DNA was visualized using UV light (Biorad Gel Doc 2000). The neomycin complex is 720bp and the LDLR complex 383bp. TABLE 4.2 summarizes the possible results.

TABLE 4.2: POSSIBLE OUTCOME COMBINATIONS OF THE GELELECTROPHORESIS. BP: BASE PAIRS

Signal		Genotype
LDLR (383bp)	NEO (720bp)	
Yes	No	LDLR +/+
Yes	Yes	LDLR +/-
No	Yes	LDLR -/-

[1] 50x TAE buffer (500 ml): 121 g Tris (Trizma-base MW= 121,14) + 28,55 ml acetic acid (99-100%) + 9,306 g EDTA (Kestranal MW=372,24). Adjust pH = 8 with NaOH.

4.3.3. HISTOLOGY

Mice were anesthetized with Domitor® (0.5mg/kg) and Ketamine (50mg/kg), intubated and ventilated with room air (270µl stroke volume, 125 strokes/min). Rectal temperature was kept at 37°C. The heart, aortic arch and thoracic aorta descendens were excised and fixated overnight in paraformaldehyde (4%), followed by dehydration (Histokinette, Microm STP120[2]) and embedding in paraffin. Serial cross-sections of the aortic root and thoracic aorta descendens (7µm, 10 slides) and longitudinal sections of the aortic arch (7µm, 10 slides) were made (Medite TES 99), which were stained afterwards.

Macrophages: Mac-3 staining After hydration (2 x 5' Xylol, 3' ethanol (EtOH) 100%, 3' EtOH 96%, 3' EtOH 70%, 3' EtOH 50%, 3' distilled water) and antigen retrieval (Target Retrieval Solution, DAKO, 95°C, 20'), endogenous peroxidases were blocked (600µl H_2O_2 + 200ml methanol). Nonspecific sites were blocked with rabbit serum (PIR, DAKO, 1/5, 45') before primary antibody (Rat-anti-Mac-3, Becton-Dickinson, 1/50) was applied overnight. The next day, secondary antibody (Rabbit-anti-Rat-B, DAKO, 1/300) was applied for 45 minutes and the signal was amplified using the Biotinyl Tyramide TSA kit from Perkin Elmer. The antigen-antibody complex was visualized by 3,3'-Diaminobenzidine (DAB) and H_2O_2 and slides were mounted using DPX (Sigma-Aldrich).

Collagen: Sirius Red staining After hydration (see Mac-3 staining), 10' of immersion in tapwater and 5' in distilled water were followed by 90' immersion in Sirius red solution (200ml distilled water, 8g picric acid (PANREAC QUIMICA, S.A.), 0.2g direct red (Sigma Aldrich)). Next, slides are rinsed (2' HCl, (0.01N) and dehydrated, 45" EtOH 70%, 2 x 5' EtOH 100%, 2 x 5' Xylol) and mounted with DPX.

[2] 1h EtOH 70%, 2x1h EtOH 96%, 2h EtOH 100%, 3h EtOH 100%, 2h Xylol/EtOH 100%, 2x3h Xylol, 2h paraffin, 2x3h paraffin

4.4. RESULTS & DISCUSSION

Genotyping confirmed full knockout of the *LDLR* gene in all mice. The collagen (Sirius red) and Mφ (Mac-3) stainings after 7, 14, 19 and 24 weeks of western diet feeding were analyzed. While mouse arteries did show evolved atherosclerotic lesions after 7 weeks of diet (FIGURE 4.1), 14 or more weeks of western diet feeding resulted in mature atherosclerotic plaque formation at the aortic sinuses and the aortic arch. It is avoided to clamp human arteries on locations with extensive atherosclerosis during surgery. Therefore it is beneficial that in the descending thoracic aorta of our mouse model only fatty streaks and less evolved lesions were detected after 14 weeks of western diet feeding. Representative images of the Mac-3 and Sirius red staining of the 14 weeks condition are displayed in FIGURE 4.2. To ensure both pathology extent and cost-effectivity, we concluded to feed the *LDLR-/-* mice for the clamping study (see chapter V) western diet for 15 weeks, starting from 5 weeks of age.

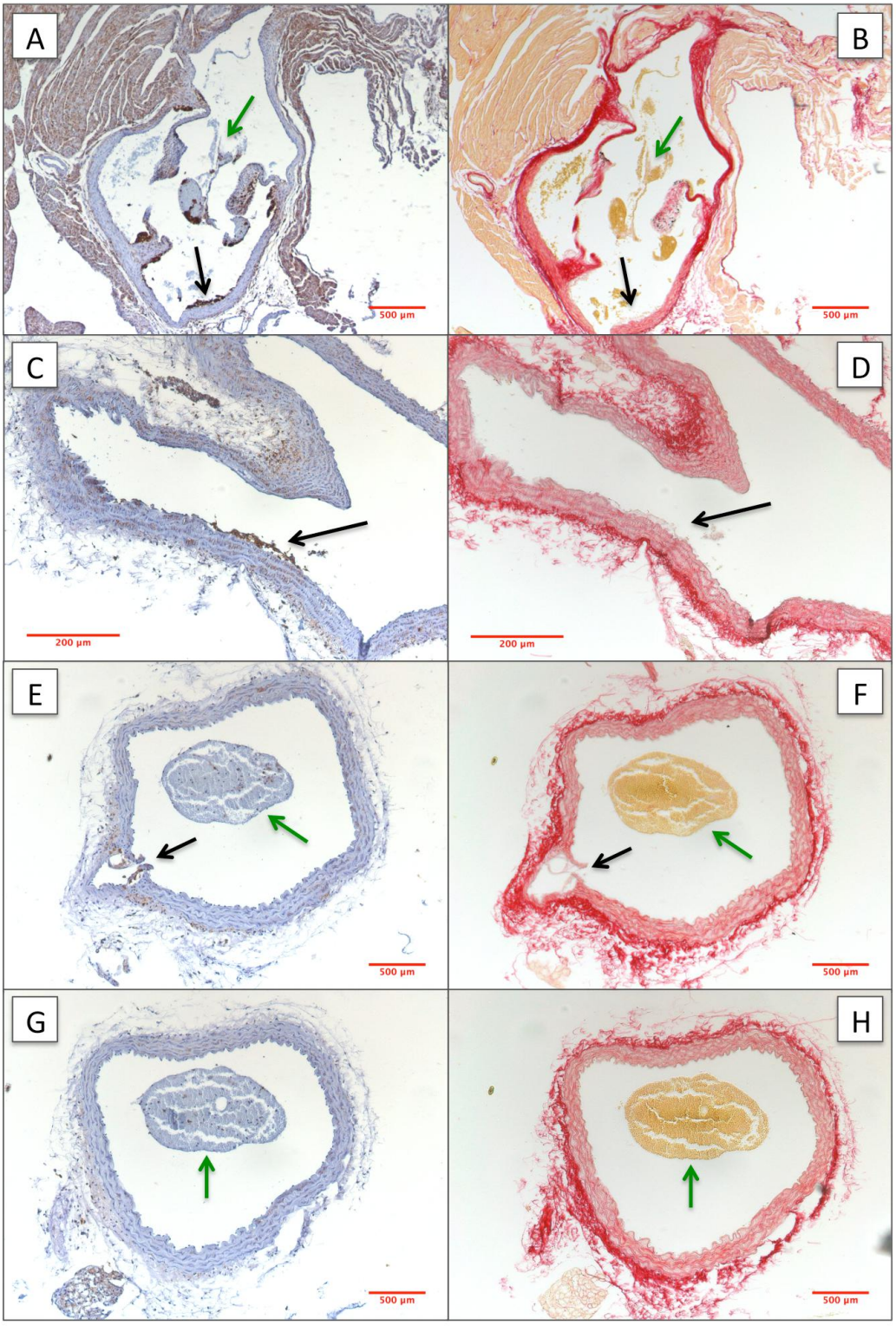

FIGURE 4.1: PARAFFIN SECTIONS (7µM) OF THE CARDIOVASCULAR TISSUE OF A MALE *LDLR*-/- MOUSE AFTER 7 WEEKS OF WESTERN DIET FEEDING. LEFT: MAC-3 STAINING; RIGHT: SIRIUS RED STAINING; A-B: HEART CROSS SECTIONS; C-D: AORTIC ARCH LONGITUDINAL SECTIONS; E-F: THORACIC DESCENDING AORTA; G-H: THORACIC DESCENDING AORTA AT INTERCOSTAL BRANCH. BLACK ARROWS SHOW ATHEROSCLEROTIC LESIONS, GREEN ARROWS SHOW BLOOD REMAINS.

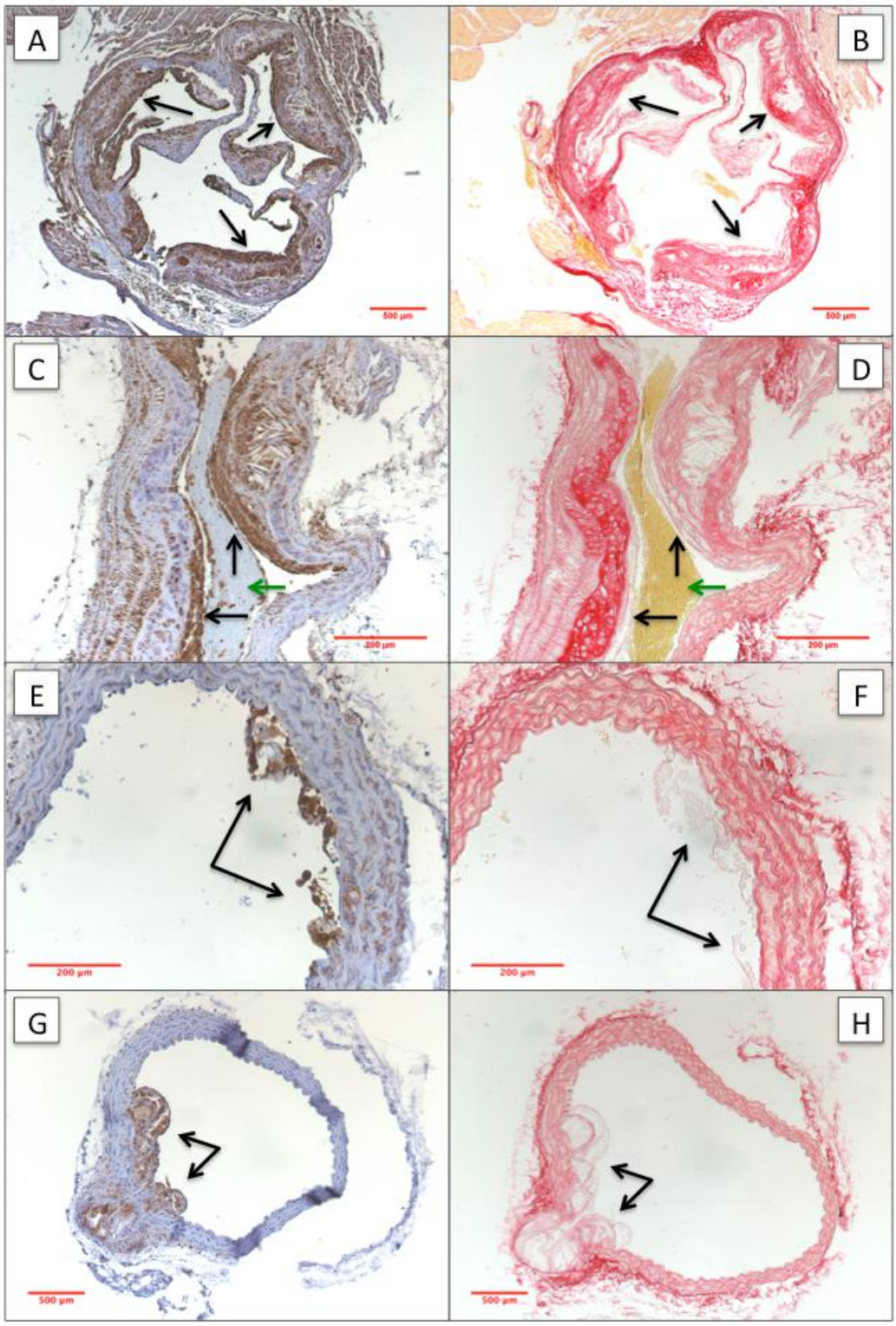

FIGURE 4.2: PARAFFIN SECTIONS (7µM) OF THE CARDIOVASCULAR TISSUE OF A MALE *LDLR*-/- MOUSE AFTER 14 WEEKS OF WESTERN DIET FEEDING. LEFT: MAC-3 STAINING; RIGHT: SIRIUS RED STAINING; A-B: HEART CROSS SECTIONS; C-D: AORTIC ARCH LONGITUDINAL SECTIONS; E-F: THORACIC DESCENDING AORTA; G-H: THORACIC DESCENDING AORTA AT INTERCOSTAL BRANCH. BLACK ARROWS SHOW ATHEROSCLEROTIC LESIONS, GREEN ARROWS SHOW BLOOD REMAINS.

4.5. REFERENCES

1. Ishibashi, S. *et al.* Hypercholesterolemia in low density lipoprotein receptor knockout mice and its reversal by adenovirus-mediated gene delivery. *J. Clin. Invest.* **92,** 883–93 (1993).

2. Getz, G. S. & Reardon, C. A. Animal models of atherosclerosis. *Arterioscler. Thromb. Vasc. Biol.* **32,** 1104–15 (2012).

3. Brousseau, M. E. & Hoeg, J. M. Transgenic rabbits as models for atherosclerosis research. *J. Lipid Res.* **40,** 365–375 (1999).

4. Famaey, N. *et al.* In vivo soft tissue damage assessment for applications in surgery. *Med. Eng. Phys.* **32,** 437–43 (2010).

5. Richardson, M. *et al.* Vasculopathy and insulin resistance in the JCR:LA-cp rat. *Atherosclerosis* **138,** 135–146 (1998).

6. Uusitupa, M. I., Niskanen, L. K., Siitonen, O., Voutilainen, E. & Pyorala, K. 5-year incidence of atherosclerotic vascular disease in relation to general risk factors, insulin level, and abnormalities in lipoprotein composition in non-insulin-dependent diabetic and nondiabetic subjects. *Circulation* **82,** 27–36 (1990).

7. Savage, P. J. & Saad, M. F. Insulin and atherosclerosis: Villain, accomplice, or innocent bystander? *British Heart Journal* **69,** 473–475 (1993).

8. Wouters, K., Shiri-Sverdlov, R., van Gorp, P. J., van Bilsen, M. & Hofker, M. H. Understanding hyperlipidemia and atherosclerosis: Lessons from genetically modified apoe and ldlr mice. *Clinical Chemistry and Laboratory Medicine* **43,** 470–479 (2005).

9. Oosterlinck, W., Vanderper, A., Flameng, W. & Herijgers, P. Glucose tolerance and left ventricular pressure-volume relationships in frequently used mouse strains. *J. Biomed. Biotechnol.* **2011,** 281312 (2011).

10. Biomarker Bliki (A service from the foundation for health improvement & technology) - http://www.biomarkerbliki.org/articles/4#/section/14.

11. Ji, Z. S., Fazio, S., Lee, Y. L. & Mahley, R. W. Secretion-capture role for apolipoprotein E in remnant lipoprotein metabolism involving cell surface heparan sulfate proteoglycans. *J. Biol. Chem.* **269,** 2764–2772 (1994).

CHAPTER V

ATHEROSCLEROSIS ALTERS LOADING-INDUCED ARTERIAL DAMAGE: IMPLICATIONS FOR ROBOTIC SURGERY

Submitted for publication in '*The Annals of Thoracic Surgery*'

Geenens R, Famaey N, Gijbels A, Verhelle S, Vinckier S, Vander Sloten J, Herijgers P

5.1. ABSTRACT

5.1.1. BACKGROUND

Lack of intra-operative haptic information during robotic surgery increases the risk for unintended tissue overload and damage. Knowledge about the acute and chronic fundamental relationship between force load and induced damage in healthy and diseased arteries is crucial to enable intra-operative haptic feedback or shared autonomy and improve patient safety.

5.1.2. METHODS

Arteries of wildtype and atherosclerotic mice were clamped *in vivo* for 2 minutes (0.0N, 0.6N or 1.27N). Histological analysis (Verhoeff's-Van Gieson, Osteopontin, CD45, CD105) was performed immediately, or after 6 hours, 2 weeks or 1 month. Endotheliumdependent and –independent vasodilatation were assessed immediately or 1 month after clamping.

5.1.3. RESULTS

Endotheliumdependent vasodilatation is worse after clamping of wildtype arteries, but is restored after one month. Clamping also results in flattening of the innermost elastic membrane of both genotypes, which is reversed over time for wildtype arteries but not for vessels from atherosclerotic mice. Higher osteopontin content in wildtype and *LDLR-/-* mice after 2 weeks suggests a phenotypic switch of the medial SMCs, an effect that is reversed after 1 month. While inflammation in the intima diminishes, medial CD45 content rises through time in both genotypes. CD105 staining shows that even manipulation without clamping results in EC loss in both *LDLR+/+* and *LDLR-/-* mice.

5.1.4. CONCLUSIONS

Arterial clamping induces different acute and long-term injury to the vessel wall of atherosclerotic and healthy arteries.

5.2. INTRODUCTION

The last decades, researchers and clinicians are developing new surgical instrumentation including robotics and implementing minimally invasive techniques to improve patient safety and satisfaction[1]. MIS is increasingly used because it limits invasiveness and tissue damage. However, surgeon feedback regarding the interaction forces between surgical instruments and tissue is worse or even completely absent during RMIS[2]. This increases the risk of undetected tissue overload that can inflict collateral damage on microscopic and even macroscopic level[3]. Tissue outside the visual field is at highest risk of accidental mechanical overload.

Therefore, it is important to determine safety thresholds above which the induced damage is unacceptable (defined as permanent and/or having irreversible consequences). Implementing these safety thresholds in robotic instruments with shared autonomy to avoid tissue overload might importantly increase surgical safety using robotic systems. Defining these thresholds requires knowledge on the quantitative relation between mechanical loading and tissue damage. In our domain intentionally clamping, or accidentally compressing arteries by instruments is an occasionally occurring condition, on which we focused. The effects of different vascular clamps and ligatures on blood vessels have been studied by several research groups. It was shown histologically and functionally that higher clamping or compression forces induce higher tissue damage[3–8] and that the extent of damage is partly time-dependent[9]. Nevertheless, a defined quantitative relation between clamping load and induced damage for mice thoracic aortas is still lacking. Furthermore, few studies focus on the long term effects of arterial clamping[10–12]. Since we define unacceptable damage as irreversible, we aim to study the intermediate term effects of well-defined clamping loads in surviving subjects.

This enabled us to investigate whether possible acute clamping-induced damage could be resolved or not.

At present, it is insufficiently known whether these safety thresholds are influenced by age or pathology, in other words, whether patient-specific safety thresholds should be implemented in robotic devices to avoid tissue overload. In our research we aimed to study the effect of age and atherosclerosis on load-induced aortic damage in well-controlled experimental mouse models, well known by our group. We have previously shown that clamping thoracic mouse aortas up to 2.0N (6 times the minimal occlusion force)[3] induces damage in C57BL/6J mice of 10, 25 and 40 weeks of age, without important differences in vascular wall response between these age groups[13]. Since a large proportion of patients undergoing surgery suffer from atherosclerosis, in this study we investigated an LDL receptor knock-out mouse model with the same genetic background, that develops atherosclerotic lesions throughout the arterial tree when fed a western diet[14].

In this chapter, acute and long-term effects of *in vivo* arterial clamping are quantified in wildtype and atherosclerotic mice. Clamps were not positioned on mature lesions. These results could be of clinical importance to ensure proper patient-specific safety during robotic MIS.

5.3. MATERIAL AND METHODS

5.3.1. ANIMALS

All animal experiments were approved by the ethical committee of the KU Leuven (project P009/2011). Mice were housed in a 12-hour light/dark cycle and were fed at libitum. Only male animals were used to avoid inter-gender differences. C57BL/6J mice knockout for the *LDLR* were used, which were fed a western diet (Ssniff® EF R/M acc.

TD88137 mod.) for 15 weeks, starting from 5 weeks of age[14]. All animals were genotyped to assure homozygous knockout of the *LDLR* (forward: 5'-CCATATGCATCCCCAGTCTT-3', reverse wildtype: 5'-GCGATGGATACACTCACTGC-3', reverse knockout: 5'-AATCCATCTTGTTCAATGGCCGATC-3', see chapter V). As wildtype control animals we used *LDLR+/+* mice, fed standard chow for 20 weeks.

5.3.2. SURGICAL PROCEDURE

Different animals were used for functional en histological tests. 108 *LDLR+/+* and 108 *LDLR-/-* mice (6 mice per condition, see TABLE 5.1 for an overview of the different experiments) of 20 weeks were anesthetized (intraperitoneally, medetomidine 0.5mg/kg, Orion Pharma and ketamine 50mg/kg, Eurovet), intubated and ventilated (250µl stroke volume, 140 strokes/min). Rectal temperature was kept at 37°C.

TABLE 5.1: OVERVIEW OF THE EXPERIMENTS THAT WERE CONDUCTED IN C57BL/6J *LDLR+/+* AND *LDLR-/-* MICE.

		TIME POINT					
		Acute		6 hours	2 weeks	1 month	
		Histology	Function	Histology	Histology	Histology	Function
LOAD	0.0N	n=6	n=6	n=6	n=6	n=6	n=6
	0.6N	n=6	n=6	n=6	n=6	n=6	n=6
	1.27N	n=6	n=6	n=6	n=6	n=6	n=6

Through a left thoracotomy, the descending thoracic aorta was carefully isolated from surrounding tissue and either used as a control sample (unclamped, 0.0N) or clamped *in vivo* for 2 minutes with a microvascular clamp at 0.6N (FST, 18055-01) or 1.27N (FST, 18055-02) (TABLE 5.1). The clamping jaws (2mm wide) are not serrated to allow homogenous distribution of the clamping forces. Afterwards, the clamp was removed and segments of the aorta were either immediately excised or the chest was closed. In

the latter case, the aortic segment was excised 6 hours, 2 weeks or 1 month after initial clamping (TABLE 5.1, anesthesia as described above). Excised segments were either tested for functional integrity or used for histological analysis.

5.3.3. FUNCTIONAL INTEGRITY TESTING

For functional integrity tests, the aortic segments (1.68 ± 0.24 mm in length) were mounted in a water-jacketed organ chamber containing Krebs solution (Sigma-Aldrich, in mM: NaCl 118.3, KCl 4.7, KH_2PO_4 1.2, $MgSO_4$ 1.2, $NaHCO_3$ 25, Na_2Ca EDTA 0.026, Glucose 5.5, $CaCl_2$ 2.5) at 37°C, aerated by 95% O_2/ 5% CO_2. Tension was measured isometrically with calibrated Type 375 force transducers (Hugo Sachs Elektronics) connected to a data acquisition system (NI-USB-6009, National Instruments). Segments were gradually stretched over 1 hour until a stable preload of 20 mN was reached. This preload was defined as optimal in preliminary tests, in which segment response to 40 mmol/l K^+ was recorded (data not shown). After preload adjustment, PC was induced by PE (Sigma-Aldrich, 10^{-6}M, 20 minutes). Subsequent cumulative addition of ACh (Sigma-Aldrich, 10^{-9}M to 10^{-5}M) during 30 minutes allowed assessment of endothelium-dependent vasodilation, expressed as % reversal of PE-induced constriction. The segment was washed 3 times with fresh Krebs solution. Afterwards, endothelium-independent vasodilation was examined by adding a direct NO donor (SNP, Fluka, 10^{-9}M to 10^{-5}M) during 30 minutes following PC by PE (10^{-6}M, 20 minutes).

5.3.4. HISTOLOGICAL ANALYSIS

Excised segments were fixated overnight in paraformaldehyde (4%), followed by dehydration (Medite TES 99) and embedding in paraffin. Serial cross-sections (7µm, 10 series) were made (Microm HM360). Stainings described below were examined using a Zeiss Axioplan 2 microscope and pictures are obtained with an Axiocam MRc5 camera.

ECs: CD105 Hydration is followed by antigen retrieval (Target Retrieval Solution, DAKO) and block of endogenous peroxidases. After application of rabbit serum (45', 1/5, DAKO X0902) to block nonspecific sites, primary antibody is incubated overnight (1/50, Goat anti-CD105, R&D AF1320). The next day, biotinylated secondary antibody containing 10% mouse serum (Sigma) is applied (45', 1/300, RaG-B, DAKO) followed by amplification of the signal (TSA Cyanine3 System, Perkin Elmer NEL704A001KT). Slides were mounted using ProLong® Gold Antifade Mountant with DAPI (Invitrogen P36935). Every section was divided in four quadrants, each of which was scored in a blinded manner (1: no fluorescence (FIGURE 5.1A), to 5: maximal fluorescence (FIGURE 5.1B)) for the staining intensity in the intima. Quadrant scores were averaged and used for analysis of endothelium presence.

Elastic membranes: Verhoeff's-Van Gieson After hydration, slides were immersed in fresh Verhoeff's elastic staining solution (as described in [15]) for 22', rinsed and immersed in 2% $FeCl_3$ (2'15"), followed by rinsing and 2' EtOH 95%. Then, slides were immersed in Van Gieson solution (Prosan) for 6'. After dehydration slides were mounted with DPX (Klinipath). The curved as well as straight-through length of the innermost elastic membrane were measured (blinded, ImageJ). The ratio (straight length divided by curved length) was used as a value for the amount of flattening: a value of 1 would mean a completely flat membrane.

Inflammation: CD45 After hydration and antigen retrieval (Target Retrieval Solution, DAKO), endogenous peroxidases were blocked. Nonspecific sites were blocked with goat serum (45', 1/5, DAKO) before primary antibody was applied overnight (1/100, Rat anti CD45, BD Pharmingen 553075). Next day, biotinylated secondary antibody was applied for 45' (1/100, GaRat-B, BD Pharmingen 559286) and the signal

was amplified (TSA Cyanine3 System, Perkin Elmer NEL704A001KT). Slides were mounted using ProLong® Gold Antifade Mountant with DAPI (Invitrogen P36935). Every section was divided in four quadrants, each of which was scored in a blinded manner (1: no fluorescence (FIGURE 5.1C), to 6: maximal fluorescence (FIGURE 5.1D)) for the staining intensity. Intima and media quadrant scores were averaged separately and used for analysis of inflammation content.

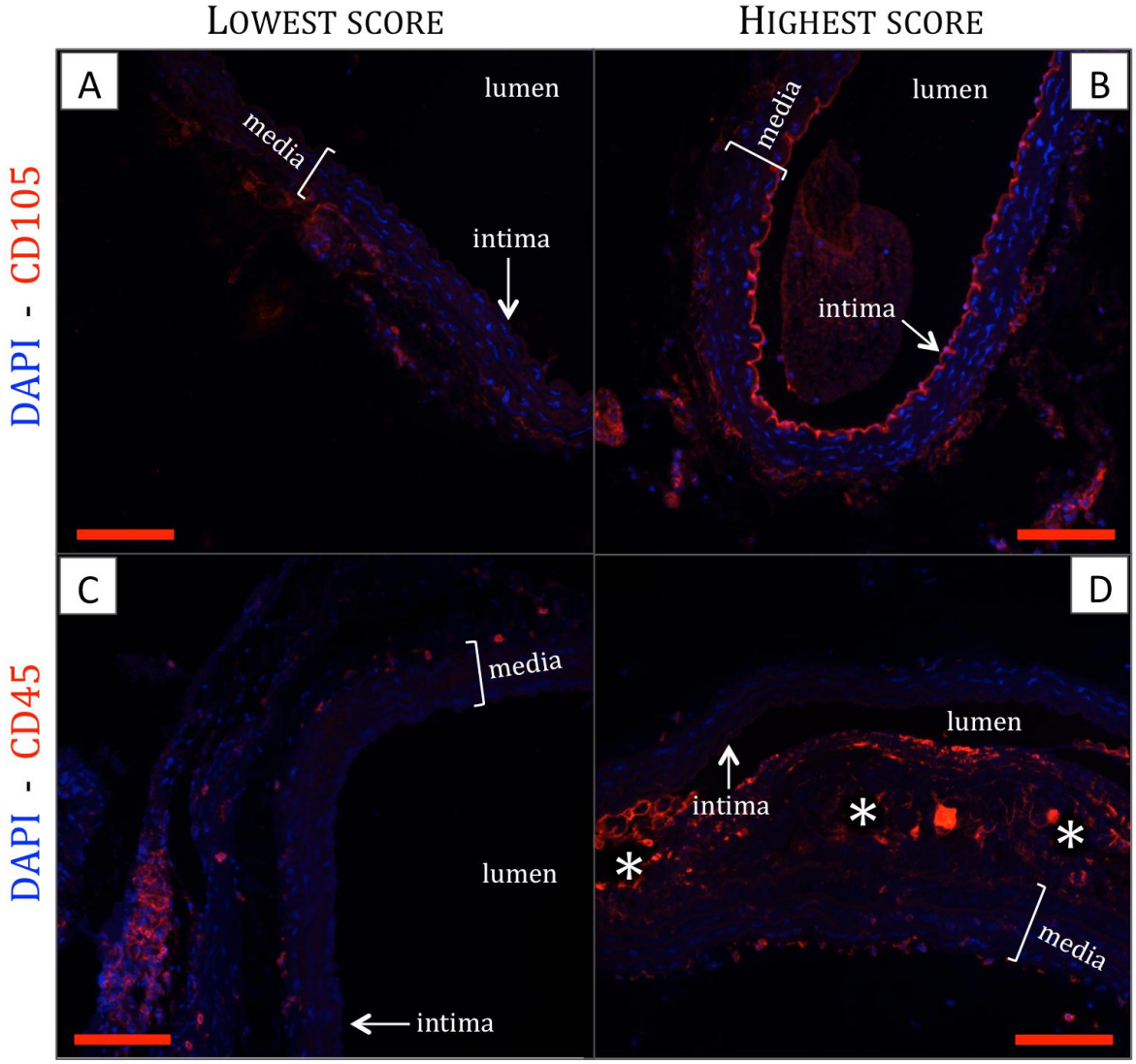

FIGURE 5.1: REPRESENTATIVE IMAGES OF CD105 (A,B) AND CD45 (C,D) STAINING, SHOWING THE CONDITION OF THE LOWEST SCORE (A,C) AND THE HIGHEST SCORE (B,D). *: ATHEROSCLEROTIC PLAQUE, SCALE BAR: 200µM.

SMC phenotype: Osteopontin – α-SMA Hydration was followed by antigen retrieval (Target Retrieval Solution, DAKO) and block of endogenous peroxidases. Application of goat serum (45', 1/5, DAKO) blocks nonspecific sites. The first primary antibody was applied overnight (1/500, rabbit anti-α-SMA, Abcam ab5694) followed by incubation with GAR-PO (45', 1/100, DAKO P0448) containing 10% mouse serum (Sigma) and visualization by DAB (DAKO K346711). After thorough rinsing and block with donkey serum (45', 1/5, Sigma), the second primary antibody is applied overnight (1/200, Goat anti-osteopontin, R&D AF808). The next day, incubation of the biotinylated secondary antibody (45', 1/300, DAG-B, Santa Cruz SC2042) is followed by signal amplification (30', Streptavidin-AP, Abcam 64268) and visualization using green chromogen (Enzo ADI-950-160-1). Slides are mounted with Faramount (DAKO, S3025). Every section was divided in four quadrants, each of which was scored (1: no osteopontin, (FIGURE 5.2A) to 5: maximal osteopontin (FIGURE 5.2B)) for osteopontin presence. Quadrant scores were averaged in a blinded manner and used for analysis of SMC phenotype.

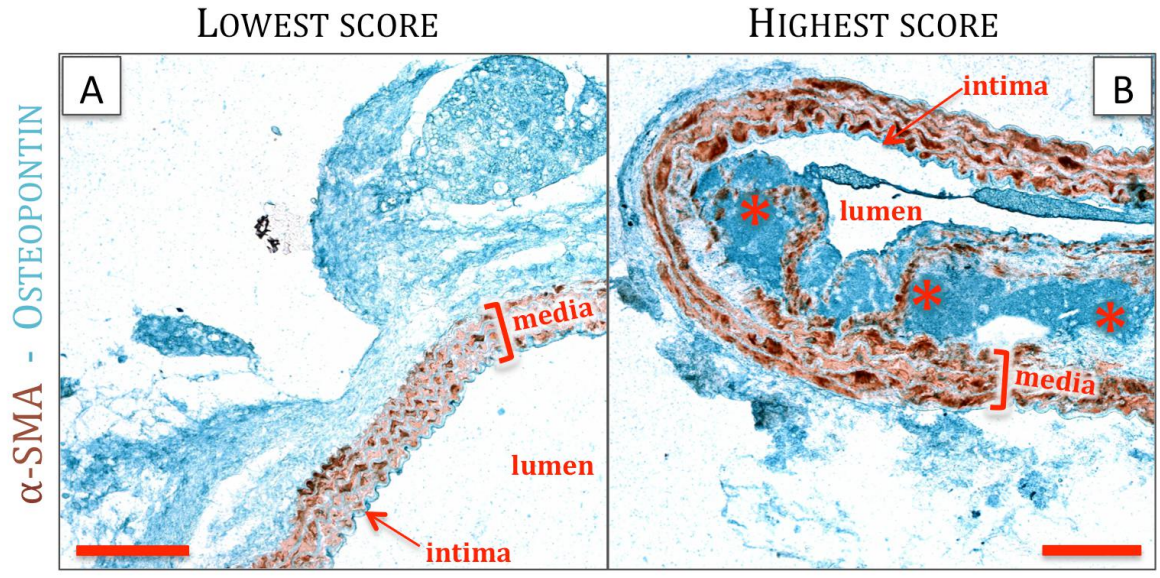

FIGURE 5.2: REPRESENTATIVE IMAGES OF OSTEOPONTIN STAINING, SHOWING THE CONDITION OF THE LOWEST SCORE (A) AND THE HIGHEST SCORE (B). *: ATHEROSCLEROTIC PLAQUE, SCALE BAR: 200μM.

5.3.5. STATISTICS

For isometric tension tests, preload was subtracted from the isometric tension value and all values were normalized for the length of the tested segment. Results are displayed as mean ± standard deviation. Statistical analyses (repeated measures two-way ANOVA) were performed with Statistica. For the histology results we aimed to analyze and pool at least 10 slices for every animal, and two way ANOVA was performed using SAS 9.4. P-values in the text represent results of the two way ANOVA testing (see also TABLE 5.2, page 88). Posthoc p-values are displayed in the graphs and the SUPPLEMENTARY TABLES. $P < 0.05$ was considered statistically significant.

5.4. RESULTS

5.4.1. ENDOTHELIUM-DEPENDENT AND –INEDPENDENT VASODILATORY FUNCTION

PC induced by PE before ACh and SNP was comparable (p=0.5309, data not shown). In the wildtype mice, we observed an acute deterioration of dose-dependent **endothelium-dependent vasodilation** after clamping (p=0.0026, FIGURE 5.3A). While maximal relaxation due to 10^{-5}M ACh additions was not impaired in arteries clamped with 0.6N (p=0.3374), segments clamped with 1.27N showed a significantly lower response compared to the unclamped segments (p=0.0130). One month after clamping, no difference in endothelium-dependent vasodilation was observed between clamped and unclamped arteries (p=0.9964, FIGURE 5.3B). In *LDLR* knockout animals with atherosclerosis, clamping did not further deteriorate endothelium-dependent vasodilatation in the acute setting (p=0.9778, FIGURE 5.4A) or after 1 month (p=0.4135, FIGURE 5.4B). No difference between wildtype and *LDLR* knockout arteries could be observed for any of the ACh concentrations. Clamping did not impair acute or 1 month **endothelium-independent vasodilation** by SNP in wildtype nor in *LDLR* knockout samples (data not shown).

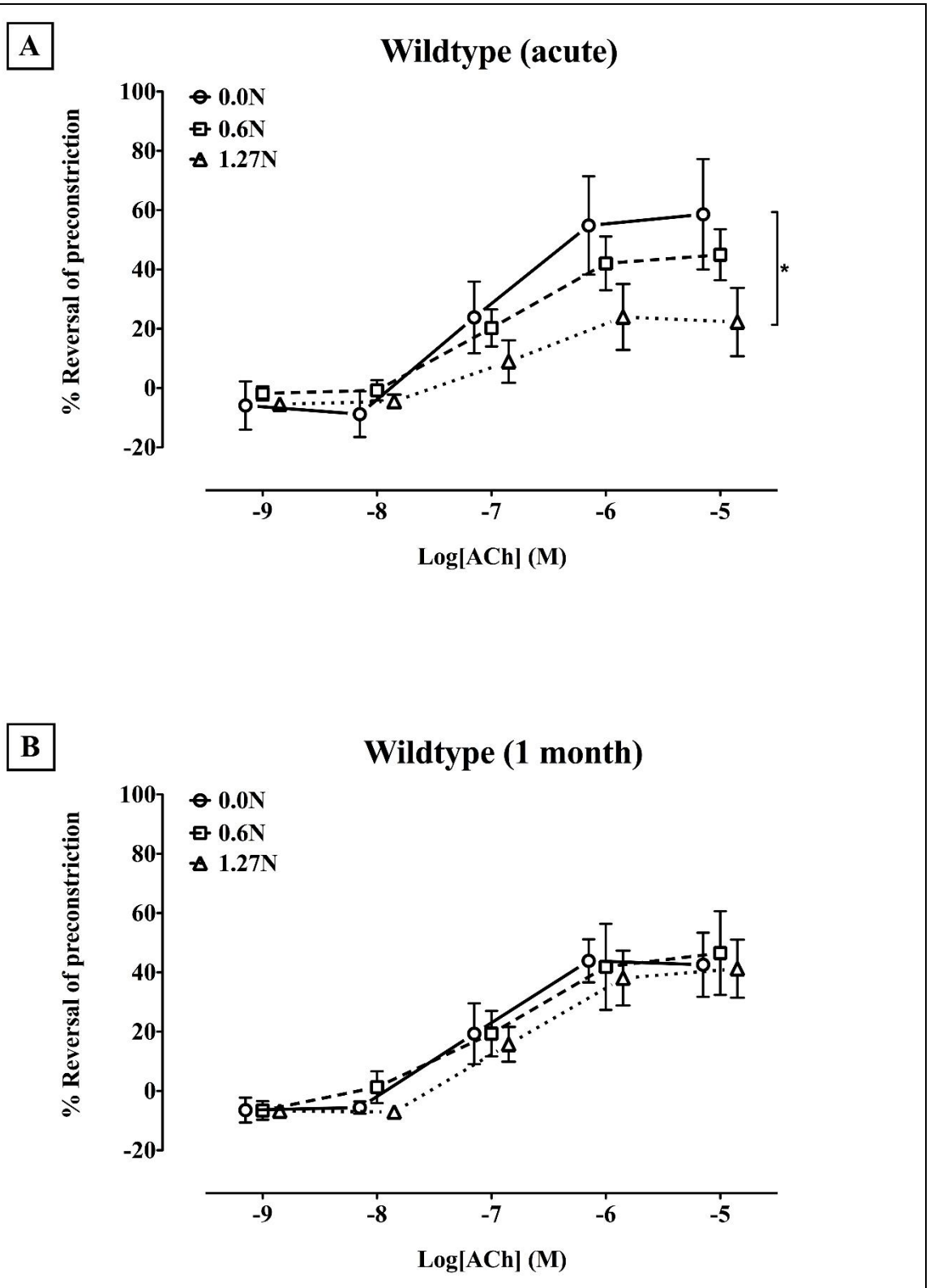

FIGURE 5.3: RELATIVE ENDOTHELIUM-DEPENDENT RELAXATION DUE TO CUMULATIVE ACH ADMINISTRATION AFTER PE-INDUCED PC (MEAN ± SD). DOSE-RESPONSE CURVES ARE SHOWN FOR WILDTYPE MICE, BOTH FOR SEGMENTS TESTED IMMEDIATELY AFTER CLAMPING (A) OR AFTER ONE MONTH SURVIVAL (B). * P<0.05.

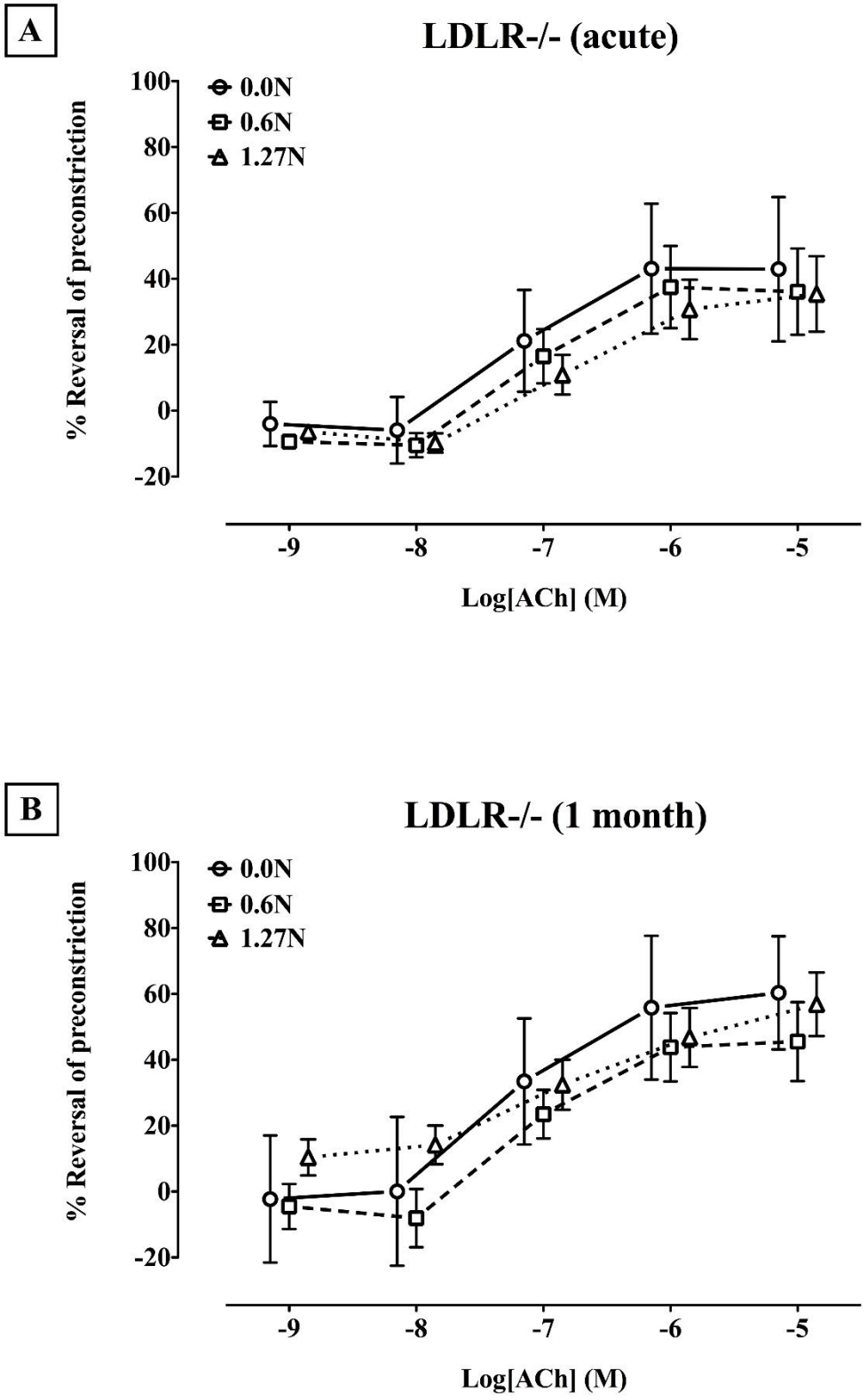

FIGURE 5.4: RELATIVE ENDOTHELIUM-DEPENDENT RELAXATION DUE TO CUMULATIVE ACH ADMINISTRATION AFTER PE-INDUCED PC (MEAN ± SD). DOSE-RESPONSE CURVES ARE SHOWN FOR *LDLR-/-* MICE, BOTH FOR SEGMENTS TESTED IMMEDIATELY AFTER CLAMPING (A) OR AFTER ONE MONTH SURVIVAL (B)..

TABLE 5.2: OVERVIEW OF THE INTERACTION AND MAIN EFFECT P-VALUES FROM THE TWO WAY ANOVA TESTS PERFORMED FOR ALL HISTOLOGICAL STAININGS. CL: CLAMP LOAD, GT: GENOTYPE, TP: TIME POINT.

			Interaction	Main Effects		
				Clamp load	Genotype	Time point
CD105	CL * GT	A	0.2074	<0.0001	<0.0001	
		6h	0.2002	0.0653	0.0385	
		2w	0.9448	0.7807	0.6680	
		1m	<0.0001	0.0011	0.0006	
	GT * TP	0.0N	0.0655		0.2113	<0.0001
		0.6N	<0.0001		0.1066	<0.0001
		1.27N	0.0002		0.0561	0.0025
	TP * CL	WT	0.1372	0.0284		<0.0001
		KO	0.0001	0.0001		<0.0001
Verhoeff's-Van Gieson	CL * GT	A	0.1755	0.0002	0.0011	
		6h	0.0013	<0.0001	0.0002	
		2w	0.5576	<0.0001	<0.0001	
		1m	0.0040	<0.0001	<0.0001	
	GT * TP	0.0N	0.2893		0.0213	0.1758
		0.6N	0.5308		<0.0001	<0.0001
		1.27N	0.1697		<0.0001	0.0525
	TP * CL	WT	0.2522	<0.0001		0.0006
		KO	0.0272	<0.0001		0.0757
Osteopontin	CL * GT	A	0.1890	0.0560	0.0018	
		6h	0.3677	0.0009	0.1661	
		2w	0.3340	<0.0001	0.0037	
		1m	0.9710	0.8969	<0.0001	
	GT * TP	0.0N	0.0056		<0.0001	<0.0001
		0.6N	0.0179		0.0024	0.0032
		1.27N	0.3600		0.0002	0.0002
	TP * CL	WT	0.0012	0.0001		0.0002
		KO	0.4440	0.0256		<0.0001
CD45 intima	CL * GT	A	0.1683	<0.0001	0.0047	
		6h	0.0903	0.0010	0.5175	
		2w	0.1104	0.0027	0.2015	
		1m	0.8710	0.0074	0.9013	
	GT * TP	0.0N	0.0867		0.9969	<0.0001
		0.6N	0.2417		0.0070	<0.0001
		1.27N	0.8588		0.4020	<0.0001
	TP * CL	WT	0.2512	<0.0001		<0.0001
		KO	0.4434	0.0021		<0.0001
CD45 media	CL * GT	A	0.0168	0.0117	0.3029	
		6h	0.0471	0.0440	0.0016	
		2w	0.3589	0.4804	0.6996	
		1m	0.9268	0.0002	0.6794	
	GT * TP	0.0N	0.3811		0.8139	0.2557
		0.6N	0.1895		0.4720	0.0004
		1.27N	0.0124		0.0010	<0.0001
	TP * CL	WT	0.0030	0.0052		0.2304
		KO	0.0548	<0.0001		0.0064

5.4.2. CD105: ENDOTHELIAL CELLS

Clamping results in lower CD105 content in the acute condition ($p<0.0001$, FIGURE 5.5). CD105 score decreases in time in both wildtype ($p<0.0001$) and atherosclerotic ($p<0.0001$) arteries, for unclamped ($p<0.0001$), 0.6N ($p<0.0001$) and 1.27N ($p=0.0025$) clamped segments. In the acute situation, wildtype samples have higher CD105 score compared to *LDLR-/-* ($p<0.0001$, FIGURE 5.5).

5.4.3. VERHOEFF'S-VAN GIESON: ELASTIC MEMBRANES

Clamping induces flattening of the innermost elastic membrane, expressed by the ratio between curved and straight-through length, in wildtype ($p<0.0001$) as well as *LDLR-/-* ($p<0.0001$) arteries (FIGURE 5.6, 5.7). Flattening is more pronounced in *LDLR-/-* compared to wildtype vessels at the acute ($p=0.0011$), 6 hours ($p=0.0002$), 2 weeks ($p<0.0001$) and 1 month ($p<0.0001$) time point. This is the case for unclamped ($p=0.0213$), 0.6N clamped ($p<0.0001$) and 1.27N clamped ($p<0.0001$) segments. While in wildtype segments the clamping-induced flattening is reversed through time ($p=0.0006$), this is not the case for atherosclerotic vessels ($p=0.0757$) (FIGURE 5.6).

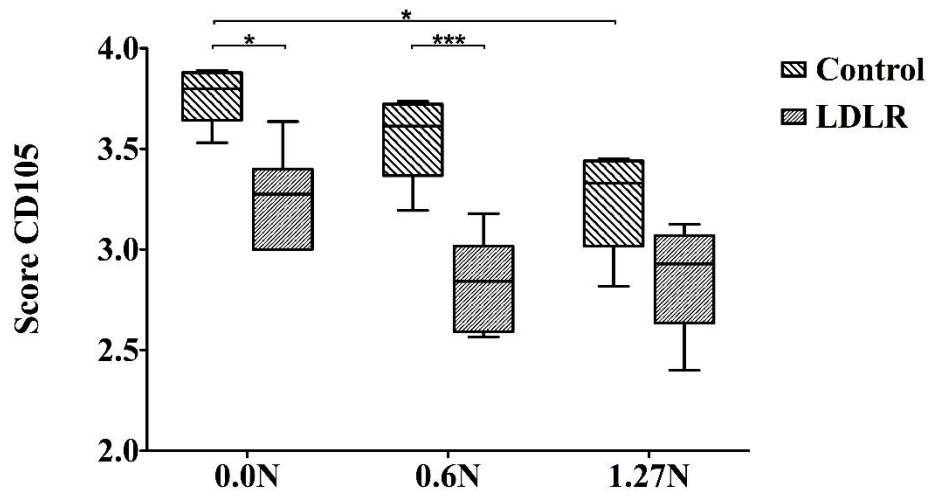

FIGURE 5.5: THE EFFECT OF CLAMPING ON CD105 PRESENCE, DISPLAYED AS PERCENTAGE FLUORESCENCE DETECTED IN INTIMA AND MEDIA. RESULTS OF WILDTYPE AND *LDLR* KNOCKOUT MICE ARE SHOWN IMMEDIATELY AFTER CLAMPING (MEDIAN AND IQR, 5-95 PERCENTILE). * P<0.05, *** P<0.0001.

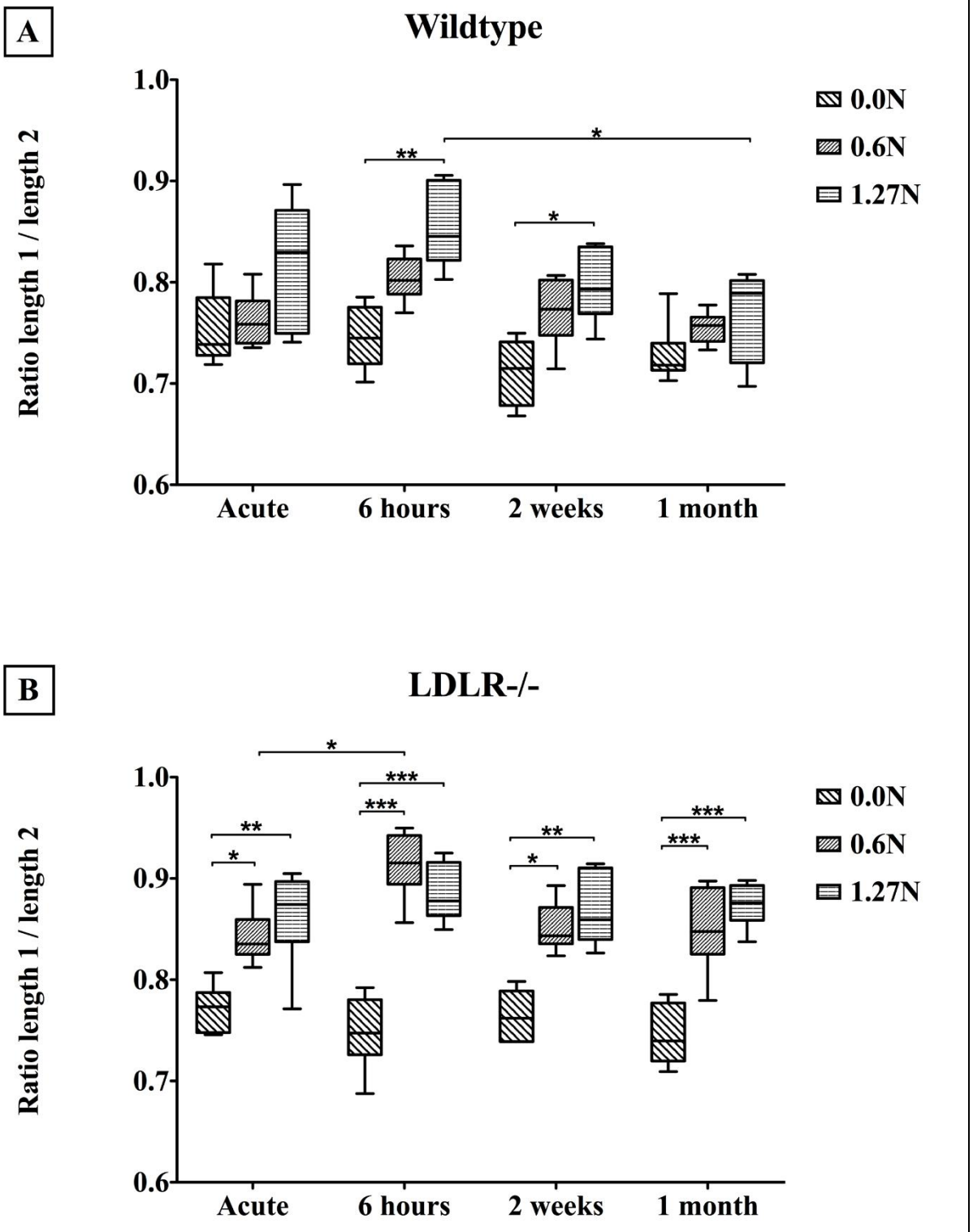

FIGURE 5.6: LONGTERM EFFECTS OF CLAMPING ON THE DEGREE OF FLATTENING OF THE INNERMOST ELASTIC MEMBRANE FOR WILDTYPE (A) AND *LDLR-/-* MICE (B) (MEDIAN AND IQR, 5-95 PERCENTILE). LENGTH 1: STRAIGHT LENGTH, LENGTH 2: CURVED LENGTH. * P<0.05, ** P<0.001, *** P<0.0001.

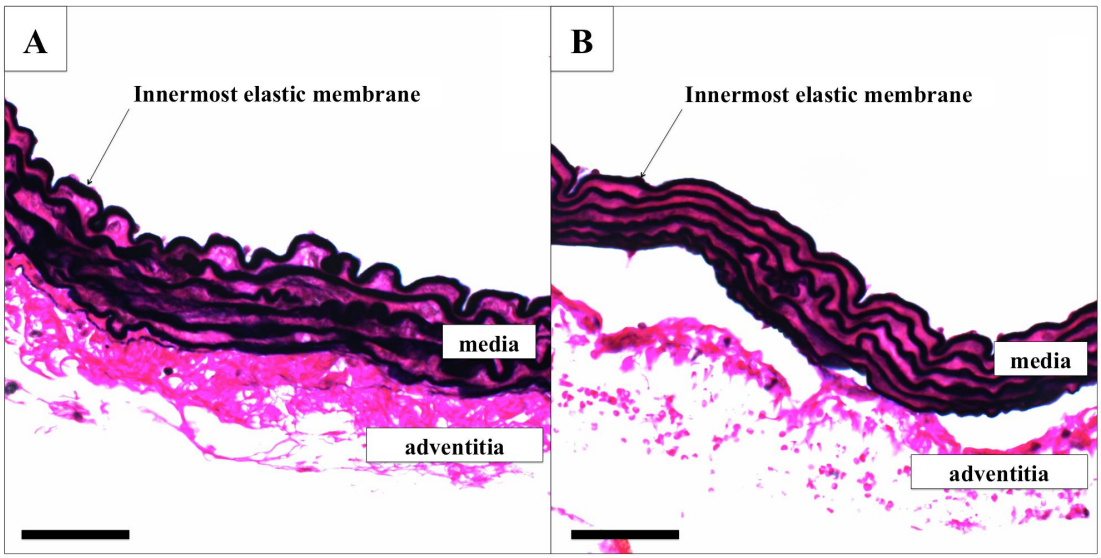

FIGURE 5.7: VERHOEFF'S-VAN GIESON STAINING OF AN UNCLAMPED (A) AND 1.27N CLAMPED (B) WILDTYPE AORTA. SCALE BAR 100µM.

5.4.4. OSTEOPONTIN: SMOOTH MUSCLE CELL PHENOTYPE

α-SMA was also stained to improve interpretation. Osteopontin score is higher in *LDLR-/-* compared to wildtype arteries in unclamped ($p<0.0001$), 0.6N clamped ($p=0.0024$) and 1.27N clamped ($p=0.0002$) samples and is higher at later time points ($p<0.0001$; $p=0.0032$ and $p=0.0002$, respectively, FIGURE 5.8). Clamping results in higher osteopontin scores in wildtype ($p=0.0001$) and *LDLR-/-* ($p=0.0256$) arteries. Moreover, there was a significant effect of clamping in the 6 hours ($p=0.0009$) and 2 weeks ($p<0.0001$) condition (FIGURE 5.8). This is not observed in the acute ($p=0.0560$) and 1 month ($p=0.8969$) condition.

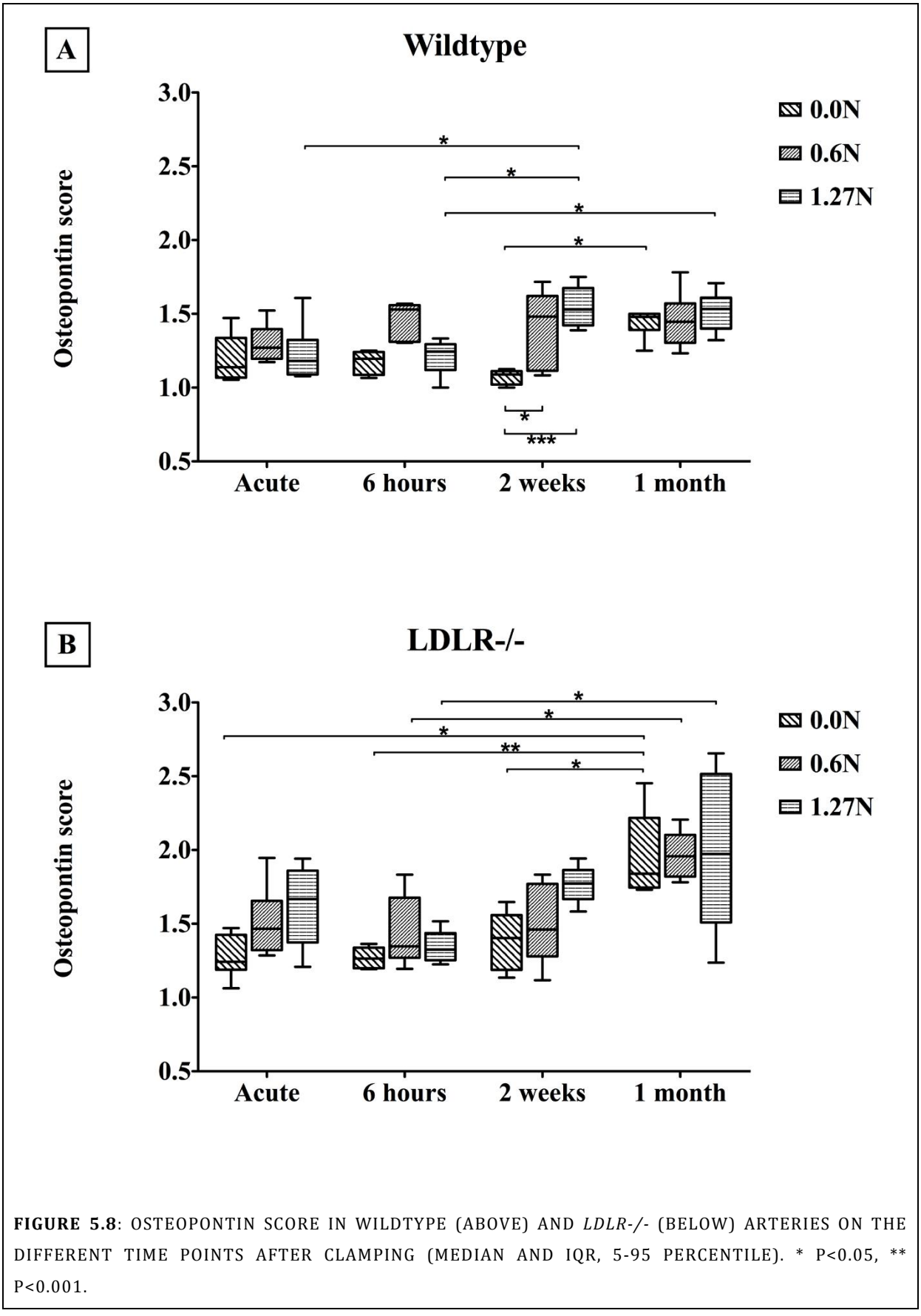

FIGURE 5.8: OSTEOPONTIN SCORE IN WILDTYPE (ABOVE) AND *LDLR-/-* (BELOW) ARTERIES ON THE DIFFERENT TIME POINTS AFTER CLAMPING (MEDIAN AND IQR, 5-95 PERCENTILE). * P<0.05, ** P<0.001.

5.4.5. CD45: INFLAMMATION

CD45 staining allowed investigation of inflammation in the tunica intima (FIGURE 5.9) and tunica media (FIGURE 5.10).

5.4.5.1. TUNICA INTIMA

Intimal CD45 score in wildtype ($p<0.0001$) as well as atherosclerotic ($p=0.0021$) vessels is elevated after clamping but diminishes through time in both genotypes ($p<0.0001$, FIGURE 5.9). While the intima in wildtype arteries shows higher CD45 content compared to *LDLR-/-* vessels in the acute condition ($p=0.0047$), no difference is observed after 6 hours ($p=0.5175$), 2 weeks ($p=0.2015$) and 1 month ($p=0.9013$). CD45 score is higher for wildtype segments compared to *LDLR-/-* samples after clamping with 0.6N ($p=0.0070$), while no difference is seen between genotypes in the unclamped ($p=0.9969$) and 1.27N ($p=0.4020$) groups.

5.4.5.2. TUNICA MEDIA

Medial CD45 in wildtype ($p=0.0052$) and atherosclerotic arteries ($p<0.0001$) was elevated after clamping (FIGURE 5.10). Through time, CD45 levels of unclamped arteries remain stable ($p=0.2557$), while CD45 score in the tunica media raises in 0.6N ($p=0.0004$) and 1.27N ($p<0.0001$) clamped vessels. Medial CD45 levels in wildtypes remain stable ($p=0.2304$, FIGURE 5.10A), but CD45 content increases through time in atherosclerotic vessels ($p=0.0064$, FIGURE 5.10B). Medial CD45 abundance is higher in *LDLR-/-* than wildtype segments in the 1.27N condition ($p=0.0010$), but does not differ between genotypes in unclamped ($p=0.8139$) and 0.6N clamped ($p=0.4720$) segments. After 6 hours, atherosclerotic arteries display a higher CD45 content in the tunica media compared to wildtype vessels ($p=0.0016$), while no difference is observed between genotypes in the acute ($p=0.3029$), 2 weeks ($p=0.6996$) and 1 month ($p=0.6794$) conditions.

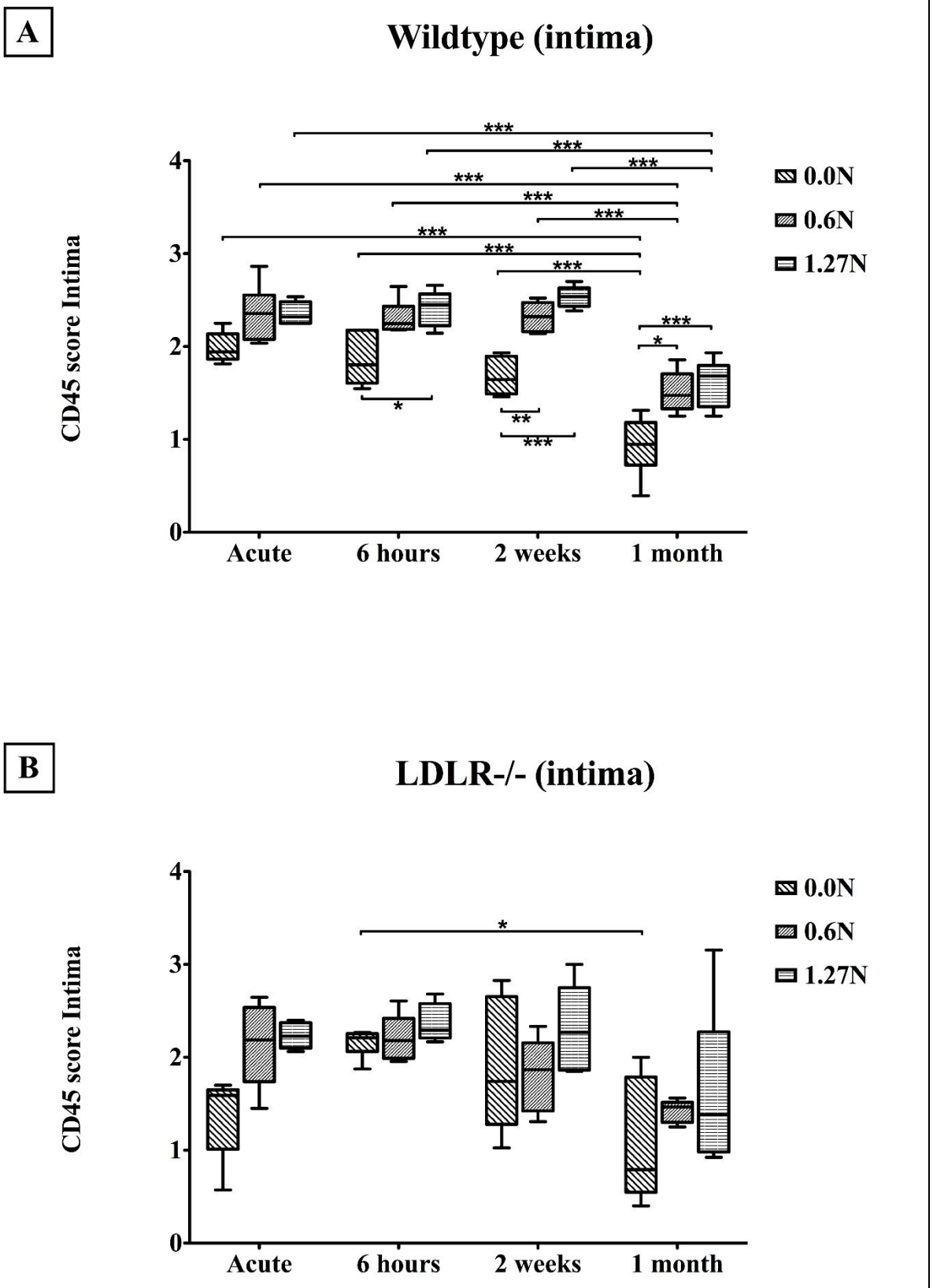

FIGURE 5.9: INFLAMMATION AFTER CLAMPING IN THE INTIMA IN WILDTYPE (A) AND *LDLR-/-* (B) ARTERIES (MEDIAN AND IQR, 5-95 PERCENTILE). * P<0.05, ** P<0.001, *** P<0.0001.

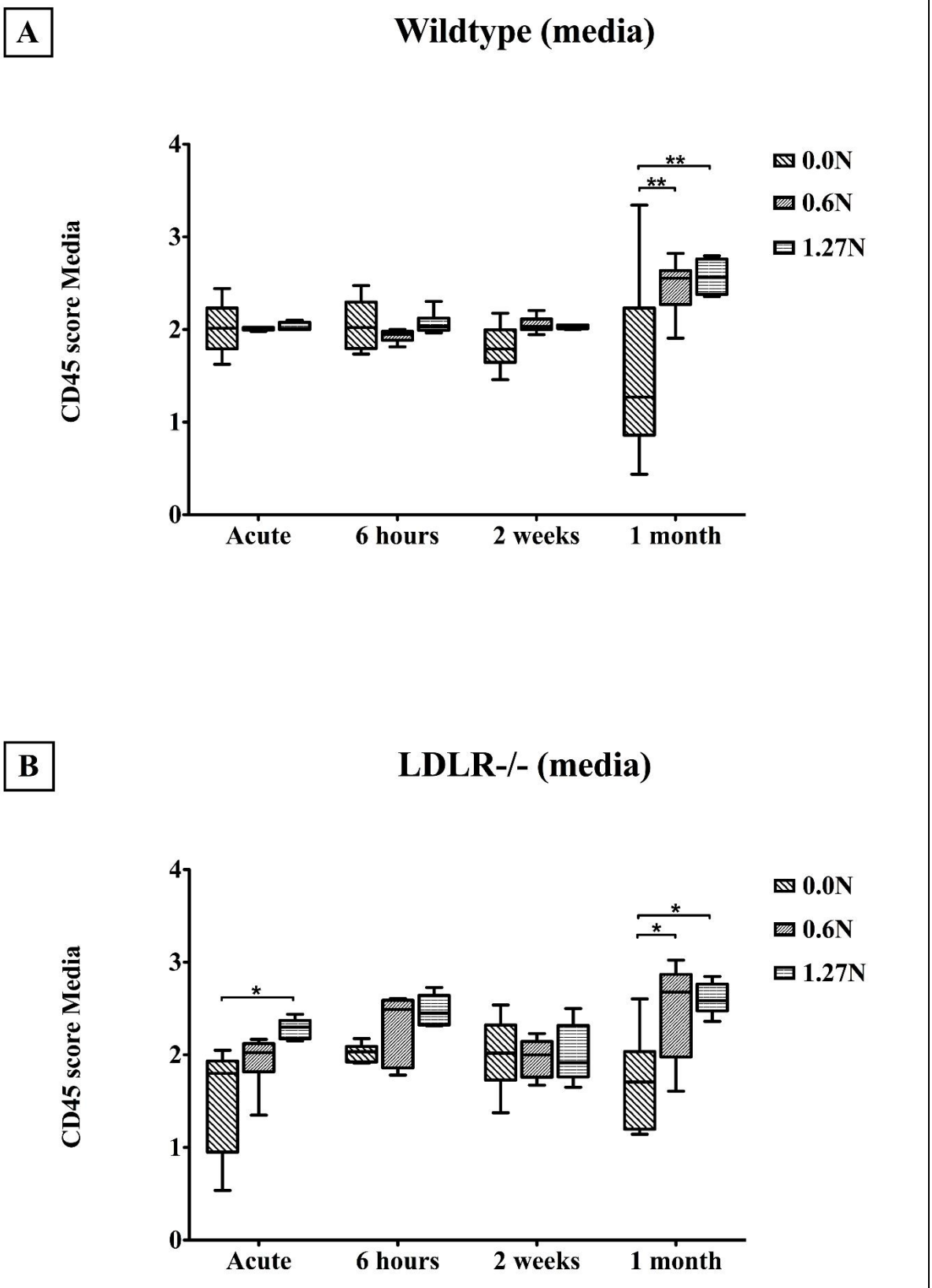

FIGURE 5.10: INFLAMMATION AFTER CLAMPING IN THE MEDIA IN WILDTYPE (A) AND *LDLR-/-* (B) ARTERIES (MEDIAN AND IQR, 5-95 PERCENTILE). * P<0.05, ** P<0.001.

5.5. DISCUSSION

In this chapter we have described that arteries of wildtype and atherosclerotic mice show a different time-dependent response to *in vivo* clamping. EC presence and function, SMC phenotype and function, the elastic membrane curvature and inflammation were investigated.

5.5.1. ENDOTHELIUM

We observed an immediate drop in endothelium-dependent vasodilatation in wildtypes. Remarkably, arteries of *LDLR* knockout mice did not show deterioration of endothelial function after clamping. This might be explained by the trend toward lower baseline relaxation in unclamped *LDLR-/-* compared to wildtype samples. Apparently, this reduces additional deterioration of endothelial function by clamping. Immunohistochemical staining of CD105 showed endothelial loss following clamping, confirming the vasoresponse tests. Endoglin or CD105 is a type I integral membrane glycoprotein located on cell surfaces. It is expressed at low levels in resting ECs, but is highly expressed in vascular ECs at sites of active angiogenesis such as tumor vessels, inflamed tissues, healing wounds and upon vascular injury[16]. While clamping-induced loss of endothelial function was recovered after one month in wildtype arteries, CD105 level did not. Since we also observed a drop in CD105 score through time in unclamped arteries, it seems that even freeing an artery of surrounding fat results in endothelial loss on the long term. This might be an explanation for the absence of a statistical effect of clamping in the chronic time points. The somewhat lower baseline endothelial function after 1 month might be caused by slow deterioration of endothelial function with aging[13].

5.5.2. INNERMOST ELASTIC MEMBRANE

The wavy pattern of medial elastic membranes of large arteries serves to enable expansion of the vessel lumen to damp the pulse waves originating from the systole, which provides energy to elastically recoil the wall during diastole (Windkessel effect). In unclamped segments, we observed a less wavy pattern of the innermost elastic membrane in *LDLR* knockout vessels compared to wildtypes samples. Furthermore, we have shown that clamping results in elastica

flattening in wildtype arteries, and to a higher extent in atherosclerotic arteries. This acute effect of arterial clamping confirms previous studies that also demonstrated flattening of medial elastic membranes following *ex vivo*[17] and *in vivo*[3] clamping. An interesting finding is that the flattening of the innermost elastic membrane in wildtype arteries after clamping is reversible in time and fully recovers within 1 month post-clamping. In contrast, arteries in atherosclerotic mice show no recovery. Local disruption of the wavy elastic membrane pattern could cause incongruence in the elastic properties of the clamped vessel, resulting in the initiation of standing waves and a change in diastolic/systolic difference. Clamping load should be limited especially when clamping atherosclerotic arteries, because they are more susceptible to elastica flattening which does not recover in the same time span as healthy vessels.

5.5.3. SMOOTH MUSCLE CELLS

Medial contractile SMC react to vascular injury such as arterial clamping by dedifferentiating into a synthetic, mobile phenotype[10]. While α-SMA is highly present in contractile SMC, the synthetic phenotype is characterized by osteopontin. As expected, immunohistochemical staining for those markers has demonstrated higher baseline osteopontin content in unclamped arteries of mice with atherosclerosis compared to wildtype vessels. This can be explained by the hyperlipidemic serum profile in *LDLR* knockout mice, which has been shown to upregulate osteopontin expression[18]. Jackiewicz et al. described a phenotypic switch to synthetic SMC (transmission electron microscopy) 7 days after *in vivo* clamping of rat arteries, which was reversed at 14 days[10]. We observed a rise in osteopontin 6 hours and 2 weeks after clamping, which was reversed after 1 month. This difference in time course could be explained by the difference in techniques used for analysis, the type of clamp or the animal model. We observed a global rise in osteopontin content through time, for wildtype as well as knockout arteries. This effect was detected not only in the clamped segments, but also in unclamped samples. Therefore we suggest that osteopontin could be upregulated during the aging process, or that manipulation to dissect the vessel from surrounding tissue is a trigger to induce a phenotypic switch. SMC function was studied by SNP, either immediately after clamping or 1 month post-op.

We did not detect a change in functional integrity of SMC at these time points, which confirms our histological findings.

5.5.4. INFLAMMATION

Our results show that clamping results in a higher CD45 content in wildtype as well as atherosclerotic arteries, both in the tunica media and tunica intima. This is consistent with studies investigating the consequences of mechanical injury to arteries[19,20]. While inflammation in the intima diminishes through time, medial CD45 score remains elevated to one month after clamping. This could be explained by an initial adherence of inflammatory cells to the damaged endothelium, with subsequent migration into the deeper arterial wall layers, since it was demonstrated that pathology could influence the permeability of the innermost elastic membrane[21]. Moreover, as has been described, inflammatory cells can also enter the media via the vasa vasorum in the tunica adventitia in response to injury[22,23]. Clamping at 1.27N results in higher medial CD45 content in arteries of atherosclerotic mice compared to healthy vessels, while a load of 0.6N leads to lower intimal CD45 score in knockout versus wildtype samples. Also, we observed that intimal inflammation in wildtypes is higher compared to *LDLR-/-* segments in the acute condition. However, medial inflammation is lower in arteries of wildtype versus knockout mice 6 hours after clamping. This suggests that inflammation after clamping in diseased arteries is most prominent in the media, and for healthy arteries in the intima. This might also be explained by a higher elastica permeability in vessels of atherosclerotic mice[21].

5.5.5. CONCLUSION

We have demonstrated that clamping up to 1.27N, which is 4.2 times the minimal occlusion force[3], induces damage to mouse thoracic aortas that is not fully repaired after one month. Interestingly, the most pronounced effect was observed on the level of the innermost elastic membrane and not at the endothelium. Also, inflammation in the tunica media appears to be of higher importance compared to the intima. Atherosclerotic arteries show a different response than healthy vessels. Therefore, it might be necessary to account for patient- or pathology-

specificity when optimizing mathematical models for arterial clamping before implementation in robotic instruments.

5.6. REFERENCES

1. Rodriguez, E. & Chitwood, W. R. Robotics in cardiac surgery. *Scandinavian Journal of Surgery* **98,** 120–124 (2009).

2. Puangmali, P., Althoefer, K., Seneviratne, L. D., Murphy, D. & Dasgupta, P. State-of-the-art in force and tactile sensing for minimally invasive surgery. *IEEE Sens. J.* **8,** 371–380 (2008).

3. Famaey, N. *et al.* In vivo soft tissue damage assessment for applications in surgery. *Med. Eng. Phys.* **32,** 437–43 (2010).

4. Margovsky, A. I., Chambers, A. J. & Lord, R. S. The effect of increasing clamping forces on endothelial and arterial wall damage: an experimental study in the sheep. *Cardiovasc. Surg.* **7,** 457–63 (1999).

5. Barone, G. W., Conerly, J. M., Farley, P. C., Flanagan, T. L. & Kron, I. L. Assessing clamp-related vascular injuries by measurement of associated vascular dysfunction. *Surgery* **105,** 465–471 (1989).

6. Hangler, H., Mueller, L., Ruttmann, E., Antretter, H. & Pfaller, K. Shunt or snare: coronary encothelial damage due to hemosttic devices for beating heart coronary surgery. *Ann. Thorac. Surg.* **86,** 1873–7 (2008).

7. Slayback, J. B., Bowen, W. W. & Hinshaw, D. B. Intimal injury from arterial clamps. *Am. J. Surg.* **132,** 183–188 (1976).

8. Vural, A. H. *et al.* Intracoronary Shunt Versus Bulldog Clamp in Off-Pump Bypass Surgery. Endothelial Trauma: Shunt Versus Clamp. *J. Surg. Res.* **150,** 261–265 (2008).

9. Margovsky, A. I., Lord, R. S. & Chambers, A. J. The effect of arterial clamp duration on endothelial injury: an experimental study. *Aust. N. Z. J. Surg.* **67,** 448–451 (1997).

10. Jackiewicz, T. A., McGeachie, J. K. & Tennant, M. Structural recovery of small arteries following clamp injury: a light and electron microscopic investigation in the rat. *Microsurgery* **17,** 674–80 (1996).

11. Hsi, C. *et al.* Experimental coronary artery occlusion: relevance to off-pump cardiac surgery. *Asian Cardiovasc. Thorac. Ann.* **10,** 293–7 (2002).

12. Dobrin, P. B., McGurrin, J. F. & McNulty, J. A. Chronic histologic changes after vascular clamping are not associated with altered vascular mechanics. *Ann. Vasc. Surg.* **6,** 153–9 (1992).

13. Geenens, R. *et al.* Arterial Vasoreactivity is Equally Affected by In Vivo Cross-Clamping with Increasing Loads in Young and Middle-Aged Mice Aortas. *Ann. Thorac. Cardiovasc. Surg.* (2015). doi:10.5761/atcs.oa.15-00225

14. Ishibashi, S. *et al.* Hypercholesterolemia in low density lipoprotein receptor knockout mice and its reversal by adenovirus-mediated gene delivery. *J. Clin. Invest.* **92,** 883–93 (1993).

15. Verhoeff-Van Gieson Staining Protocol for Elastic Fibers - http://www.ihcworld.com/_protocols/special_stains/vvg.htm. at <http://www.ihcworld.com/_protocols/special_stains/vvg.htm>

16. Atlas Genetics Oncology - http://atlasgeneticsoncology.org/Genes/ENGID40452ch9q34.html.

17. Harvey, J. G. & Gough, M. H. A comparison of the traumatic effects of vascular clamps. *Br. J. Surg.* **68,**

267–72 (1981).

18. Shao, J.-S. *et al.* Vascular calcification and aortic fibrosis: a bifunctional role for osteopontin in diabetic arteriosclerosis. *Arterioscler. Thromb. Vasc. Biol.* **31,** 1821–33 (2011).

19. Rinaldi, B. *et al.* Inflammatory events in a vascular remodeling model induced by surgical injury to the rat carotid artery. *Br. J. Pharmacol.* **147,** 175–82 (2006).

20. Tanaka, H. *et al.* Sustained activation of vascular cells and leukocytes in the rabbit aorta after balloon injury. *Circulation* **88,** 1788–1803 (1993).

21. Sandow, S. L., Gzik, D. J. & Lee, R. M. K. W. Arterial internal elastic lamina holes: relationship to function? *J. Anat.* **214,** 258–66 (2009).

22. Mulligan-Kehoe, M. J. & Simons, M. Vasa vasorum in normal and diseased arteries. *Circulation* **129,** 2557–66 (2014).

23. Maiellaro, K. & Taylor, W. R. The role of the adventitia in vascular inflammation. *Cardiovasc. Res.* **75,** 640–648 (2007).

CHAPTER VI

OVERALL DISCUSSION

The lack of haptic feedback during robotic minimally invasive procedures encloses a potential risk of avoidable collateral damage due to accidental tissue overload. Implementing these safety thresholds in robotic instruments with shared autonomy could avoid tissue overload and might importantly increase surgical safety using robotic systems. The required mathematical models to make this possible can only be validated if substantial *in vivo* data is available. **The goal of this dissertation was to gather this biological information by studying the relationship between force application on mouse aortas and the hereby-induced tissue damage, acutely and its long-term consequences. Moreover, we wanted to evaluate whether patient-specific characteristics like age and pathology should be accounted for.**

6.1. HAPTIC FEEDBACK

Visual information is very important for accurate execution of surgical procedures. In the Da Vinci surgical robot, a state of the art camera system creates a three dimensional image of the site of interest at the master console[1]. This enables intuitive manipulation and provides excellent visualization of the instrument tip interaction with body tissues. However, despite this optimal visual feedback, the lack of **force information** creates difficulties. For example, excessive force application can cause fine suture material to break or can induce unnecessary injury to soft tissue. On the other hand, if exerted forces are too low, knots might not hold or tissue structures might slip[2]. Moreover, body structures out of sight might be crushed when manoeuvring the instruments to the desired location. Direct haptic feedback would notify the surgeon about the forces that are exerted at all times during the operation. Obviously, for this information to be meaningful the **relationship between force load and tissue response** has to be known. In this context our interdisciplinary project was set up, combining insight from

engineers, surgeons and basic researchers. **This PhD dissertation concerns the biologic part of this research, in which *in vivo* and *in vitro* experiments have been conducted to study the response of soft tissue to mechanical manipulation.**

6.2. EFFECT OF CLAMPING ON ARTERIES

To study accidental tissue overload to blood vessels in a controlled setting we decided to clamp mouse arteries for a short time period. Margovsky and colleagues published that clamping sheep carotid arteries for 30 minutes induces the maximal amount of endothelial injury, since longer **clamping times** did not cause additional damage[3]. However, 3 years later it was demonstrated that 1 minute of clamping already disrupts the endothelial layer of pig aorta[4]. In preliminary experiments of our research group[5], rat abdominal aortas were clamped for 2 minutes. When instruments are manoeuvred to the desired location during MIS they can accidentally crush soft tissue out of the visual field for short time intervals.

It has been demonstrated in many studies that mechanical manipulation of arteries and other soft tissues induces damage[3–17]. Comparison between different types of vascular occlusion devices and clamp loads has shown that even so-called atraumatic arterial clamps damage the vessel wall[5–13,16–18]. Therefore, we decided to choose the **clamping loads** for our study as low as possible to minimize damage. Meanwhile, effectiveness was ensured since forces were higher than the minimal occlusion force[5].

The **clamping device** was developed for the rat model we initially intended to use for this study. Thanks to miniaturisation of the clamping jaws we could use this device in mice. However, for the clamp to be positioned correctly, osteotomy of several ribs was required so we could only use this system for acute experiments. For the long-term and pathology study, micro bulldog clamps were used that are commercially available.

Forces exerted by the instrument tips were measured before experiments were conducted. Clamping surfaces of commercially available occlusion devices are often serrated to avoid slippage. However, we used non-serrated clamps to ensure that force execution was distributed equally over the arterial wall.

Clamping-induced injury to the vessel wall can be visualized and quantified on different levels. Most studies, like ours, are based on the assessment of vasoreactivity[5–7] and/or histological stainings[3–6,8–10,14,16,17], or electron microscopy[3,6–9,11–14,16]. As shown in this project, organ bath tests provide information about remaining **functional integrity** of a specific cell type in the tissue of interest. In the case of blood vessels, the availability of vasoactive agents that do -or do not- need intact ECs enables quantification of damage to the endothelium versus the SMCs in the media. If these data are combined and compared with **histology** results, this provides a more complete insight into the effects of a certain tissue manipulation. Standard histological stainings like Verhoeff's-Van Gieson provide general information about structural morphological changes. Additionally, we performed immunohistochemical stainings using antibodies against endoglin (CD105), osteopontin – α-SMA, and CD45. This provided us with information about elastic membrane curvature, EC presence, SMC phenotype, and inflammation, respectively, to complete our results of the vasoreactivity tests. A very interesting extension of this research would be to investigate changes in gene expression using quantitative PCR, to clarify the molecular pathways involved.

6.3. EFFECT OF AGE

Mechanical properties of the arterial wall change when blood vessels **age**[19], which might lead to a different response to arterial clamping. As we expected and was described in previous studies[5–7], clamping impaired endothelial function in all age groups. We

observed a trend toward diminished endothelial function in older animals, which might reach significance in mice older than 40 weeks[20]. Therefore, it could be a useful extension of our study to include additional age groups to our existent results. Also, it would be an asset to also have morphological information by performing histological stainings and include survival experiments to study long-term consequences of mechanical manipulation.

6.4. EFFECT OF PATHOLOGY

Another factor that changes mechanical properties of blood vessels is vascular pathology. **Atherosclerosis** accounts for 84.5% of cardiovascular deaths and 28.2% of all-cause mortality[21]. Keeping this striking prevalence in mind, we decided to include an animal model with this pathology in our study. As discussed previously (see chapter IV), multiple atherosclerosis models are available[22]. Although using mice for our purpose is challenging given their small size, the advantages (easy breeding, low cost, well established models) even this out. Moreover, these advantages gave us the opportunity to extend our study with more testing conditions, by investigating multiple clamp loads on several time points. *ApoE-/-* and *LDLR-/-* mice are the most frequently used mouse model to study atherosclerosis[22]. ApoE has multiple functions that could have an indirect impact on atherosclerosis, independent of plasma lipid levels[22]. Therefore we decided to use ***LDLR* knockout mice fed western diet**, since we do not need the extensive and fast development of atherosclerotic lesion associated with the *ApoE* knockout mouse model.

We could not find a consistent genotype-based difference in **intima** response to arterial clamping. In the acute and 1 month condition, endoglin (CD105) level was higher in knockout samples, while 6 hours after clamping it was lower compared to wildtypes. No

difference was observed 2 weeks after clamping. Moreover, although staining of endoglin (CD105) showed loss of EC presence after clamping, we only observed a loss of EC function in wildtype arteries that were tested immediately. This corresponds well with previous study results which stated no clear relationship of clamp load and intimal injury could be demonstrated in atherosclerotic arteries[11,13].

However, investigation of effects located in the tunica **media** provided more consistent results. Osteopontin score is higher in atherosclerotic arteries compared to wildtype vessels, which means that knockout of the *LDLR* combined with western diet feeding results in a higher synthetic to contractile SMC ratio. This might explain our finding that atherosclerotic arteries that are not or lightly (0.6N) clamped, relax less compared to healthy vessels in response to SNP. Quantification of curvature showed more flattening of the innermost elastic membrane in atherosclerotic samples compared to wildtype segments. While flattening occured in both genotypes, no recovery was observed in *LDLR-/-* arteries. These conclusions suggest that atherosclerotic arteries are more prone to medial damage, especially in the lighter clamping load range.

Looking at **inflammation** by means of CD45 staining, we observed a consistent rise after clamping. Interestingly, wildtype CD45 scores were higher than *LDLR-/-* levels in the intima, while media analysis showed a reversed pattern.

6.5. FUTURE PERSPECTIVES

A **Finite Element Model** was developed to model the responses of arteries to mechanical loading (Nele Famaey, Biomechanics, KU Leuven). To approach the values of the parameters in this model, biological data are necessary. Apart from the results obtained in this study, tests need to be performed to determine and model the mechanical behaviour of healthy, undamaged arteries. We have collected arterial

samples for examination of pressure-diameter relation in nonclamped arteries (Heleen Fehervary, Biomechanics, KU Leuven). Later on, a damage component can be included in the model. The results reported in this dissertation allow estimation of these injury parameters.

Once the parameters have been determined, the FEM will be implemented in a robotic vascular clamp prototype after which additional mouse experiments will allow **validation** and further optimisation. The ultimate goal is to be able to monitor online if the exerted forces rise too high and to provide a notification if this happens. To this purpose, preoperative information will have to be linked to intra-operative force measurements.

To investigate whether **extrapolation** to human surgery is possible, experiments using the prototype will also be conducted in a large animal model. Four locations of the arteria renalis of healthy sheep will be clamped simultaneously with different forces, while the contralateral artery is used as a nonclamped control. Excised segments will be studied conform the mouse study, using the techniques that are defined in this dissertation. Moreover, *ex vivo* loaded human arteria mammaria interna segments will be processed and studied with these protocols.

When the FEM is optimized for human arteries, it can be implemented in a simplified master-slave surgical system, a surgical robot provided with an intelligent component which limits forces exerted by the instruments, improving patient safety. Inquiry of experienced surgeons would allow determination of the most efficient way of providing force feedback. Our final aim is to transfer this concept to the operating theater, where it could be implemented in surgical robots to improve patient safety during RMIS procedures.

6.6. REFERENCES

1. Lanfranco, A. R., Castellanos, A. E., Desai, J. P. & Meyers, W. C. Robotic surgery: a current perspective. *Ann. Surg.* **239,** 14–21 (2004).

2. Okamura, A. M. Methods for haptic feedback in teleoperated robot-assisted surgery. *Industrial Robot: An International Journal* **31,** 499–508 (2004).

3. Margovsky, A. I., Lord, R. S. & Chambers, A. J. The effect of arterial clamp duration on endothelial injury: an experimental study. *Aust. N. Z. J. Surg.* **67,** 448–451 (1997).

4. Babin-Ebell, J., Gimpel-Henning, K., Sievers, H.-H. & Scharfschwerdt, M. Influence of clamp duration and pressure on endothelial damage in aortic cross-clamping. *Interact. Cardiovasc. Thorac. Surg.* **10,** 168–71 (2010).

5. Famaey, N. *et al.* In vivo soft tissue damage assessment for applications in surgery. *Med. Eng. Phys.* **32,** 437–43 (2010).

6. Barone, G. W., Conerly, J. M., Farley, P. C., Flanagan, T. L. & Kron, I. L. Assessing clamp-related vascular injuries by measurement of associated vascular dysfunction. *Surgery* **105,** 465–471 (1989).

7. Gersak, B., Trobec, R., Krisch, I. & Psenicnik, M. Loss of endothelium-mediated vascular relaxation as a response to various clamping pressures. *Eur. J. Cardiothorac. Surg.* **10,** 684–9 (1996).

8. Margovsky, A. Artery wall damage and platelet uptake from so-called atraumatic arterial clamps: an experimental study. *Cardiovasc. Surg.* **5,** 42–47 (1997).

9. Margovsky, A. I., Chambers, A. J. & Lord, R. S. The effect of increasing clamping forces on endothelial and arterial wall damage: an experimental study in the sheep. *Cardiovasc. Surg.* **7,** 457–63 (1999).

10. Darçin, O. T. *et al.* Pressure-controlled Vascular Clamp: A Novel Device for Atraumatic Vessel Occlusion. *Ann. Vasc. Surg.* **18,** 254–256 (2004).

11. Slayback, J. B., Bowen, W. W. & Hinshaw, D. B. Intimal injury from arterial clamps. *Am. J. Surg.* **132,** 183–188 (1976).

12. Manship, L. L. *et al.* Differential endothelial injury caused by vascular clamps and vessel loops. I. Normal vessels. *Am. Surg.* **51,** 392–400 (1985).

13. Manship, L. L., Moore, W. M., Bynoe, R. & Bunt, T. J. Differential endothelial injury caused by vascular clamps and vessel loops. II. Atherosclerotic vessels. *Am. Surg.* **51,** 401–6 (1985).

14. Jackiewicz, T. A., McGeachie, J. K. & Tennant, M. Structural recovery of small arteries following clamp injury: a light and electron microscopic investigation in the rat. *Microsurgery* **17,** 674–80 (1996).

15. Vriens, B. H. R. *et al.* Arterial clamping leads to stenosis at clamp sites after femoropopliteal bypass surgery. *Am. J. Surg.* **210,** 536–44 (2015).

16. Dobrin, P. B., McGurrin, J. F. & McNulty, J. A. Chronic histologic changes after vascular clamping are not associated with altered vascular mechanics. *Ann. Vasc. Surg.* **6,** 153–9 (1992).

17. Hsi, C. *et al.* Experimental coronary artery occlusion: relevance to off-pump cardiac surgery. *Asian Cardiovasc. Thorac. Ann.* **10,** 293–7 (2002).

18. De, S. *et al.* Assessment of Tissue Damage due to Mechanical Stresses. *Int. J. Rob. Res.* **26,** 1159–1171 (2007).

19. Ungvari, Z., Kaley, G., de Cabo, R., Sonntag, W. E. & Csiszar, A. Mechanisms of vascular aging: New

perspectives. *J. Gerontol. A. Biol. Sci. Med. Sci.* **65 A,** 1028–1041 (2010).

20. Geenens, R. *et al.* Arterial Vasoreactivity is Equally Affected by In Vivo Cross-Clamping with Increasing Loads in Young and Middle-Aged Mice Aortas. *Ann. Thorac. Cardiovasc. Surg.* (2015). doi:10.5761/atcs.oa.15-00225

21. Global, regional, and national age–sex specific all-cause and cause-specific mortality for 240 causes of death, 1990–2013: a systematic analysis for the Global Burden of Disease Study 2013. *Lancet* **385,** 117–171 (2014).

22. Getz, G. S. & Reardon, C. A. Animal models of atherosclerosis. *Arterioscler. Thromb. Vasc. Biol.* **32,** 1104–15 (2012).

SUMMARY

The lack of intraoperative haptic feedback limits the benefits that are associated with robotic minimally invasive surgery. The development of mathematical models to implement force information in surgical robots requires biological data describing the **relationship between mechanical loading and consequential tissue damage**. In this dissertation we aimed to quantify this relationship for aortic clamping, a procedure that is often crucial during surgery. We have shown that *in vivo* clamping of mouse thoracic aorta results in damage on both the functional and morphological level, which partly persists up to one month after the initial clamping injury.

To investigate if implementation of patient-specific information is necessary in the developed models, we examined whether or not age and pathology influence the relation between clamping force and tissue injury.

We observed a trend towards impaired endothelium-dependent relaxation in **aging** mice, Probably this difference in response would become significant when mice older than 40 weeks would be included in the study.

Given the high prevalence of **atherosclerosis** in patients who need surgery, we also studied the effect of aortic clamping in a mouse model displaying atherosclerotic lesions (*LDLR* knockout mice fed western diet). We could not find a consistent genotype-based difference in response to arterial clamping at intima level. However, investigation of effects located in the tunica media showed that atherosclerotic arteries have a higher osteopontin score (synthetic smooth muscle cells) compared to wildtype vessels. Quantification of curvature showed more flattening of the innermost elastic membrane in response to clamping in atherosclerotic samples compared to wildtype segments.

While flattening did occur in both genotypes, no recovery was observed in *LDLR-/-* arteries. These conclusions suggest that atherosclerotic arteries are more prone to medial damage, especially in the lighter clamping load range. Additionally, we observed a consistent rise in inflammatory cells (CD45) after clamping. Interestingly, wildtype inflammation scores were higher than *LDLR-/-* levels in the intima, while media analysis showed an opposite pattern.

We can **conclude** that *in vivo* clamping of arteries results in damage to the vessel wall, even when utilizing low clamp loads. While the comorbid factor aging did not affect the results significantly, atherosclerotic arteries respond differently to mechanical injury compared to healthy vessels. These results suggest that mathematical models to be implemented in surgical robots should account for possible pathology at the tissue of interest. This would improve safety during and after minimally invasive surgery.

SAMENVATTING

Het gebrek aan intraoperatieve haptische terugkoppeling limiteert de voordelen die geassocieerd zijn met robotische minimaal invasieve chirurgie. De ontwikkeling van mathematische modellen om krachtinformatie in chirurgische robots te implementeren vereist kennis over de **verhouding tussen mechanische belasting en hieruit resulterende weefselschade**. Het doel van deze doctoraatsthesis was om deze relatie te kwantificeren voor het klemmen van arteries, een procedure die vaak noodzakelijk is tijdens chirurgische ingrepen. We hebben aangetoond dat *in vivo* klemmen van murine thoracale aorta's resulteert in schade op zowel het functionele als morfologisch niveau, en dat deze schade gedeeltelijk behouden blijft tot 1 maand na de mechanische belasting.

Om te bepalen of het noodzakelijk is om patiënt-specifieke informatie in de mathematische modellen te includeren, werd onderzocht of de factoren leeftijd en pathologie een invloed uitoefenen op de relatie tussen mechanische klemkracht en weefselschade.

We observeerden een trend naar verminderde endotheelafhankelijke relaxatie in oudere muizen. Vermoedelijk zou deze trend significant worden indien muizen van nog oudere **leeftijd** (> 40 weken) in de studie opgenomen zouden worden.

Gezien de hoge prevalentie van **atherosclerose** in patiënten die chirurgische ingrepen ondergaan, werd het effect van arterieel klemmen ook onderzocht in muizen die atherosclerotische letsels vertonen (*LDLR* knockout muizen op westers dieet). We vonden geen consistent effect van genotype ter hoogte van de tunica intima. In de media toonden onze resultaten echter een hogere osteopontine aanwezigheid aan

(synthetische gladde spiercellen) in atherosclerotische arteries vergeleken met wildtype bloedvaten. Verder gaf kwantificatie van klem-geïnduceerde afplatting van de binnenste elastische membraan aan dat atherosclerotische stalen meer afplatting vertonen na het klemmen. Terwijl deze afplatting niet reversibel was in *LDLR* knockout arteries, zagen we in wildtype bloedvaten wel herstel doorheen de tijd. Deze conclusies suggereren dat arteries in atherosclerotische dieren meer vatbaar zijn voor schade ter hoogte van de tunica media. CD45 kleuring toonde een consistente stijging aan van inflammatoire cellen na klemmen. Terwijl CD45 scores in wildtype arteries in de tunica intima hoger zijn dan in *LDLR* knockout vaten, zagen we in de media een omgekeerd patroon.

We kunnen **concluderen** dat *in vivo* klemmen van arteries deze bloedvaten beschadigt, zelfs wanneer de klemkracht laag is. Terwijl we geen significant effect van leeftijd konden aantonen, zagen we wel een verschillende respons van arteries in gezonde en atherosclerotische muizen. Deze resultaten suggereren dat patiënt-specifieke informatie geïmplementeerd zou moeten worden in de mathematische modellen voor chirurgische robots. Dit zou de veiligheid tijdens en na minimaal invasieve chirurgische procedures verhogen.

SUPPLEMENTARY TABLES

SUPPLEMENTARY TABLES I: CD105 STAINING

Post-hoc P-values after two way ANOVA

WT: wildtype, KO: *LDLR* knockout

Acute	0.0N WT	0.0N KO	0.6N WT	0.6N KO	1.27N WT	1.27N KO
0.0N, WT		0.0061	0.5929	<.0001	0.0050	<.0001
0.0N, KO	0.0061		0.2337	0.0349	10000	0.0548
0.6N, WT	0.5929	0.2337		<.0001	0.2042	0.0001
0.6N, KO	<.0001	0.0349	<.0001		0.0417	10000
1.27N, WT	0.0050	10000	0.2042	0.0417		0.0649
1.27N, KO	<.0001	0.0548	0.0001	10000	0.0649	

6h	0.0N WT	0.0N KO	0.6N WT	0.6N KO	1.27N WT	1.27N KO
0.0N, WT		10000	0.7758	0.9969	0.0580	0.9997
0.0N, KO	10000		0.6329	0.9839	0.0277	0.9968
0.6N, WT	0.7758	0.6329		0.9467	0.5071	0.9103
0.6N, KO	0.9969	0.9839	0.9467		0.1195	10000
1.27N, WT	0.0580	0.0277	0.5071	0.1195		0.1097
1.27N, KO	0.9997	0.9968	0.9103	10000	0.1097	

2w	0.0N WT	0.0N KO	0.6N WT	0.6N KO	1.27N WT	1.27N KO
0.0N, WT		10000	10.000	0.9909	0.9999	10000
0.0N, KO	10000		10000	0.9990	0.9987	0.9994
0.6N, WT	10.000	10000		0.9947	0.9998	0.9999
0.6N, KO	0.9909	0.9990	0.9947		0.9653	0.9785
1.27N, WT	0.9999	0.9987	0.9998	0.9653		10000
1.27N, KO	10000	0.9994	0.9999	0.9785	10000	

1m	0.0N WT	0.0N KO	0.6N WT	0.6N KO	1.27N WT	1.27N KO
0.0N, WT		10000	0.9999	0.9973	0.9961	<.0001
0.0N, KO	10000		10000	0.9980	0.9949	<.0001
0.6N, WT	0.9999	10000		0.9999	0.9804	<.0001
0.6N, KO	0.9973	0.9980	0.9999		0.9311	<.0001
1.27N, WT	0.9961	0.9949	0.9804	0.9311		<.0001
1.27N, KO	<.0001	<.0001	<.0001	<.0001	<.0001	

0.0N	WT Acute	WT 6 hours	WT 2 weeks	WT 1 month	KO Acute	KO 6 hours	KO 2 weeks	KO 1 month
WT, Acute		0.0012	<.0001	<.0001	0.0657	0.0012	<.0001	<.0001
WT, 6 hours	0.0012		0.6711	0.9839	0.7290	10.000	0.8546	0.9798
WT, 2 weeks	<.0001	0.6711		0.9877	0.0227	0.4642	10000	0.9906
WT, 1 month	<.0001	0.9839	0.9877		0.1672	0.9308	0.9992	10000
KO, Acute	0.0657	0.7290	0.0227	0.1672		0.8173	0.0662	0.1548
KO, 6 hours	0.0012	10.000	0.4642	0.9308	0.8173		0.6973	0.9191
KO, 2 weeks	<.0001	0.8546	10000	0.9992	0.0662	0.6973		0.9995
KO, 1 month	<.0001	0.9798	0.9906	10000	0.1548	0.9191	0.9995	

0.6N	WT Acute	WT 6 hours	WT 2 weeks	WT 1 month	KO Acute	KO 6 hours	KO 2 weeks	KO 1 month
WT, Acute		<.0001	<.0001	<.0001	0.0001	0.0003	<.0001	<.0001
WT, 6 hours	<.0001		10000	0.9951	0.9200	0.8395	0.9658	10000
WT, 2 weeks	<.0001	10000		0.9987	0.9574	0.8998	0.9851	10.000
WT, 1 month	<.0001	0.9951	0.9987		0.9997	0.9969	10000	0.9999
KO, Acute	0.0001	0.9200	0.9574	0.9997		10000	10000	0.9868
KO, 6 hours	0.0003	0.8395	0.8998	0.9969	10000		0.9999	0.9579
KO, 2 weeks	<.0001	0.9658	0.9851	10000	10000	0.9999		0.9969
KO, 1 month	<.0001	10000	10.000	0.9999	0.9868	0.9579	0.9969	

1.27N	WT Acute	WT 6 hours	WT 2 weeks	WT 1 month	KO Acute	KO 6 hours	KO 2 weeks	KO 1 month
WT, Acute		0.0303	0.3784	0.9440	0.8719	0.9399	0.4623	<.0001
WT, 6 hours	0.0303		0.9221	0.3351	0.4605	0.4353	0.9276	0.1690
WT, 2 weeks	0.3784	0.9221		0.9621	0.9895	0.9802	10000	0.0090
WT, 1 month	0.9440	0.3351	0.9621		10.000	10000	0.9763	0.0004
KO, Acute	0.8719	0.4605	0.9895	10.000		10000	0.9941	0.0008
KO, 6 hours	0.9399	0.4353	0.9802	10000	10000		0.9879	0.0010
KO, 2 weeks	0.4623	0.9276	10000	0.9763	0.9941	0.9879		0.0132
KO, 1 month	<.0001	0.1690	0.0090	0.0004	0.0008	0.0010	0.0132	

WT	Acute 0.0N	Acute 0.6N	Acute 1.27N	6 hours 0.0N	6 hours 0.6N	6 hours 1.27N	2 weeks 0.0N	2 weeks 0.6N	2 weeks 1.27N	1 month 0.0N	1 month 0.6N	1 month 1.27N
Acute, 0.0N		0.9965	0.3536	0.0254	0.0001	<.0001	0.0001	0.0002	<.0001	0.0014	0.0006	0.0073
Acute, 0.6N	0.9965		0.9380	0.2652	0.0038	<.0001	0.0041	0.0052	0.0019	0.0327	0.0174	0.1225
Acute, 1.27N	0.3536	0.9380		0.9816	0.2149	0.0011	0.2250	0.2588	0.1366	0.6445	0.4937	0.9186
6 hours, 0.0N	0.0254	0.2652	0.9816		0.9595	0.0876	0.9638	0.9750	0.9022	0.9999	0.9985	10000
6 hours, 0.6N	0.0001	0.0038	0.2149	0.9595		0.7709	10.000	10.000	10.000	0.9999	10000	0.9844
6 hours, 1.27N	<.0001	<.0001	0.0011	0.0876	0.7709		0.7573	0.7126	0.8786	0.3129	0.4472	0.1067
2 weeks, 0.0N	0.0001	0.0041	0.2250	0.9638	10.000	0.7573		10000	10000	0.9999	10000	0.9865
2 weeks, 0.6N	0.0002	0.0052	0.2588	0.9750	10.000	0.7126	10000		10.000	10000	10000	0.9918
2 weeks, 1.27N	<.0001	0.0019	0.1366	0.9022	10.000	0.8786	10000	10.000		0.9986	0.9999	0.9501
1 month, 0.0N	0.0014	0.0327	0.6445	0.9999	0.9999	0.3129	0.9999	10000	0.9986		10000	10000
1 month, 0.6N	0.0006	0.0174	0.4937	0.9985	10000	0.4472	10000	10000	0.9999	10000		0.9998
1 month, 1.27N	0.0073	0.1225	0.9186	10000	0.9844	0.1067	0.9865	0.9918	0.9501	10000	0.9998	

KO	Acute 0.0N	Acute 0.6N	Acute 1.27N	6 hours 0.0N	6 hours 0.6N	6 hours 1.27N	2 weeks 0.0N	2 weeks 0.6N	2 weeks 1.27N	1 month 0.0N	1 month 0.6N	1 month 1.27N
Acute, 0.0N		0.6344	0.7185	0.9859	0.7252	0.8723	0.3372	0.5471	0.1545	0.5428	0.2611	<.0001
Acute, 0.6N	0.6344		10.000	0.9991	10.000	10.000	10000	10.000	0.9981	10000	10000	<.0001
Acute, 1.27N	0.7185	10.000		0.9998	10.000	10.000	0.9999	10.000	0.9947	10000	0.9999	<.0001
6 hours, 0.0N	0.9859	0.9991	0.9998		0.9998	10.000	0.9617	0.9971	0.8187	0.9969	0.9422	<.0001
6 hours, 0.6N	0.7252	10.000	10.000	0.9998		10000	0.9999	10.000	0.9943	10000	0.9998	<.0001
6 hours, 1.27N	0.8723	10.000	10.000	10.000	10000		0.9995	10.000	0.9858	10000	0.9990	<.0001
2 weeks, 0.0N	0.3372	10000	0.9999	0.9617	0.9999	0.9995		10000	10000	10000	10000	<.0001
2 weeks, 0.6N	0.5471	10.000	10.000	0.9971	10.000	10.000	10000		0.9995	10000	10000	<.0001
2 weeks, 1.27N	0.1545	0.9981	0.9947	0.8187	0.9943	0.9858	10000	0.9995		0.9995	10000	0.0001
1 month, 0.0N	0.5428	10000	10000	0.9969	10000	10000	10000	10000	0.9995		10000	<.0001
1 month, 0.6N	0.2611	10000	0.9999	0.9422	0.9998	0.9990	10000	10000	10000	10000		<.0001
1 month, 1.27N	<.0001	<.0001	<.0001	<.0001	<.0001	<.0001	<.0001	<.0001	0.0001	<.0001	<.0001	

SUPPLEMENTARY TABLES II: VERHOEFF'S-VAN GIESON STAINING

Post-hoc P-values after two way ANOVA

WT: wildtype, KO: *LDLR* knockout

Acute	0.0N WT	0.0N KO	0.6N WT	0.6N KO	1.27N WT	1.27N KO
0.0N, WT		0.9657	0.9984	0.0059	0.0731	0.0005
0.0N, KO	0.9657		0.9987	0.0422	0.3278	0.0044
0.6N, WT	0.9984	0.9987		0.0166	0.1679	0.0016
0.6N, KO	0.0059	0.0422	0.0166		0.8996	0.9421
1.27N, WT	0.0731	0.3278	0.1679	0.8996		0.3945
1.27N, KO	0.0005	0.0044	0.0016	0.9421	0.3945	

6h	0.0N WT	0.0N KO	0.6N WT	0.6N KO	1.27N WT	1.27N KO
0.0N, WT		10000	0.0746	<.0001	0.0001	<.0001
0.0N, KO	10000		0.0629	<.0001	<.0001	<.0001
0.6N, WT	0.0746	0.0629		<.0001	0.1110	0.0029
0.6N, KO	<.0001	<.0001	<.0001		0.0393	0.7536
1.27N, WT	0.0001	<.0001	0.1110	0.0393		0.5665
1.27N, KO	<.0001	<.0001	0.0029	0.7536	0.5665	

2w	0.0N WT	0.0N KO	0.6N WT	0.6N KO	1.27N WT	1.27N KO
0.0N, WT		0.1126	0.0339	<.0001	0.0011	<.0001
0.0N, KO	0.1126		0.9985	0.0014	0.5433	0.0002
0.6N, WT	0.0339	0.9985		0.0024	0.7487	0.0002
0.6N, KO	<.0001	0.0014	0.0024		0.0651	0.8922
1.27N, WT	0.0011	0.5433	0.7487	0.0651		0.0072
1.27N, KO	<.0001	0.0002	0.0002	0.8922	0.0072	

1m	0.0N WT	0.0N KO	0.6N WT	0.6N KO	1.27N WT	1.27N KO
0.0N, WT		0.9408	0.6969	<.0001	0.2837	<.0001
0.0N, KO	0.9408		0.9940	<.0001	0.8070	<.0001
0.6N, WT	0.6969	0.9940		0.0003	0.9788	<.0001
0.6N, KO	<.0001	<.0001	0.0003		0.0018	0.7962
1.27N, WT	0.2837	0.8070	0.9788	0.0018		<.0001
1.27N, KO	<.0001	<.0001	<.0001	0.7962	<.0001	

0.0N	WT Acute	WT 6 hours	WT 2 weeks	WT 1 month	KO Acute	KO 6 hours	KO 2 weeks	KO 1 month
WT, Acute		10.000	0.3071	0.8551	0.9698	10.000	0.9993	0.9998
WT, 6 hours	10.000		0.5644	0.9712	0.8972	10.000	0.9899	10000
WT, 2 weeks	0.3071	0.5644		0.9807	0.0363	0.4646	0.1352	0.5721
WT, 1 month	0.8551	0.9712	0.9807		0.2687	0.9493	0.5762	0.9790
KO, Acute	0.9698	0.8972	0.0363	0.2687		0.8977	0.9999	0.8247
KO, 6 hours	10.000	10.000	0.4646	0.9493	0.8977		0.9915	10000
KO, 2 weeks	0.9993	0.9899	0.1352	0.5762	0.9999	0.9915		0.9759
KO, 1 month	0.9998	10000	0.5721	0.9790	0.8247	10000	0.9759	

0.6N	WT Acute	WT 6 hours	WT 2 weeks	WT 1 month	KO Acute	KO 6 hours	KO 2 weeks	KO 1 month
WT, Acute		0.2386	0.9994	0.9998	0.0006	<.0001	0.0001	0.0001
WT, 6 hours	0.2386		0.5320	0.0998	0.3159	<.0001	0.1164	0.1302
WT, 2 weeks	0.9994	0.5320		0.9778	0.0029	<.0001	0.0006	0.0007
WT, 1 month	0.9998	0.0998	0.9778		0.0002	<.0001	<.0001	<.0001
KO, Acute	0.0006	0.3159	0.0029	0.0002		0.0027	0.9995	0.9997
KO, 6 hours	<.0001	<.0001	<.0001	<.0001	0.0027		0.0120	0.0103
KO, 2 weeks	0.0001	0.1164	0.0006	<.0001	0.9995	0.0120		10000
KO, 1 month	0.0001	0.1302	0.0007	<.0001	0.9997	0.0103	10000	

1.27N	WT Acute	WT 6 hours	WT 2 weeks	WT 1 month	KO Acute	KO 6 hours	KO 2 weeks	KO 1 month
WT, Acute		0.8147	0.9831	0.4522	0.5998	0.1528	0.4339	0.3223
WT, 6 hours	0.8147		0.2760	0.0213	10000	0.8949	0.9968	0.9909
WT, 2 weeks	0.9831	0.2760		0.9390	0.1392	0.0199	0.0869	0.0498
WT, 1 month	0.4522	0.0213	0.9390		0.0081	0.0009	0.0051	0.0022
KO, Acute	0.5998	10000	0.1392	0.0081		0.9785	10000	0.9998
KO, 6 hours	0.1528	0.8949	0.0199	0.0009	0.9785		0.9989	0.9995
KO, 2 weeks	0.4339	0.9968	0.0869	0.0051	10000	0.9989		10000
KO, 1 month	0.3223	0.9909	0.0498	0.0022	0.9998	0.9995	10000	

WT	Acute 0.0N	Acute 0.6N	Acute 1.27N	6 hours 0.0N	6 hours 0.6N	6 hours 1.27N	2 weeks 0.0N	2 weeks 0.6N	2 weeks 1.27N	1 month 0.0N	1 month 0.6N	1 month 1.27N
Acute, 0.0N		10.000	0.0990	10.000	0.4079	0.0006	0.6912	0.9992	0.6399	0.9871	10000	0.9998
Acute, 0.6N	10.000		0.2589	0.9999	0.7067	0.0025	0.3929	10.000	0.8901	0.8852	10000	10000
Acute, 1.27N	0.0990	0.2589		0.0712	0.9999	0.8575	0.0002	0.5121	0.9955	0.0031	0.1253	0.4271
6 hours, 0.0N	10.000	0.9999	0.0712		0.3092	0.0005	0.8915	0.9932	0.5150	0.9992	10000	0.9975
6 hours, 0.6N	0.4079	0.7067	0.9999	0.3092		0.4113	0.0023	0.9179	10.000	0.0275	0.4734	0.8686
6 hours, 1.27N	0.0006	0.0025	0.8575	0.0005	0.4113		<.0001	0.0098	0.2233	<.0001	0.0008	0.0066
2 weeks, 0.0N	0.6912	0.3929	0.0002	0.8915	0.0023	<.0001		0.1797	0.0070	0.9996	0.6239	0.2332
2 weeks, 0.6N	0.9992	10.000	0.5121	0.9932	0.9179	0.0098	0.1797		0.9861	0.6482	0.9998	10000
2 weeks, 1.27N	0.6399	0.8901	0.9955	0.5150	10.000	0.2233	0.0070	0.9861		0.0695	0.7063	0.9703
1 month, 0.0N	0.9871	0.8852	0.0031	0.9992	0.0275	<.0001	0.9996	0.6482	0.0695		0.9761	0.7315
1 month, 0.6N	10000	10000	0.1253	10000	0.4734	0.0008	0.6239	0.9998	0.7063	0.9761		10.000
1 month, 1.27N	0.9998	10000	0.4271	0.9975	0.8686	0.0066	0.2332	10000	0.9703	0.7315	10.000	

KO	Acute 0.0N	Acute 0.6N	Acute 1.27N	6 hours 0.0N	6 hours 0.6N	6 hours 1.27N	2 weeks 0.0N	2 weeks 0.6N	2 weeks 1.27N	1 month 0.0N	1 month 0.6N	1 month 1.27N
Acute, 0.0N		0.0168	0.0005	0.9832	<.0001	<.0001	10000	0.0040	0.0002	0.9586	0.0046	<.0001
Acute, 0.6N	0.0168		0.9933	0.0003	0.0156	0.5002	0.0085	10.000	0.9342	0.0002	10000	0.8624
Acute, 1.27N	0.0005	0.9933		<.0001	0.2436	0.9841	0.0003	10.000	10.000	<.0001	0.9999	10000
6 hours, 0.0N	0.9832	0.0003	<.0001		<.0001	<.0001	0.9997	<.0001	<.0001	10000	<.0001	<.0001
6 hours, 0.6N	<.0001	0.0156	0.2436	<.0001		0.9659	<.0001	0.0572	0.5945	<.0001	0.0506	0.6063
6 hours, 1.27N	<.0001	0.5002	0.9841	<.0001	0.9659		<.0001	0.7912	0.9998	<.0001	0.7653	0.9999
2 weeks, 0.0N	10000	0.0085	0.0003	0.9997	<.0001	<.0001		0.0021	0.0001	0.9984	0.0024	<.0001
2 weeks, 0.6N	0.0040	10.000	10.000	<.0001	0.0572	0.7912	0.0021		0.9954	<.0001	10000	0.9843
2 weeks, 1.27N	0.0002	0.9342	10.000	<.0001	0.5945	0.9998	0.0001	0.9954		<.0001	0.9935	10000
1 month, 0.0N	0.9586	0.0002	<.0001	10000	<.0001	<.0001	0.9984	<.0001	<.0001		<.0001	<.0001
1 month, 0.6N	0.0046	10000	0.9999	<.0001	0.0506	0.7653	0.0024	10000	0.9935	<.0001		0.9790
1 month, 1.27N	<.0001	0.8624	10000	<.0001	0.6063	0.9999	<.0001	0.9843	10000	<.0001	0.9790	

SUPPLEMENTARY TABLES III: OSTEOPONTIN STAINING

Post-hoc P-values after two way ANOVA

WT: wildtype, KO: *LDLR* knockout

Acute	0.0N WT	0.0N KO	0.6N WT	0.6N KO	1.27N WT	1.27N KO
0.0N, WT		0.9780	0.9409	0.1158	0.9995	0.0132
0.0N, KO	0.9780		10000	0.3502	0.9982	0.0520
0.6N, WT	0.9409	10000		0.4624	0.9888	0.0805
0.6N, KO	0.1158	0.3502	0.4624		0.1729	0.9142
1.27N, WT	0.9995	0.9982	0.9888	0.1729		0.0195
1.27N, KO	0.0132	0.0520	0.0805	0.9142	0.0195	

6h	0.0N WT	0.0N KO	0.6N WT	0.6N KO	1.27N WT	1.27N KO
0.0N, WT		0.8440	0.0162	0.0339	0.9965	0.3937
0.0N, KO	0.8440		0.1656	0.2922	0.9762	0.9524
0.6N, WT	0.0162	0.1656		0.9995	0.0354	0.6676
0.6N, KO	0.0339	0.2922	0.9995		0.0732	0.8387
1.27N, WT	0.9965	0.9762	0.0354	0.0732		0.6305
1.27N, KO	0.3937	0.9524	0.6676	0.8387	0.6305	

2w	0.0N WT	0.0N KO	0.6N WT	0.6N KO	1.27N WT	1.27N KO
0.0N, WT		0.0778	0.0469	0.0081	0.0023	<.0001
0.0N, KO	0.0778		0.9999	0.9282	0.7011	0.0295
0.6N, WT	0.0469	0.9999		0.9772	0.8266	0.0489
0.6N, KO	0.0081	0.9282	0.9772		0.9962	0.2012
1.27N, WT	0.0023	0.7011	0.8266	0.9962		0.4217
1.27N, KO	<.0001	0.0295	0.0489	0.2012	0.4217	

1m	0.0N WT	0.0N KO	0.6N WT	0.6N KO	1.27N WT	1.27N KO
0.0N, WT		0.0312	10.000	0.0273	0.9968	0.0213
0.0N, KO	0.0312		0.0388	10000	0.0903	10000
0.6N, WT	10.000	0.0388		0.0340	0.9989	0.0266
0.6N, KO	0.0273	10000	0.0340		0.0802	10000
1.27N, WT	0.9968	0.0903	0.9989	0.0802		0.0641
1.27N, KO	0.0213	10000	0.0266	10000	0.0641	

0.0N	WT Acute	WT 6 hours	WT 2 weeks	WT 1 month	KO Acute	KO 6 hours	KO 2 weeks	KO 1 month
WT, Acute		10.000	0.9185	0.1702	0.9829	0.9898	0.4421	<.0001
WT, 6 hours	10.000		0.9676	0.1120	0.9493	0.9653	0.3263	<.0001
WT, 2 weeks	0.9185	0.9676		0.0052	0.3495	0.3954	0.0256	<.0001
WT, 1 month	0.1702	0.1120	0.0052		0.6101	0.5577	0.9988	<.0001
KO, Acute	0.9829	0.9493	0.3495	0.6101		10000	0.9178	<.0001
KO, 6 hours	0.9898	0.9653	0.3954	0.5577	10000		0.8891	<.0001
KO, 2 weeks	0.4421	0.3263	0.0256	0.9988	0.9178	0.8891		<.0001
KO, 1 month	<.0001	<.0001	<.0001	<.0001	<.0001	<.0001	<.0001	

0.6N	WT Acute	WT 6 hours	WT 2 weeks	WT 1 month	KO Acute	KO 6 hours	KO 2 weeks	KO 1 month
WT, Acute		0.8540	0.9790	0.8913	0.6539	0.9335	0.7386	<.0001
WT, 6 hours	0.8540		0.9998	10000	10000	10.000	10.000	0.0035
WT, 2 weeks	0.9790	0.9998		10000	0.9919	10000	0.9974	0.0009
WT, 1 month	0.8913	10000	10000		0.9998	10000	10000	0.0027
KO, Acute	0.6539	10000	0.9919	0.9998		0.9990	10000	0.0098
KO, 6 hours	0.9335	10.000	10000	10000	0.9990		0.9998	0.0019
KO, 2 weeks	0.7386	10.000	0.9974	10000	10000	0.9998		0.0066
KO, 1 month	<.0001	0.0035	0.0009	0.0027	0.0098	0.0019	0.0066	

1.27N	WT Acute	WT 6 hours	WT 2 weeks	WT 1 month	KO Acute	KO 6 hours	KO 2 weeks	KO 1 month
WT, Acute		10.000	0.3699	0.4966	0.1406	0.9948	0.0205	0.0002
WT, 6 hours	10.000		0.3042	0.4208	0.1085	0.9877	0.0151	0.0001
WT, 2 weeks	0.3699	0.3042		10000	0.9994	0.8693	0.8259	0.0754
WT, 1 month	0.4966	0.4208	10000		0.9948	0.9384	0.7149	0.0459
KO, Acute	0.1406	0.1085	0.9994	0.9948		0.5781	0.9795	0.2286
KO, 6 hours	0.9948	0.9877	0.8693	0.9384	0.5781		0.1557	0.0031
KO, 2 weeks	0.0205	0.0151	0.8259	0.7149	0.9795	0.1557		0.8351
KO, 1 month	0.0002	0.0001	0.0754	0.0459	0.2286	0.0031	0.8351	

WT	Acute 0.0N	Acute 0.6N	Acute 1.27N	6 hours 0.0N	6 hours 0.6N	6 hours 1.27N	2 weeks 0.0N	2 weeks 0.6N	2 weeks 1.27N	1 month 0.0N	1 month 0.6N	1 month 1.27N
Acute, 0.0N		0.9866	10.000	10.000	0.1223	10.000	0.9785	0.3888	0.0114	0.2232	0.1592	0.0300
Acute, 0.6N	0.9866		0.9995	0.9557	0.7363	0.9965	0.3009	0.9744	0.1850	0.8885	0.8083	0.3574
Acute, 1.27N	10.000	0.9995		10.000	0.2303	10.000	0.8180	0.6054	0.0239	0.3890	0.2911	0.0618
6 hours, 0.0N	10.000	0.9557	10.000		0.0735	10.000	0.9949	0.2697	0.0059	0.1429	0.0982	0.0164
6 hours, 0.6N	0.1223	0.7363	0.2303	0.0735		0.1505	0.0016	10.000	0.9986	10000	10000	10000
6 hours, 1.27N	10.000	0.9965	10.000	10.000	0.1505		0.9081	0.4666	0.0132	0.2736	0.1960	0.0360
2 weeks, 0.0N	0.9785	0.3009	0.8180	0.9949	0.0016	0.9081		0.0117	<.0001	0.0043	0.0025	0.0002
2 weeks, 0.6N	0.3888	0.9744	0.6054	0.2697	10.000	0.4666	0.0117		0.9212	10000	10000	0.9874
2 weeks, 1.27N	0.0114	0.1850	0.0239	0.0059	0.9986	0.0132	<.0001	0.9212		0.9851	0.9956	10000
1 month, 0.0N	0.2232	0.8885	0.3890	0.1429	10000	0.2736	0.0043	10000	0.9851		10000	0.9992
1 month, 0.6N	0.1592	0.8083	0.2911	0.0982	10000	0.1960	0.0025	10000	0.9956	10000		0.9999
1 month, 1.27N	0.0300	0.3574	0.0618	0.0164	10000	0.0360	0.0002	0.9874	10000	0.9992	0.9999	

KO	Acute 0.0N	Acute 0.6N	Acute 1.27N	6 hours 0.0N	6 hours 0.6N	6 hours 1.27N	2 weeks 0.0N	2 weeks 0.6N	2 weeks 1.27N	1 month 0.0N	1 month 0.6N	1 month 1.27N
Acute, 0.0N		0.9044	0.4364	10.000	0.9923	10.000	0.9998	0.9399	0.0847	0.0010	0.0008	0.0006
Acute, 0.6N	0.9044		0.9997	0.8850	10.000	0.9937	0.9994	10.000	0.8706	0.1146	0.0992	0.0754
Acute, 1.27N	0.4364	0.9997		0.4043	0.9814	0.7862	0.8953	0.9989	0.9985	0.4972	0.4562	0.3846
6 hours, 0.0N	10.000	0.8850	0.4043		0.9891	10.000	0.9996	0.9254	0.0752	0.0009	0.0007	0.0005
6 hours, 0.6N	0.9923	10.000	0.9814	0.9891		10000	10.000	10.000	0.6061	0.0345	0.0291	0.0211
6 hours, 1.27N	10.000	0.9937	0.7862	10.000	10000		10000	0.9974	0.2735	0.0084	0.0070	0.0050
2 weeks, 0.0N	0.9998	0.9994	0.8953	0.9996	10.000	10000		0.9999	0.3769	0.0121	0.0101	0.0071
2 weeks, 0.6N	0.9399	10.000	0.9989	0.9254	10.000	0.9974	0.9999		0.8188	0.0876	0.0753	0.0565
2 weeks, 1.27N	0.0847	0.8706	0.9985	0.0752	0.6061	0.2735	0.3769	0.8188		0.9820	0.9747	0.9556
1 month, 0.0N	0.0010	0.1146	0.4972	0.0009	0.0345	0.0084	0.0121	0.0876	0.9820		10000	10000
1 month, 0.6N	0.0008	0.0992	0.4562	0.0007	0.0291	0.0070	0.0101	0.0753	0.9747	10000		10.000
1 month, 1.27N	0.0006	0.0754	0.3846	0.0005	0.0211	0.0050	0.0071	0.0565	0.9556	10000	10.000	

SUPPLEMENTARY TABLES IV: CD45 STAINING - INTIMA

Post-hoc P-values after two way ANOVA

WT: wildtype, KO: *LDLR* knockout

Acute	0.0N WT	0.0N KO	0.6N WT	0.6N KO	1.27N WT	1.27N KO
0.0N, WT		0.0373	0.3526	0.9661	0.3586	0.7633
0.0N, KO	0.0373		0.0001	0.0037	0.0001	0.0009
0.6N, WT	0.3526	0.0001		0.7860	10.000	0.9770
0.6N, KO	0.9661	0.0037	0.7860		0.7923	0.9924
1.27N, WT	0.3586	0.0001	10.000	0.7923		0.9786
1.27N, KO	0.7633	0.0009	0.9770	0.9924	0.9786	

6h	0.0N WT	0.0N KO	0.6N WT	0.6N KO	1.27N WT	1.27N KO
0.0N, WT		0.2685	0.0218	0.1191	0.0030	0.0102
0.0N, KO	0.2685		0.7976	0.9969	0.3142	0.5496
0.6N, WT	0.0218	0.7976		0.9642	0.9588	0.9966
0.6N, KO	0.1191	0.9969	0.9642		0.5820	0.8112
1.27N, WT	0.0030	0.3142	0.9588	0.5820		0.9995
1.27N, KO	0.0102	0.5496	0.9966	0.8112	0.9995	

2w	0.0N WT	0.0N KO	0.6N WT	0.6N KO	1.27N WT	1.27N KO
0.0N, WT		0.9458	0.0869	0.9877	0.0099	0.1369
0.0N, KO	0.9458		0.4197	0.9998	0.0800	0.5287
0.6N, WT	0.0869	0.4197		0.2846	0.9355	10000
0.6N, KO	0.9877	0.9998	0.2846		0.0451	0.3830
1.27N, WT	0.0099	0.0800	0.9355	0.0451		0.9207
1.27N, KO	0.1369	0.5287	10000	0.3830	0.9207	

1m	0.0N WT	0.0N KO	0.6N WT	0.6N KO	1.27N WT	1.27N KO
0.0N, WT		0.9978	0.3068	0.4758	0.1597	0.1351
0.0N, KO	0.9978		0.5561	0.7434	0.3391	0.2964
0.6N, WT	0.3068	0.5561		0.9996	0.9990	0.9972
0.6N, KO	0.4758	0.7434	0.9996		0.9829	0.9712
1.27N, WT	0.1597	0.3391	0.9990	0.9829		10000
1.27N, KO	0.1351	0.2964	0.9972	0.9712	10000	

0.0N	WT Acute	WT 6 hours	WT 2 weeks	WT 1 month	KO Acute	KO 6 hours	KO 2 weeks	KO 1 month
WT, Acute		0.9999	0.9258	0.0050	0.3538	0.9979	0.9999	0.0178
WT, 6 hours	0.9999		0.9942	0.0168	0.6156	0.9551	10.000	0.0540
WT, 2 weeks	0.9258	0.9942		0.0773	0.9448	0.5344	0.9901	0.2124
WT, 1 month	0.0050	0.0168	0.0773		0.6568	0.0004	0.0096	0.9997
KO, Acute	0.3538	0.6156	0.9448	0.6568		0.0847	0.5428	0.8990
KO, 6 hours	0.9979	0.9551	0.5344	0.0004	0.0847		0.9509	0.0016
KO, 2 weeks	0.9999	10.000	0.9901	0.0096	0.5428	0.9509		0.0341
KO, 1 month	0.0178	0.0540	0.2124	0.9997	0.8990	0.0016	0.0341	

0.6N	WT Acute	WT 6 hours	WT 2 weeks	WT 1 month	KO Acute	KO 6 hours	KO 2 weeks	KO 1 month
WT, Acute		10.000	10000	0.0001	0.8476	0.9833	0.0331	<.0001
WT, 6 hours	10.000		10000	0.0003	0.9493	0.9984	0.0677	<.0001
WT, 2 weeks	10000	10000		0.0002	0.9338	0.9972	0.0587	<.0001
WT, 1 month	0.0001	0.0003	0.0002		0.0078	0.0018	0.5272	0.9994
KO, Acute	0.8476	0.9493	0.9338	0.0078		0.9996	0.5248	0.0017
KO, 6 hours	0.9833	0.9984	0.9972	0.0018	0.9996		0.2454	0.0004
KO, 2 weeks	0.0331	0.0677	0.0587	0.5272	0.5248	0.2454		0.2337
KO, 1 month	<.0001	<.0001	<.0001	0.9994	0.0017	0.0004	0.2337	

1.27N	WT Acute	WT 6 hours	WT 2 weeks	WT 1 month	KO Acute	KO 6 hours	KO 2 weeks	KO 1 month
WT, Acute		10.000	0.9906	0.0302	0.9990	10.000	10.000	0.0396
WT, 6 hours	10.000		0.9991	0.0152	0.9900	10.000	0.9996	0.0203
WT, 2 weeks	0.9906	0.9991		0.0032	0.8540	0.9961	0.9653	0.0044
WT, 1 month	0.0302	0.0152	0.0032		0.1151	0.0374	0.0810	10000
KO, Acute	0.9990	0.9900	0.8540	0.1151		0.9984	10000	0.1446
KO, 6 hours	10.000	10.000	0.9961	0.0374	0.9984		10.000	0.0483
KO, 2 weeks	10.000	0.9996	0.9653	0.0810	10000	10.000		0.1020
KO, 1 month	0.0396	0.0203	0.0044	10000	0.1446	0.0483	0.1020	

WT	Acute 0.0N	Acute 0.6N	Acute 1.27N	6 hours 0.0N	6 hours 0.6N	6 hours 1.27N	2 weeks 0.0N	2 weeks 0.6N	2 weeks 1.27N	1 month 0.0N	1 month 0.6N	1 month 1.27N
Acute, 0.0N		0.2090	0.2158	0.9994	0.3955	0.0816	0.4476	0.3513	0.0059	<.0001	0.0285	0.1930
Acute, 0.6N	0.2090		10.000	0.0243	10.000	10.000	<.0001	10.000	0.9574	<.0001	<.0001	<.0001
Acute, 1.27N	0.2158	10.000		0.0255	10.000	10.000	<.0001	10.000	0.9538	<.0001	<.0001	<.0001
6 hours, 0.0N	0.9994	0.0243	0.0255		0.0634	0.0070	0.9373	0.0525	0.0003	<.0001	0.2333	0.7145
6 hours, 0.6N	0.3955	10.000	10.000	0.0634		0.9996	0.0003	10.000	0.8229	<.0001	<.0001	<.0001
6 hours, 1.27N	0.0816	10.000	10.000	0.0070	0.9996		<.0001	0.9998	0.9978	<.0001	<.0001	<.0001
2 weeks, 0.0N	0.4476	<.0001	<.0001	0.9373	0.0003	<.0001		0.0002	<.0001	<.0001	0.9743	10000
2 weeks, 0.6N	0.3513	10.000	10.000	0.0525	10.000	0.9998	0.0002		0.8602	<.0001	<.0001	<.0001
2 weeks, 1.27N	0.0059	0.9574	0.9538	0.0003	0.8229	0.9978	<.0001	0.8602		<.0001	<.0001	<.0001
1 month, 0.0N	<.0001	<.0001	<.0001	<.0001	<.0001	<.0001	<.0001	<.0001	<.0001		0.0012	<.0001
1 month, 0.6N	0.0285	<.0001	<.0001	0.2333	<.0001	<.0001	0.9743	<.0001	<.0001	0.0012		0.9996
1 month, 1.27N	0.1930	<.0001	<.0001	0.7145	<.0001	<.0001	10000	<.0001	<.0001	<.0001	0.9996	

KO	Acute 0.0N	Acute 0.6N	Acute 1.27N	6 hours 0.0N	6 hours 0.6N	6 hours 1.27N	2 weeks 0.0N	2 weeks 0.6N	2 weeks 1.27N	1 month 0.0N	1 month 0.6N	1 month 1.27N
Acute, 0.0N		0.2771	0.1358	0.2384	0.1574	0.0585	0.8304	0.9187	0.1086	0.9889	10000	0.9989
Acute, 0.6N	0.2771		10.000	10.000	10.000	0.9994	0.9985	0.9905	10.000	0.0088	0.2953	0.7916
Acute, 1.27N	0.1358	10.000		10.000	10.000	10.000	0.9764	0.9294	10.000	0.0028	0.1413	0.5561
6 hours, 0.0N	0.2384	10.000	10.000		10.000	0.9998	0.9967	0.9835	10.000	0.0068	0.2530	0.7426
6 hours, 0.6N	0.1574	10.000	10.000	10.000		10000	0.9845	0.9483	10.000	0.0035	0.1647	0.6041
6 hours, 1.27N	0.0585	0.9994	10.000	0.9998	10000		0.8455	0.7273	10.000	0.0010	0.0597	0.3068
2 weeks, 0.0N	0.8304	0.9985	0.9764	0.9967	0.9845	0.8455		10000	0.9425	0.1122	0.8675	0.9988
2 weeks, 0.6N	0.9187	0.9905	0.9294	0.9835	0.9483	0.7273	10000		0.8688	0.1834	0.9443	0.9999
2 weeks, 1.27N	0.1086	10.000	10.000	10.000	10.000	10.000	0.9425	0.8688		0.0025	0.1135	0.4664
1 month, 0.0N	0.9889	0.0088	0.0028	0.0068	0.0035	0.0010	0.1122	0.1834	0.0025		0.9594	0.5717
1 month, 0.6N	10000	0.2953	0.1413	0.2530	0.1647	0.0597	0.8675	0.9443	0.1135	0.9594		0.9997
1 month, 1.27N	0.9989	0.7916	0.5561	0.7426	0.6041	0.3068	0.9988	0.9999	0.4664	0.5717	0.9997	

SUPPLEMENTARY TABLES IV: CD45 STAINING - MEDIA

Post-hoc P-values after two way ANOVA

WT: wildtype, KO: *LDLR* knockout

Acute	0.0N WT	0.0N KO	0.6N WT	0.6N KO	1.27N WT	1.27N KO
0.0N, WT		0.0944	10.000	0.9983	10.000	0.6173
0.0N, KO	0.0944		0.0789	0.1679	0.0575	0.0015
0.6N, WT	10.000	0.0789		0.9986	10.000	0.5454
0.6N, KO	0.9983	0.1679	0.9986		0.9934	0.3196
1.27N, WT	10.000	0.0575	10.000	0.9934		0.6406
1.27N, KO	0.6173	0.0015	0.5454	0.3196	0.6406	

6h	0.0N WT	0.0N KO	0.6N WT	0.6N KO	1.27N WT	1.27N KO
0.0N, WT		10000	0.9552	0.3382	10.000	0.0341
0.0N, KO	10000		0.9732	0.2296	0.9993	0.0177
0.6N, WT	0.9552	0.9732		0.0510	0.8802	0.0029
0.6N, KO	0.3382	0.2296	0.0510		0.3923	0.7761
1.27N, WT	10.000	0.9993	0.8802	0.3923		0.0381
1.27N, KO	0.0341	0.0177	0.0029	0.7761	0.0381	

2w	0.0N WT	0.0N KO	0.6N WT	0.6N KO	1.27N WT	1.27N KO
0.0N, WT		0.7337	0.5420	0.8747	0.6376	0.7418
0.0N, KO	0.7337		0.9996	0.9997	10000	10000
0.6N, WT	0.5420	0.9996		0.9906	10.000	0.9999
0.6N, KO	0.8747	0.9997	0.9906		0.9977	0.9995
1.27N, WT	0.6376	10000	10.000	0.9977		10000
1.27N, KO	0.7418	10000	0.9999	0.9995	10000	

1m	0.0N WT	0.0N KO	0.6N WT	0.6N KO	1.27N WT	1.27N KO
0.0N, WT		0.9930	0.0533	0.0474	0.0248	0.0189
0.0N, KO	0.9930		0.1700	0.1540	0.0883	0.0693
0.6N, WT	0.0533	0.1700		10000	0.9994	0.9977
0.6N, KO	0.0474	0.1540	10000		0.9998	0.9987
1.27N, WT	0.0248	0.0883	0.9994	0.9998		10000
1.27N, KO	0.0189	0.0693	0.9977	0.9987	10000	

0.0N	WT Acute	WT 6 hours	WT 2 weeks	WT 1 month	KO Acute	KO 6 hours	KO 2 weeks	KO 1 month
WT, Acute		10.000	0.9977	0.7738	0.7805	10.000	10.000	0.9724
WT, 6 hours	10.000		0.9949	0.7209	0.7305	10.000	10.000	0.9559
WT, 2 weeks	0.9977	0.9949		0.9793	0.9777	0.9957	0.9974	10.000
WT, 1 month	0.7738	0.7209	0.9793		10.000	0.7072	0.7399	0.9989
KO, Acute	0.7805	0.7305	0.9777	10.000		0.7200	0.7508	0.9984
KO, 6 hours	10.000	10.000	0.9957	0.7072	0.7200		10.000	0.9568
KO, 2 weeks	10.000	10.000	0.9974	0.7399	0.7508	10.000		0.9673
KO, 1 month	0.9724	0.9559	10.000	0.9989	0.9984	0.9568	0.9673	

0.6N	WT Acute	WT 6 hours	WT 2 weeks	WT 1 month	KO Acute	KO 6 hours	KO 2 weeks	KO 1 month
WT, Acute		0.9998	10000	0.1300	0.9999	0.6186	10.000	0.1053
WT, 6 hours	0.9998		0.9956	0.0463	10000	0.3406	10.000	0.0363
WT, 2 weeks	10000	0.9956		0.2252	0.9973	0.7867	0.9995	0.1871
WT, 1 month	0.1300	0.0463	0.2252		0.0532	0.9763	0.0779	10000
KO, Acute	0.9999	10000	0.9973	0.0532		0.3720	10000	0.0419
KO, 6 hours	0.6186	0.3406	0.7867	0.9763	0.3720		0.4692	0.9601
KO, 2 weeks	10.000	10.000	0.9995	0.0779	10000	0.4692		0.0620
KO, 1 month	0.1053	0.0363	0.1871	10000	0.0419	0.9601	0.0620	

1.27N	WT Acute	WT 6 hours	WT 2 weeks	WT 1 month	KO Acute	KO 6 hours	KO 2 weeks	KO 1 month
WT, Acute		0.9999	10000	<.0001	0.1475	0.0014	10.000	<.0001
WT, 6 hours	0.9999		0.9999	0.0001	0.2922	0.0038	0.9995	<.0001
WT, 2 weeks	10000	0.9999		<.0001	0.1441	0.0013	10000	<.0001
WT, 1 month	<.0001	0.0001	<.0001		0.0777	0.9787	<.0001	0.9999
KO, Acute	0.1475	0.2922	0.1441	0.0777		0.5414	0.1360	0.0316
KO, 6 hours	0.0014	0.0038	0.0013	0.9787	0.5414		0.0015	0.8909
KO, 2 weeks	10.000	0.9995	10000	<.0001	0.1360	0.0015		<.0001
KO, 1 month	<.0001	<.0001	<.0001	0.9999	0.0316	0.8909	<.0001	

WT	Acute 0.0N	Acute 0.6N	Acute 1.27N	6 hours 0.0N	6 hours 0.6N	6 hours 1.27N	2 weeks 0.0N	2 weeks 0.6N	2 weeks 1.27N	1 month 0.0N	1 month 0.6N	1 month 1.27N
Acute, 0.0N		10.000	10.000	10.000	10.000	10.000	0.9977	10.000	10.000	0.4745	0.5640	0.2627
Acute, 0.6N	10.000		10.000	10.000	10.000	10.000	0.9974	10.000	10.000	0.4214	0.4697	0.1902
Acute, 1.27N	10.000	10.000		10.000	10.000	10.000	0.9926	10.000	10.000	0.3433	0.5563	0.2457
6 hours, 0.0N	10.000	10.000	10.000		10.000	10.000	0.9929	10.000	10.000	0.3865	0.6570	0.3358
6 hours, 0.6N	10.000	10.000	10.000	10.000		0.9999	10.000	10.000	10.000	0.6760	0.2496	0.0802
6 hours, 1.27N	10.000	10.000	10.000	10.000	0.9999		0.9770	10.000	10.000	0.2512	0.6738	0.3366
2 weeks, 0.0N	0.9977	0.9974	0.9926	0.9929	10.000	0.9770		0.9848	0.9929	0.9566	0.0626	0.0150
2 weeks, 0.6N	10.000	10.000	10.000	10.000	10.000	10.000	0.9848		10.000	0.2853	0.6281	0.2987
2 weeks, 1.27N	10.000	10.000	10.000	10.000	10.000	10.000	0.9929	10.000		0.3464	0.5526	0.2432
1 month, 0.0N	0.4745	0.4214	0.3433	0.3865	0.6760	0.2512	0.9566	0.2853	0.3464		0.0008	0.0001
1 month, 0.6N	0.5640	0.4697	0.5563	0.6570	0.2496	0.6738	0.0626	0.6281	0.5526	0.0008		10.000
1 month, 1.27N	0.2627	0.1902	0.2457	0.3358	0.0802	0.3366	0.0150	0.2987	0.2432	0.0001	10.000	

KO	Acute 0.0N	Acute 0.6N	Acute 1.27N	6 hours 0.0N	6 hours 0.6N	6 hours 1.27N	2 weeks 0.0N	2 weeks 0.6N	2 weeks 1.27N	1 month 0.0N	1 month 0.6N	1 month 1.27N
Acute, 0.0N		0.6999	0.0302	0.4399	0.0233	0.0038	0.4898	0.6167	0.5334	0.9990	0.0018	0.0003
Acute, 0.6N	0.6999		0.8677	10.000	0.8207	0.3694	10000	10.000	10.000	0.9904	0.2804	0.0781
Acute, 1.27N	0.0302	0.8677		0.9786	10.000	0.9991	0.9668	0.9183	0.9809	0.1922	0.9980	0.9199
6 hours, 0.0N	0.4399	10.000	0.9786		0.9634	0.6252	10000	10.000	10.000	0.9164	0.5295	0.1965
6 hours, 0.6N	0.0233	0.8207	10.000	0.9634		0.9997	0.9463	0.8821	0.9677	0.1563	0.9992	0.9475
6 hours, 1.27N	0.0038	0.3694	0.9991	0.6252	0.9997		0.5737	0.4481	0.6593	0.0308	10000	10000
2 weeks, 0.0N	0.4898	10000	0.9668	10000	0.9463	0.5737		10000	10000	0.9401	0.4761	0.1664
2 weeks, 0.6N	0.6167	10.000	0.9183	10.000	0.8821	0.4481	10000		10.000	0.9779	0.3528	0.1073
2 weeks, 1.27N	0.5334	10.000	0.9809	10.000	0.9677	0.6593	10000	10.000		0.9486	0.5731	0.2359
1 month, 0.0N	0.9990	0.9904	0.1922	0.9164	0.1563	0.0308	0.9401	0.9779	0.9486		0.0168	0.0027
1 month, 0.6N	0.0018	0.2804	0.9980	0.5295	0.9992	10000	0.4761	0.3528	0.5731	0.0168		10.000
1 month, 1.27N	0.0003	0.0781	0.9199	0.1965	0.9475	10000	0.1664	0.1073	0.2359	0.0027	10.000	

CURRICULUM VITAE

Personalia

Rachel GEENENS

rachel.geenens@hotmail.com

Born July 24, 1986, Kortrijk, Belgium

Married August 28, 2015, Aarschot, Belgium

Education

1998-2004: Science-Math, Sint-Jan Berchmanscollege, Avelgem

2004-2009: Master of Biology, KU Leuven – Summa Cum Laude

PDL Award: Laureate Class of 2009

2009-2010: Specific Teacher Training (Science), KU Leuven – Cum Laude

2010-2016: PhD training: Laboratory of Experimental Cardiac Surgery, KU Leuven

Promotor: Prof. Dr. P. Herijgers

Funding: IWT (Agentschap voor Innovatie door Wetenschap & Technologie) and IDO project (3E100307)

Certificates

Radioprotection and biosafety

Laboratory animal science Module I

Laboratory animal science Module II

Labview core training

Publications

Geenens R, Famaey N, Gijbels A, Verhelle S, Vranken E, Ginckels A, Vinckier S, Vander Sloten J, Herijgers P. Atherosclerosis alters loading-induced arterial damage: implications for robotic surgery. [*Submitted for publication in 'The Annals of Thoracic Surgery'*].

Geenens R, Famaey N, Gijbels A, Verhulst V, Vinckier S, Vander Sloten J, Herijgers P. Arterial Vasoreactivity is Equally Affected by In Vivo Cross-Clamping with Increasing Loads in Young and Middle-Aged Mice Aortas. Ann Thorac Cardiovasc Surg. 2016 Feb 20;22(1):38-43,Epub 2015 Nov 6.

Vandenbriele C, Kauskot A, Vandersmissen I, Criel M, **Geenens R**, Craps S, Luttun A, Janssens S, Hoylaerts MF, Verhamme P. Platelet Endothelial Aggregation Receptor -1: A novel modifier of neoangiogenesis. Cardiovasc Res. 2015 Oct 1;108(1):124-38.

Verleden SE, Vasilescu DM, McDonough JE, Ruttens D, Vos R, Vandermeulen E, Bellon H, **Geenens R**, Verbeken EK, Verschakelen J, Van Raemdonck DE, Wuyts WA, Sokolow Y, Knoop C, Cooper JD, Hogg JC, Verleden GM, Vanaudenaerde BM. Linking clinical phenotypes of chronic lung allograft dysfunction to changes in lung structure. Eur Respir J. 2015 Nov;46(5):1430-9.

Jacobs G, Oosterlinck W, Dresselaers T, **Geenens R**, Kerselaers S, Himmelreich U, Herijgers P, Vennekens R. Enhanced β-adrenergic cardiac reserve in Trpm4^{-}/$^{-}$ mice with ischaemic heart failure. Cardiovasc Res. 2015 Mar 1;105(3):330-9.

Feng Y, Schouteden S, **Geenens R**, Van Duppen V, Herijgers P, Holvoet P, Van Veldhoven PP, Verfaillie CM. Hematopoietic stem/progenitor cell proliferation and differentiation is differentially regulated by high-density and low-density lipoproteins in mice. PLoS One 2012;7(11).

Verleden SE, Scheers H, Nawrot TS, Vos R, Fierens F, **Geenens R**, Yserbyt J, Wauters S, Verbeken EK, Nemery B, Dupont LJ, Van Raemdonck DE, Verleden GM, Vanaudenaerde BM. Lymphocytic bronchiolitis after lung transplantation is associated with daily changes in air pollution. Am J Transplant 2012 Jul;12(7):1831-8.

Verleden SE, Vos R, **Geenens R**, Ruttens D, Vaneylen A, Dupont LJ, Verleden GM, van Raemdonck DE, Vanaudenaerde BM. Vitamin D deficiency in lung transplant patients: is it important? Transplantation 2012 Jan 27;93(2):224-9.

Vanaudenaerde BM, Verleden SE, Vos R, De Vleeschauwer SI, Willems-Widyastuti A, **Geenens R**, Van Raemdonck DE, Dupont LJ, Verbeken EK, Meyts I. Innate and adaptive interleukin-17-producing lymphocytes in chronic inflammatory lung disorders. Am J Respir Crit Care Med. 2011 Apr 15;183(8):977-86.

Oral and poster presentations

Geenens R, Famaey N, Gijbels A, Verhulst V, Vinckier S, Vander Sloten J, Herijgers P. Age does not influence the effect of in vivo aortic clamping on vascular function in mice. Poster presentation at Canadian Cardio Congress, Vancouver, 2014.

Geenens R. Analysis of tissue damage after in vivo arterial clamping. Oral presentation research seminar, Leuven, 2014.

Geenens R, Famaey N, Gijbels A, Vinckier S, Vander Sloten J, Herijgers P. Age does not influence the effect of in vivo aortic clamping on vascular function in mice. Poster presentation at IRB 'The clock of life', Barcelona, 2013.

Mariën R, Smoljkic M, **Geenens R**, Roeffaers M, Vander Sloten J, Famaey N. Mechanical characterization of arterial tissue: Simultaneous confocal imaging and tensile testing. Poster presentation: Proceedings of the 3rd Joint Workshop on New Technologies for Computer/Robot Assisted Surgery, Verona, 2013.

Feng Y, Schouteden S, Geeraert B, **Geenens R**, Van Duppen V, Van Welden T, Herijgers P, Holvoet P, Van Veldhoven P, Verfaillie C. LDL and HDL counteract hematopoietic stem/progenitor cells in regulation of inflammation and atherosclerosis. Oral presentation by Yingmei Feng: ISA 2012.

Feng Y, Schouteden S, Geeraert B, Van Duppen V, **Geenens R**, Herijgers P, Holvoet P, Rye K, Verfaillie C. LDL and HDL counteract hematopoietic stem/progenitor cells in regulation of inflammation and atherosclerosis. Poster presentation by Yingmei Feng: ASH, 2012.

Geenens R, Famaey N, Vinckier S, Vander Sloten J, Herijgers P. Safety margins for minimally invasive surgery. Poster presentation at Vascular Biology Summer School, Papendal, 2011.